OPTIMAL HELICOPTER TRAJECTORY PLANNING FOR TERRAIN FOLLOWING FLIGHT

FINAL REPORT

March 1990

Research Supported by

NASA AMES Research Center

NASA Contract Number NAG2-463

Principal Investigator: P. K. A. Menon

Graduate Research Assistant: E. Kim

School of Aerospace Engineering

Georgia Institute of Technology

Atlanta, Georgia 30332

NASA Contract Monitor: V. H. L. Cheng

TABLE OF CONTENTS

LIST OF TABLES

LIST OF FIGURES

LIST OF SYMBOLS

ALPHABET

d	radius of the capture set, feet
f(x,y)	terrain altitude, feet
g	gravitational acceleration, feet/second^2
h	altitude, feet
H	variational Hamiltonian
J	performance index, payoff, cost function
K	weighting factor for composite performance index, $0 \leq K \leq 1$
m	helicopter mass, slugs
P	terminal constraint
$\Re$	real number
R	initial constraint
S	switching function

t	time, seconds
T	main rotor thrust, lb
V	velocity, feet/second
W	weighting factor for composite performance index
x	down-range, feet
y	cross-range, feet

GREEK

χ	heading angle on the local tangent plane, radians
ϕ	bank angle, radians
γ	flight path angle, radians
λ	costates
ν	multiplier for terminal constraint
θ	pitch angle, radians
ψ	heading angle on the inertial coordinate, radians

SUBSCRIPTS

c	clearance between helicopter and the terrain
e	evader
f	terminal time
ℓ	local coordinate system
o	initial time
p	pursuer

SUPERSCRIPTS

a	augmented
T	transpose
o	optimal

ACRONYMS

ARMCOP	A single main rotor helicopter simulation program (U.S. Army)
E-L	Euler - Lagrange
HELCOMP	A helicopter air - to - air combat simulation program

HJB	Hamilton - Jacobi - Bellman
L-C	Legendre - Clebsch
LHX	Light Helicopter eXperimental
NOE	Nap - of - the - Earth
ORP	Optimal Route Planning
P.I.	discreet Performance Index
TMAN	6 DOF helicopter simulation program (NASA Ames Research Center)
TPBVP	Two Point Boundary Value Problem
WKB	Wentzel - Kramers - Brillouin

SUMMARY

Helicopters operating in high threat areas have to fly close to the earth surface to minimize the risk of being detected by the adversaries. This report presents techniques for low altitude helicopter trajectory planning. These methods are based on optimal control theory and appear to be implementable onboard in realtime. Second order necessary conditions are obtained to provide a criterion for finding the optimal trajectory when more than one extremal passes through a given point. A second trajectory planning method incorporating a quadratic performance index is also discussed. In a later part of the thesis, trajectory planning problem is formulated as a differential game. The objective here is to synthesize optimal trajectories in the presence of an actively maneuvering adversary. Numerical methods for obtaining solutions to these problems are outlined. As an alternative to numerical method, feedback linearizing transformations are combined with the linear quadratic game results to synthesize explicit nonlinear feedback strategies for helicopter pursuit-evasion. Some of the trajectories generated from this research are evaluated on a six-degree-of-freedom helicopter simulation incorporating an advanced autopilot. The optimal trajectory planning methods presented here are also useful for autonomous land vehicle guidance.

CHAPTER I

INTRODUCTION

1.1 Introduction

Recent years have seen an increased interest in helicopter operations near the ground as evident in the literature [1-3]. In a high threat environment, helicopters have to fly close to the earth surface to minimize the risk of being detected by the enemy [4-5]. The objective here is to use terrain and surrounding objects to mask the helicopter during the mission .

Due to data processing limitations, a hierarchical system architecture is essential for nap-of-the-earth flight guidance. This concept provides a natural way of decomposing a complex control process into simpler and more manageable components. Thus, the guidance functions are divided into three levels, namely, far-field, mid-field, and near-field [6].

The far-field planning task involves off-line mission planning to generate mission way-points and goals. Mission requirements, global threat information and vehicle resources on-board are taken into account. The mid-field planning function generates the flight route using the way-points data given by the far-field planner. High resolution digital map, threat information, and vehicle limitations are included in performing real-time guidance computations. The near-field guidance function provides a least expected deviation path from the mid-field nominal path due to the vehicle dynamics limitations and

obstacles detected by on-board sensors. The focus of this report will be on the mid-field route planning problem.

Most route planning methods given in the literature [7-11] appear to use the terrain altitude and lateral deviations from a nominal trajectory as the performance index. These methods are based on the heuristic search techniques including variants of dynamic programming such as the A^*-algorithm. All these approaches employ the discretization of the terrain spatial coordinates before carrying out a systematic search for optimal trajectory. On a rough terrain, these approaches require an enormous amount of computation and storage to generate sufficiently smooth trajectories [12].

An alternative formulation for the trajectory planning is based on Pontryagin's maximum principle and was first outlined in Reference 13. State equations in this formulation include the terrain constraint, incorporated via a coordinate transformation. The performance index is a linear combination of flight time and terrain altitude. The resulting nonlinear two-point boundary value problem is then converted to a one-dimensional search process by incorporating a constant of motion and employing an adjoint-control transformation. The solution is implementable in near real time and is capable of detecting situations where more than one extremal passes through a given point. The second-order necessary condition for this problem is studied in detail. This trajectory planning method automatically accomplishes known-threat avoidance and is similar to the classical Zermelo's navigation problem [14]. In this method, the computational algorithm requires the second partial derivatives of the terrain profile to generate extremals. As a result, the terrain profile needs to be represented by quadratic or cubic splines lattices. This feature can sometimes make the extremals sensitive to the error in the terrain data.

In an alternative formulation [15], the need for second partial derivatives is eliminated by avoiding the coordinate transformation approach. The performance index in this

problem consists of a quadratic form in the terrain altitude, lateral deviation from the nominal trajectory, and heading angle. By changing the independent variable from time to down-range, the order of the problem is reduced. As in the first method, the extremals are obtained using the optimal control theory and necessary conditions are tested along the extremals. An approximate second variation test is developed for this problem using the WKB method [16]. A special case that can result in singular arcs in this trajectory planning problem is also outlined.

So far, the route planning problem for single vehicle has been discussed. As a natural extension, the guidance for two or more vehicles that cooperate or compete against each other is considered next. This results in a differential game formulation for the trajectory planning problem. Since the publication of a book by Isaacs [17] on differential games in 1965, a body of research is available on differential games with kinematic models in a plane. With such simple modeling, it is possible to obtain elegant results. The well-known homicidal chauffeur problem is an example. On the other hand, the helicopter guidance problem requires the use of a model in which the coefficients vary as a function of the vehicle position on the terrain. The method proposed in this report uses the terrain profile data to formulate a differential game between two helicopters.

In conjunction with the recent theory of nonlinear transformations, Menon [18] showed that a class of differential games with nonlinear dynamics can be transformed into the well known linear quadratic pursuit-evasion game form. Compared with the previous derivations of pursuit-evasion guidance laws which completely ignore the dynamic nonlinearities in the vehicle models, the nonlinear transformation approach continuously compensates for the vehicle nonlinearities. In the present work, this formalism is used to study a helicopter pursuit-evasion game at nap-of-the-earth flight altitudes.

Finally, in order to verify whether the trajectories generated using various planning schemes discussed in the foregoing satisfy the helicopter physical constraints, these need to be evaluated on a detailed helicopter simulation. An advanced autopilot developed by Heiges [19] together with a six-degree-of-freedom helicopter simulation is used in this investigation. The helicopter simulation was originally developed at NASA Ames Research Center for the study of Air-to-Air combat [20-21].

1.2 Contributions of the Report

In contrast with the existing literature, this report develops techniques for trajectory planning based on the Calculus of Variation. Numerical algorithms are given for the determination of optimal trajectories with various performance indices. Additionally, tests are developed for verifying the optimality of the emerging trajectories.

Methods developed in the present research will aid in constructing an integrated methodology for low altitude flight guidance of helicopters. The trajectory planning solution is also useful for autonomous surface/underwater vehicle guidance, terrain following guidance for cruise missiles and aircraft [22-24] and optimal trajectory planning for robots.

1.3 Organization of the Report

This report is organized as follows:

Chapter II gives a brief description of previous research on helicopter low-altitude flight trajectory planning and air-to-air combat. It was the work in this area that motivated the present research topic. This chapter also covers a few well-known results in optimal

control theory and differential game theory. Background on the nonlinear transformation techniques to control nonlinear systems is also presented.

Two optimal trajectory planning schemes useful for the terrain-following/terrain-avoidance guidance of helicopter are presented in Chapter III. This chapter illustrates how the nonlinear two-point boundary value problem can be solved using a one-dimensional searching method. To ensure that the extremals obtained by this approach are optimal, second-order necessary conditions are also developed in this chapter.

In Chapter IV, research on the helicopter pursuit-evasion is discussed. A backward integration method and a nonlinear transformation method are given in this chapter.

Chapter V discusses the implementation and test of the generated trajectories in a realistic six degrees of freedom helicopter simulation. The helicopter physical variables along the trajectories obtained from Chapter III are examined here.

Chapter VI evaluates the results obtained from present research. Suggestions for future work are also outlined.

Finally, the appendices contain some of the analysis used in the main body of the report. In Appendix A, the transformation from local tangent plane to inertial coordinates is derived. This transformation is employed in developing the first trajectory planning scheme (ORP #1). Various numerical conjugate point tests and their relationships are discussed in Appendix B. These tests are used to verify the optimality of the synthesized trajectories. In Appendix C, separability of the Hamiltonian and its consequence on Differential Game solutions are discussed. A necessary condition for global minimum is given in Appendix D.

All numerical results are obtained with VAX-11/750™. Contour maps are drawn by DISSPLA™ graphics routine. Algebraic equations are derived by symbolic program

MACSYMA™. Unless otherwise mentioned, British Units, i.e., pound (lb) - foot (ft) - second (sec), are the basic units used in this report.

CHAPTER II

BACKGROUND

2.1 Introduction

In this chapter, previous research on the helicopter trajectory planning problem and air-to-air combat are reviewed. An overview of Dynamic Programming used in several of these research is given in Section 2.4. This section also provides an outline on optimal control theory. Section 2.5 provides a review of several notions involved in differential games. Finally, some recent results in nonlinear transformations for feedback control are reviewed in Section 2.6.

2.2 Previous Research on Helicopter Trajectory Planning

Historically, terrain information has been used for low altitude flight guidance of deep penetration attack aircraft and cruise missiles. Since these vehicles fly a considerable time over the opponent's territory, they are vulnerable to detection by the enemy. The objective of low altitude flight guidance using terrain map is to minimize the influence of air defense threats on the mission profile [25-26]. Trajectory generated by such a guidance scheme is composed of a terrain-following path in the vertical plane. In the nap-of-the-earth guidance of helicopters, on the other hand, both vertical and lateral maneuvers are employed.

Reference 7 discusses the computation of vertical and lateral helicopter trajectories using a combination of discrete dynamic programming [27] and tree searching [28]. They considered the performance indices for the lateral and vertical planes as follows:

$$J_L = \sum_i [wD_i^2 + (h_{cl} + H_i)^2] \tag{2.1}$$

$$J_V = \sum_i (h_{cl} + H_i)^2 \tag{2.2}$$

where, w is the terrain-following/terrain-avoidance ratio, D_i the lateral deviation from reference path, H_i terrain altitude at location index i, and h_{cl} helicopter clearance altitude. Note that the two performance indices do not include control terms.

Reference 11 developed an algorithm to generate a low altitude threat penetration trajectory which minimizes the performance index:

$$J = \sum_i (D_i + C_t)\Delta t_i \tag{2.3}$$

Here, D_i is the value of the danger array at the *i*th cell, Δt_i the transition time, and C_t the cost of time. Danger arrays D_i depends on the vehicle position (x,y,h), and the heading angle χ. C_t is a coefficient including flight time and fuel. Decoupled vertical and lateral threat penetration trajectories were obtained by dynamic programming and tree search.

Reference 29 describes a three-dimensional dynamic programming approach to maximize the overall probability of survival $\mathbf{P_s}$ along any path defined by:

$$\mathbf{P_s} = \prod_{path} P_s(x,y,z,j) \tag{2.4}$$

where, $P_s(x,y,z,j)$ is the probability of survival through cell (x,y,z) in the *j*th direction to an adjacent cell. In the actual implementation, the values assigned to each cell are negative logarithms of the probabilities of survival. The problem is thereby transformed from one

of maximizing the product of survival probabilities to minimizing the sum of negative logarithmic probabilities. The probability is a function of terrain masking, fuel constraint, or time constraint.

The investigators in artificial intelligence area [10] have suggested to use the heuristic search to find a near-optimal routes for autonomous helicopter. Two of the most commonly used heuristic search techniques for finding optimal path are the branch-and-bound and the A*-algorithm, discussed in Reference 10. The branch-and-bound is an exhaustive search method similar to both depth-first and breadth-first schemes. They search all possible paths until the goal is found. A*-algorithm is the branch-and-bound search in conjunction with the dynamic programming principle to reduce computations [28].

All these approaches employ the discretization of the terrain spatial coordinates before carrying out the search for the optimal trajectory. As a result, they assume that the route consists of straight line segments. On an uneven terrain, this implies that a large number of discretization intervals will be required to generate sufficiently smooth trajectories. Unfortunately, this increase in the number of discretization intervals is accompanied by an enormous increase in computational complexity. For example, in the case of discrete dynamic programming, this is of order $\{(n+1)^2+1\}$, where n is the number of discretization intervals in one spatial direction [12]. A solution advanced by some researchers for handling this "curse of dimensionality" is the use of parallel-computing architectures [30].

This report will propose alternative trajectory planning schemes based on the Euler-Lagrange equations [12]. These approaches require a one-dimensional search to determine optimal trajectories. Further details will be discussed in Chapter III.

2.3 Previous Research on Helicopter Pursuit-Evasion

Unlike the one-sided trajectory planning problem, reported research on two-sided trajectory planning has been very sparse. A previous research [31] employed a discrete matrix game approach for generating maneuvering decisions for low altitude flying helicopter during one-on-one air combat over a hilly terrain. Each player had seven maneuvering strategies, and thus the game matrix consisted of 49 payoff elements. Each element in this matrix represented the score evaluated using a scoring function. Under the perfect information assumption, the scoring function was composed of an orientation, a relative range, a velocity, and a terrain profile. The state variables required in evaluating the scoring function were obtained by numerically integrating the equations of motion for each of the seven strategies of the participants. After numerical integration, the saddle point was searched and optimal maneuvering strategies for each player were obtained. This procedure was repeated until terminal conditions are satisfied.

According to Von Neumann and Mongenstern [32], every finite and discrete game can be cast in the matrix form. However, the dimensions of this matrix will be astronomical except for very simple problems. Additionally, the computational effort in conducting a search for the optimum can be prohibitive. R. Isaacs [17] provided the framework for obtaining solutions to continuous games with differential constraints. This will be further elaborated in Section 2.5.

In this report, the helicopter pursuit-evasion problem will be studied as two one-sided optimal control problem using differential game theory. Two different formulations will be discussed. The first one requires two-dimensional search to determine optimal strategies. Another approach using nonlinear transformation techniques demands the specification of the terminal time. Details of these approaches will be given in Chapter IV.

2.4 A Review of The Optimal Control Theory

In order to motivate subsequent development, this section will present a review of the central results from optimal control theory [12].

Given the state equations:

$$\dot{x} = f(x,u,t) \ , \qquad x(t_0) = x_0 \tag{2.5}$$

where, $x(t)$: = state vector of dimension n, $x \in X$

$u(t)$: = control function of dimension m, $u \in U$

Initial constraints:

$$R\ (x(t_0),t_0) = 0 \tag{2.6}$$

Terminal constraints:

$$P\ (x(t_t),t_f) = 0 \text{ and } t_f \text{ is free} \tag{2.7}$$

Performance Index:

$$J\ [u] = g(x(t_f),t_f) + \int_{t_0}^{t_f} L(x,u,t)\ dt \tag{2.8}$$

The optimal control problem is to pick u(t) to minimize J[u] while satisfying the state equations and the boundary constraints.

The optimal control can be obtained using Dynamic Programming [27] or Pontryagin's Minimum Principle [33]. For most problems encountered in applications, these two approaches can be shown to be equivalent [12].

2.4.1 Continuous Dynamic Programming

Define the continuous optimal return function as

$$J^{o}[x(t),t] = \min_{u \in U} J[x(t),u(t),t] \tag{2.9}$$

To simplify presentation, it is assumed here that the terminal cost is zero. Next, assuming the optimal return function to be continuous, one can write [34]

$$J^{o}[x(t),t] = \min_{u \in U} \{ \int_{t}^{t+\varepsilon} L(x,u,\tau)d\tau + \int_{t+\varepsilon}^{t_f} L(x,u,\tau)d\tau \} \tag{2.10}$$

for sufficiently small ε. If the vector functions u(τ) and L are both continuous at t, there exist an ε sufficiently small such that expression (2.10) can be approximated as:

$$J^{o}[x(t),t] = \min_{u \in U} \{ \varepsilon L(x,u,\tau) + \int_{t+\varepsilon}^{t_f} L(x,u,\tau)\,d\tau \} \tag{2.11}$$

From the definition of J^{o} the optimal return function (2.9), this amounts to

$$J^{o}[x(t),t] = \min_{u \in U} \{\varepsilon L(x,u,t) + J^{o}[x(t+\varepsilon),t+\varepsilon]\} \tag{2.12}$$

The state evolution may next be approximated by

$$x(t+\varepsilon) = x(t) + \varepsilon f(x,u,t) \tag{2.13}$$

Substituting equation (2.13) into (2.12), for sufficiently small positive ε, and retaining only the first-order terms, one has

$$J^{o}[x(t),t] = \min_{u \in U} \{\varepsilon L(x,u,t) + J^{o}[x(t)+\varepsilon f(x,u,t),t+\varepsilon]\} \qquad (2.14)$$

Taking a Taylor's series expansion of $J^{o}[x(t)+\varepsilon f(x,u,t), t+\varepsilon]$, and retaining only the first order terms,

$$J^{o}[x(t)+\varepsilon f(x,u,t),t+\varepsilon] = J^{o}[x(t),t] + \varepsilon J^{o}_{x}[x(t),t]\ f(x,u,t) + \varepsilon\, J^{o}_{t}[x(t),t] \qquad (2.15)$$

Next, substituting (2.15) into (2.14), and cancelling the $J^{o}[x(t),t]$ term and dividing by ε, one has

$$J^{o}_{t}[x(t),t] = - \min_{u \in U} \{\ L(x(t),u(t),t) + J^{o}_{x}[x(t),t]\ f(x,u,t)\} \qquad (2.16)$$

Let $u^{o}(x,t)$ denote the optimal control given x and t. This control must yield a minimum for the right hand side of equation (2.16). Thus,

$$J^{o}_{t}[x,t] = - L(x,u^{o},t) - J^{o}_{x}[x,t]\ f(x,u^{o},t) \qquad (2.17)$$

Equation (2.17) is known as the Hamilton-Jacobi-Bellman (HJB) equation. This is a first order nonlinear partial differential equation.

This equation is difficult to solve if the functions L and f are highly nonlinear. As a result, this equation is often solved using the method of characteristics. The characteristics of the HJB equation are called the Euler-Lagrange (E-L) equations [12]. The E-L equations are first order nonlinear ordinary differential equations with prescribed boundary conditions. In the following we will indicate the derivation of E-L equations using the HJB equation.

Differentiating the expression (2.17) partially with respect to x, and noting that the control variables are independent of the state variables results in the expression

$$J^{\circ}_{tx}[x,t] = - L_x(x,u^{\circ},t) - J^{\circ}_{xx}[x,t]\ f(x,u^{\circ},t) - f_x(x,u^{\circ},t)\ J^{\circ}_x[x,t] \tag{2.18}$$

Now, the total derivative to $J^{\circ}_x[x,t]$ is given by

$$\frac{dJ^{\circ}_x[x,t]}{dt} = J^{\circ}_{xt}[x,t] + J^{\circ}_{xx}[x,t]f(x,u^{\circ},t) \tag{2.19}$$

Substituting (2.18) into (2.19), one has

$$\frac{dJ^{\circ}_x[x,t]}{dt} = - L_x(x,\ u^{\circ},\ t) -\ f_x(x,\ u^{\circ},\ t)\ J^{\circ}_x[x,t] \tag{2.20}$$

This set of first-order ordinary differential equations for $J_x{}^{\circ}[x,t]$ can be solved if x and u° were known for all t and initial conditions for $J_x{}^{\circ}[x,t]$ were given. $J_x{}^{\circ}[x,t]$ are called the costates of the systems, often denoted by the variable λ.

2.4.2 Pontryagin's Minimum Principle

Introducing a new variable called the Hamiltonian [12],

$$H\ (x,u,\lambda,t) = L\ (x,u,t) + \lambda^{T}\ f\ (x,u,t) \tag{2.21}$$

The Euler-Lagrange equations (2.5), (2.20) can be written as

$$\dot{x} = f(x,u,t), \tag{2.22a}$$

$$\dot{\lambda} = - H_x \tag{2.22b}$$

The fact that optimal control u has to minimize the quantities within braces in (2.16) leads to the so called optimality condition

$$H_u = 0 \tag{2.23}$$

Equations (2.22) must satisfy the given boundary conditions. For additional details on this problem, see Reference 12.

While the satisfaction of HJB is sufficient for optimality, additional conditions must be imposed while solving the optimal control problem using the E-L equations. In this case, the optimal controls emerging from (2.22), (2.23) should additionally satisfy the following condition [12]:

(i) Legendre-Clebsch condition

$$H_{uu} \geq 0 \tag{2.24}$$

(ii) Weierstrass condition

$$\delta H\ (x, \lambda^{o}, u^{o}, u, t) \geq 0 \tag{2.25}$$

(iii) Jacobi condition

Nonexistence of conjugate point in (t_0, t_f)

Conditions (i) and (iii) are necessary for weak local minimum, while condition (ii) is necessary for strong local minimum. Strengthening conditions (i) and (ii) and closing the interval in condition (iii) constitute the sufficient condition [12]. In some situations, normality condition [12] has to be verified before testing the conditions (i) - (iii).

Additional conditions can be obtained using various combinations of these necessary conditions [35].

2.5 A Review of Differential Games

If optimal control theory briefly reviewed in the previous section can be considered a theory for one-sided control problems, differential game theory may be identified as a theory for two-sided control problems. It has been shown [36] that the problem definitions and solution methods used in optimal control theory can be extended into the game theory.

The theory of differential games is a subject concerned with the optimization of dynamic systems involving two or more players with conflicting interests. The study of differential games was initiated by Isaacs in 1954. In 1965, Isaacs published a book which details various aspects of differential games [17]. In 1957, Berkovitz and Fleming [37] solved a simple differential game using the calculus of variations. In a later research, Berkovitz treated a wider class of differential games using the calculus of variations [38]. Friedman's book [39] discusses the necessary conditions in differential games in terms of the more familiar optimal control theory notation.

The aforementioned differential games mostly dealt with problems of the pursuit-evasion type having the zero-sum property, i.e., one player's loss being the other player's gain. Dropping the zero-sum hypothesis adds both conceptual and analytic complexity, but it may extend the utility of the theory of differential games to a much wider class of applications. Two typical non-zero-sum games are the Nash game and Stackelberg game, in which each participant has its own performance criterion.

Assuming that the players have perfect information of the current states and that their respective roles are determined before the game begins, a differential game may be stated as follows:

Given differential constraints:

$$\dot{x} = f(x,\phi,\psi,t), \qquad x(t_0)=x_0 \tag{2.26}$$

where, $x(t)$: = state vector of dimension n, $x \in X$

$\phi(t)$: = control of Player 1 of dimension ℓ, $\phi \in \Phi$

$\psi(t)$: = control of Player 2 of dimension m, $\psi \in \Psi$

Initial constraints:

$$R(x(t_0),t_0) = 0 \tag{2.27}$$

and terminal constraints:

$$P(x(t_f),t_f) = 0,\ t_f \text{ is free} \tag{2.28}$$

The terminal constraints define the stopping condition for the game. For example, if the participants have a "capture set", the game terminates at the instant the adversary enters the capture set.

The performance index or payoff for the *i* th player may be defined as

$$J_i[x,\phi,\psi,t] = g_i(x(t_f),t_f) + \int_{t_0}^{t_f} L_i(x,\phi,\psi,t)\, dt \tag{2.29}$$

Each player involved in the game attempts to optimize its own performance index with due attention to the other player's state-control variable evolution. Once the differential constraints, initial and terminal constraints and the performance index are defined, one may describe three different game scenarios.

2.5.1 Nash Non-Zero-Sum Game

If an optimal solution exists, optimal closed loop control pair (ϕ^o, ψ^o) must satisfy the Nash inequalities condition [40]:

$$J_1(\phi^o,\psi^o) \leq J_1(\phi^o,\psi), \quad \forall\, \psi \in \Psi \tag{2.30}$$

$$J_2(\phi^o,\psi^o) \leq J_2(\phi,\psi^o), \quad \forall\, \phi \in \Phi \tag{2.31}$$

Inequalities (2.30) and (2.31) imply that optimal strategies for each player should yield the smallest cost for individual participants. Any deviation from the optimal strategy will yield a higher cost.

2.5.2 Stackelberg Non-Zero-Sum Game

In this game, one assumes that the second player is the leader while the first player is the follower. As a result, the first player is operating a purely reactive fashion. If there exists a mapping $M:\Psi \rightarrow \Phi$, and the following conditions are satisfied, then the pair $(\phi^*, \psi^*) \in \Phi \times \Psi$ is called a Stakelberg strategy pair with Player 2 as a leader and Player 1 as follower [41]:

$$J_1(M\psi, \psi) \leq J_1(\phi, \psi) \tag{2.32}$$

$$J_2(\phi^*, \psi^*) \leq J_2(M\psi,\psi) \tag{2.33}$$

$$\phi^* = M\,\psi^* \tag{2.34}$$

In other words, the Stackelberg strategy is the optimal strategy for the leader when the follower reacts by playing optimally. An interesting property relating the Nash and Stakelberg strategies can be derived from equations (2.30) - (2.34) as follows [41]:

$$J_2(\phi^*, \psi^*) \leq J_2(\phi^o, \psi^o) \tag{2.35}$$

which means that the leader in the Stackelberg solution achieves at least as good a cost function as the corresponding Nash solution.

2.5.3 Zero-Sum Game

Zero-sum games result when the two decision-makers are adversaries. One decision-maker's loss is the other decision-maker's gain. In this case, the equilibrium solution has the property that

$$J_1 = -J_2 = J \tag{2.36}$$

The above Nash inequalities criterion (2.30) and (2.31) may be reduced to

$$J\,[x,\phi^o,\psi,t] \leq J\,[x,\phi^o,\psi^o,t] \leq J\,[x,\phi,\psi^o,t] \tag{2.37}$$

where, $J\,[x,\phi^o,\psi^o,t] \equiv V\,[x_0,t_0]$ is called the value of the game. In such a differential game both players have the same performance index, with the first player minimizing it while the second player attempts to maximize. Equation (2.37) suggests that if the minimizing player deviates from his optimal strategy, the game will have a higher game value. Alternatively, if maximizing player deviates from the optimal strategy, the game will have a lower value than if the two were employing optimal strategies. This is the well-known saddle point condition in the game theory [32]. A similar saddle point condition may also be derived from the Stackelberg inequality conditions.

Introducing the variational Hamiltonian

$$H\,(x,\phi,\psi,\lambda,t) = L + \lambda^T f \tag{2.38}$$

and define the terminal conditions as:

$$Q(x(t_f),t_f) = g(x(t_f),t_f) + \nu^T P\,(x(t_f),t_f) \tag{2.39}$$

Since $\dot{x} = f(x,u,t)$, one may write the performance index as

$$J^a = Q(x(t_f),t_f) + \int_{t_0}^{t_f} (H - \lambda^T \dot{x})\ dt \tag{2.40}$$

Since the control terms appear only in the function H, the saddle point condition (2.37) can be written as [42].

$$\int_{t_0}^{t} H(x,\phi^o,\psi,\lambda,t)\ dt \le \int_{t_0}^{t} H(x,\phi^o,\psi^o,\lambda,t)\ dt \le \int_{t_0}^{t} H(x,\phi,\psi^o,\lambda,t)\ dt \tag{2.41}$$

If for all t, functions L and f are continuous, the inequality (2.41) can be changed to the pointwise form [42] by using the principle of optimality which requires that at every instant controls should be chosen to make system optimal:

$$H(x,\phi^o,\psi,\lambda,t) \le H(x,\phi^o,\psi^o,\lambda,t) \le H(x,\phi,\psi^o,\lambda,t) \tag{2.42}$$

Equation (2.42) is a sufficient condition for the inequality (2.41) and a differential game version of Weierstrass condition in the optimal control.

Generally, by the order of action it is known [35] that

$$\max_{\psi}\ \min_{\phi}\ H(x,\phi,\psi,\lambda,t) = \min_{\phi}\ \max_{\psi}\ H(x,\phi,\psi,\lambda,t) \tag{2.43}$$

Additional conditions sufficient for satisfying the above equation (2.43) as equality for a special case was given by Von Neumann and Morgenstern [32]. This is known in the literature as the Isaacs principle.

If H is separable in ϕ and ψ, i.e.,

$$f(x, \phi, \psi, t) = f_1(x, \phi, t) + f_2(x, \psi, t) \tag{2.44}$$

$$L(x,\phi,\psi,t) = L_1(x, \phi, t) + L_2(x, \psi, t) \tag{2.45}$$

it may be shown [39] that

$$\max_{\psi} \min_{\phi} H(x,\phi,\psi,\lambda,t) = \min_{\phi} \max_{\psi} H(x,\phi,\psi,\lambda,t) = H(x,\phi^{o},\psi^{o},\lambda,t) \tag{2.46}$$

Since the stationarity conditions (first-order necessary conditions) are the same for minimization or maximization, the differential game can be defined as a two-sided optimal control problem with coupling appearing via the transversality conditions. In this case, the necessary conditions for $\phi(t)$ and $\psi(t)$ to be optimal are:

1) Euler-Lagrange equations

$$\dot{x} = f(x,\phi,\psi,t) \tag{2.47}$$

$$\dot{\lambda} = - H_x \tag{2.48}$$

2) Transversality conditions at t_f

$$\lambda^{T}(t_f) = Q_x(x(t_f),t_f) \tag{2.49}$$

$$P\,(x(t_f),t_f) = 0 \tag{2.50}$$

$$H(t_f) = 0 \text{ , } t_f \text{ is free} \tag{2.51}$$

3) Optimality conditions

$$H_\phi = 0 \tag{2.52}$$

$$H_\psi = 0 \tag{2.53}$$

4) Isaacs principle

$$\max_{\psi} \min_{\phi} H(x, \phi, \psi, \lambda, t) = \min_{\phi} \max_{\psi} H(x, \phi, \psi, \lambda, t) \tag{2.54}$$

It may be shown that this solution can be also obtained by solving a partial differential equation similar to the HJB equation [39]. In the differential game context, this PDE is called the Hamilton-Jacobi-Isaacs equation for the optimal J [39], viz,

$$J^o_t(x,t) = - \min_{\phi} \max_{\psi} H(x, \phi, \psi, J^o_x, t) \tag{2.55}$$

$$J^o(x(t_f),t_f) = g(x(t_f),t_f) \tag{2.56}$$

The similarity of the differential game and optimal control is apparent from the foregoing. However, it is important to note that certain differences exist between optimal control problems and differential games [43]. First, although feedback control is not essential in the optimal control problems it becomes the central requirement in differential games. Secondly, the solution is characterized by regions where solutions exist and where they do not. Moreover, verification of the second-order necessary conditions, while not routinely employed in optimal control, becomes mandatory in differential game solutions.

2.6 Transformation of Nonlinear Systems

Even though differential game theory has several potential applications in economics, military, and engineering, it has not been employed to the same degree as optimal control theory. However, linear-quadratic differential games have received considerable interest in the differential games literature [40, 41, 43, 44]. These games have been important in studying the local behavior of certain nonlinear differential games. Recently, it has been shown that a class of nonlinear differential games may be solved in closed form using transformations [18]. In that work it was shown that nonlinear transformation techniques are useful for implementing linear-quadratic differential game solutions in nonlinear differential games.

2.6.1 Kronecker Indices and Brunovsky Form

Before tackling the nonlinear system control problem, a brief review of linear system theory in the state space will be given. For a given multivariable system

$$\dot{x}(t) = A\,x(t) + B\,u(t)\,,\quad x \in \Re^n,\ u \in \Re^m \tag{2.57}$$

the first step in designing control laws is to test for controllability. This involves the computation of a controllability matrix C{A, B} [45] as

$$\left\{b_1,\ Ab_1,\ A^2b_1,\ \ldots.\ A^{k_1-1}b_1,\ b_2\,,\ Ab_2,\ \ldots\ldots,A^{k_m-1}b_m\right\} \tag{2.58}$$

For the system to be controllable, this matrix must have a rank n [45]. Next, this matrix may be normalized to determine a transformation matrix

$$T = \{e_{11},\ e_{12},\ \ldots.\ e_{1k_1},\ e_{21},\ \ldots..\ ,e_{m1},\ ..\ e_{mk_m}\} \tag{2.59}$$

Defining a new set of state variable x = Ty and substituting in (2.57), one has

$$\dot{y} = T^{-1}AT\, y + T^{-1}B\, u \tag{2.60}$$

or,

$$\dot{y} = A_c\, y + B_c\, u \tag{2.61}$$

with

$$A_c = T^{-1}AT \quad , \; B_c = T^{-1}B$$

Under this transformation the matrices A_c and B_c will have mostly zero or one entries together with a specific structure. For example, n=10, m=3, k_1=3, k_2=3, k_3=4

$$A_c = \begin{bmatrix} \bullet & \bullet & \bullet & \bullet & \bullet & \bullet & \bullet & \bullet & \bullet & \bullet \\ 1 & 0 & 0 & 0 & 0 & 0 & 0 & 0 & 0 & 0 \\ 0 & 1 & 0 & 0 & 0 & 0 & 0 & 0 & 0 & 0 \\ \bullet & \bullet & \bullet & \bullet & \bullet & \bullet & \bullet & \bullet & \bullet & \bullet \\ 0 & 0 & 0 & 1 & 0 & 0 & 0 & 0 & 0 & 0 \\ 0 & 0 & 0 & 0 & 1 & 0 & 0 & 0 & 0 & 0 \\ \bullet & \bullet & \bullet & \bullet & \bullet & \bullet & \bullet & \bullet & \bullet & \bullet \\ 0 & 0 & 0 & 0 & 0 & 1 & 0 & 0 & 0 & 0 \\ 0 & 0 & 0 & 0 & 0 & 0 & 1 & 0 & 0 & 0 \\ 0 & 0 & 0 & 0 & 0 & 0 & 0 & 1 & 0 & 0 \end{bmatrix} \qquad B_c = \begin{bmatrix} 1 & \bullet & \bullet \\ 0 & 0 & 0 \\ 0 & 0 & 0 \\ 0 & 1 & \bullet \\ 0 & 0 & 0 \\ 0 & 0 & 0 \\ 0 & 0 & 1 \\ 0 & 0 & 0 \\ 0 & 0 & 0 \\ 0 & 0 & 0 \end{bmatrix} \tag{2.62}$$

where symbol • means any numeric entry. In this controller canonical form, the canonical invariant parameters are

$$\{k_i, \alpha_j\} \tag{2.63}$$

where, k_i is called the controllability indices, or Kronecker indices and α_j eigenvalues of system.

Using control law

$$u(t) = G\, v(t) - K\, y(t) \tag{2.64}$$

the system (2.61) becomes

$$\dot{y} = (A_c - B_c K)\, y + B_c G\, v \tag{2.65}$$

By suitable choice of input transformation G and state feedback gain K, the entries marked • in the {1st, (k_1+1)st, (k_1+k_2+1)st,....} rows of A_c and B_c can be zeroed out to get the special controller form as follows:

$$\dot{y} = A^{\bullet}\, y + B^{\bullet}\, v \tag{2.66}$$

For the aforementioned example (2.62),

$$A^{*} = \begin{bmatrix} 0 & 0 & 0 & 0 & 0 & 0 & 0 & 0 & 0 & 0 \\ 1 & 0 & 0 & 0 & 0 & 0 & 0 & 0 & 0 & 0 \\ 0 & 1 & 0 & 0 & 0 & 0 & 0 & 0 & 0 & 0 \\ 0 & 0 & 0 & 0 & 0 & 0 & 0 & 0 & 0 & 0 \\ 0 & 0 & 0 & 1 & 0 & 0 & 0 & 0 & 0 & 0 \\ 0 & 0 & 0 & 0 & 1 & 0 & 0 & 0 & 0 & 0 \\ 0 & 0 & 0 & 0 & 0 & 0 & 0 & 0 & 0 & 0 \\ 0 & 0 & 0 & 0 & 0 & 0 & 1 & 0 & 0 & 0 \\ 0 & 0 & 0 & 0 & 0 & 0 & 0 & 1 & 0 & 0 \\ 0 & 0 & 0 & 0 & 0 & 0 & 0 & 0 & 1 & 0 \end{bmatrix} \quad B^{*} = \begin{bmatrix} 1 & 0 & 0 \\ 0 & 0 & 0 \\ 0 & 0 & 0 \\ 0 & 1 & 0 \\ 0 & 0 & 0 \\ 0 & 0 & 0 \\ 0 & 0 & 1 \\ 0 & 0 & 0 \\ 0 & 0 & 0 \\ 0 & 0 & 0 \end{bmatrix} \tag{2.67}$$

As we can see in (2.67), all eigenvalues of system can be zeroed out. The only remaining invariants are the Kronecker indices. This special controller canonical form is called the Brunovsky canonical form [45] and exhibits a parallel array of m decoupled subsystems of dynamic order k_1, k_2, k_3,...., k_m [46].

2.6.2 Nonlinear Transformation

In the differential geometry, the Brunovsky canonical form can be viewed as a group acting on the space of linear systems. Each subsystem forms a single orbit under the group action and new system pair $\{A^{*}, B^{*}\}$ are cyclic (single-companion-matrix). Such differential geometric concepts in linear control theory have been extended into nonlinear

systems with control variables appearing linearly in the dynamics by Krener [47] and Brockett [48]. An infinitesimal group theory and tangential transformations for nonlinear differential equations studied by Marius Sophus Lie [49] forms the basis for transforming a nonlinear system to linear system. Compared with the usual linearization using a Taylor series expansion about a fixed equilibrium point, local tangential transformations expand Taylor series continuously along the trajectory. Thus, the approximation, like a turtle, carries its convergence house with it [50].

Consider the nonlinear system

$$\dot{x} = f(x) + \sum_{i=1}^{m} g_i(x)u_i(t) \tag{2.68}$$

where x, f(x), $g_i(x)$ are n vectors with the hypothesis that f(0) = 0, causality condition, and u are the m control variables. This system may be transformed to Brunovsky's canonical form using two distinct approaches. Each of these are discussed below.

2.6.2.1 Hunt & Su's Approach

References 51 and 52 showed that the transformation $T = (T_1, T_2, ..., T_n, T_{n+1}, ..., T_{n+m})$ is required to have the following properties

(i) $T(0) = 0$.

(ii) $T_1, T_2, ..., T_n$ are functions of $x_1, x_2, ..., x_n$.

(iii) $T_{n+1}, T_{n+2}, ..., T_{n+m}$, are functions of $x_1, x_2, ..., x_n, u_1, u_2, ..., u_m$.

(iv) T maps the open set U of $\Re^n$ into $\Re^n$ with a nonsingular Jacobian matrix.

(v) $T_1, T_2, ..., T_n$ are the state variables and $T_{n+1}, T_{n+2}, ..., T_{n+m}$ are the controls for a linear time-invariant system in the Brunovsky form.

Reference 53 gives necessary and sufficient conditions to map to the Brunovsky form with m Kronecker indices $\kappa_1, \kappa_2, ..., \kappa_m$. Because the Lie bracket operation on pairs of

vectors keeps invariant characteristics independent of the choice of coordinate systems used, introduce the Lie brackets

$$[f,g] = \frac{\partial g}{\partial x} f - \frac{\partial f}{\partial x} g \tag{2.69}$$

where $\partial g/\partial x$ and $\partial f/\partial x$ are $n \times n$ Jacobian matrix. One may define an alternative notation to simplify the analysis. Thus, let

$$[f,g] = (ad^1 f,g) \tag{2.70}$$

Successive Lie Brackets can then be expressed as

$$\begin{aligned} g &= (ad^0 f,g) \\ [f,g] &= (ad^1 f,g) \\ [f,[f,g]] &= (ad^2 f,g) \\ [f,(ad^2 f,g)] &= (ad^3 f,g) \\ [f,(ad^{n-1} f,g)] &= (ad^n f,g) \end{aligned} \tag{2.71}$$

The transformation $T = (T_1, T_2, ..., T_n, T_{n+1}, ..., T_{n+m})$ exists if and only if

(i) the set $C = \{(ad^0 f,g_1), (ad^1 f,g_1), ..., (ad^{\kappa_1-1} f,g_1), (ad^0 f,g_2), (ad^1 f,g_2), ..., (ad^{\kappa_2-1} f,g_2), ..., (ad^0 f,g_m), (ad^1 f,g_m), ..., (ad^{\kappa_m-1} f,g_m)\}$ spans R^n about the origin.

(ii) the sets $C_j = \{(ad^0 f,g_1), (ad^1 f,g_1), ..., (ad^{\kappa_j-2} f,g_1), (ad^0 f,g_2), (ad^1 f,g_2), ..., (ad^{\kappa_j-2} f,g_2), ..., (ad^0 f,g_m), (ad^1 f,g_m), ..., (ad^{\kappa_j-2} f,g_m)\}$ are involute for $j = 1, 2, ..., m$.

(iii) the span of each C_j is equal to the span of $C_j \cap C$.

By definition, a linearly independent set of vector fields $\{x_1, x_2, ..., x_n\}$ is *involute* if and only if there are scalar functions α_{ijk} such that

$$[x_i, x_j] = \sum_{k=1}^{n} \alpha_{ijk} x_k \quad \text{for all } i,j,k \tag{2.72}$$

2.6.2.2 Meyer's Approach

This approach is more intuitive. In this technique, the states to be controlled are successively differentiated until control terms appear in the equations. Various steps during these differentiations form the mapping.

2.6.2.3 Comparison of Two Approaches

Although Hunt and Su's approach is more systematic than Meyer's, it is nearly impossible to solve partial differential equations for T-transformations except in very simple problems. Meyer's approach is a special case of Hunt and Su's approach.

If system equations are derived by the classical dynamics with forces and moments as control variables, then control terms will appear in the second-order kinematic equations. In this case, Meyer's approach can be easily implemented and the transformed system is always a double integrator system. This technique has been used in Robotics for several years and called the Computed Torque Method.

For comparisons, a simple example is provided by the problem of a vertically moving vehicle of unit mass which has thrust u and drag being proportional to the square of the speed. The equation of motion can be written

$$\ddot{x} = -G - K\dot{x}^2 + u \tag{2.73}$$

with G denoting gravity. In state variable form, the system can be expressed as follows:

$$\dot{x}_1 = x_2 \tag{2.74}$$

$$\dot{x}_2 = - G - Kx_2^2 + u \tag{2.75}$$

In the standard notation (2.68), it can be expressed as follows:

$$f = \begin{bmatrix} x_2 \\ - G - Kx_2^2 \end{bmatrix} \qquad g = \begin{bmatrix} 0 \\ 1 \end{bmatrix} \tag{2.76}$$

First, consider Hunt and Su's Method. The necessary and sufficient conditions are that rank {g, [f,g]} =2 and that {g, [f,g]} be involute. It is easy to check that

$$[f,g] = 0 - \begin{bmatrix} 0 & 1 \\ 0 & - 2Kx_2 \end{bmatrix} \begin{bmatrix} 0 \\ 1 \end{bmatrix} = - \begin{bmatrix} 1 \\ - 2Kx_2 \end{bmatrix} \tag{2.77}$$

$$|g, [f,g]| = \begin{vmatrix} 0 & - 1 \\ 1 & 2Kx_2 \end{vmatrix} = 1 \neq 0 \tag{2.78}$$

which has rank 2 and the vector field {g, $ad_f(g)$} is involute. Then, the method begins with writing a Brunovsky form

$$\begin{bmatrix} \dot{y}_1 \\ \dot{y}_2 \end{bmatrix} = \begin{bmatrix} 0 & 1 \\ 0 & 0 \end{bmatrix} \begin{bmatrix} y_1 \\ y_2 \end{bmatrix} + \begin{bmatrix} 0 \\ 1 \end{bmatrix} v \tag{2.79}$$

where

$$y_1 = T_1(x_1,x_2) \tag{2.80}$$

$$y_2 = T_2(x_1,x_2) \tag{2.81}$$

$$v = T_3(x_1,x_2,u) \tag{2.82}$$

From Brunovsky form,

$$\dot{y}_1 = \dot{T}_1(x_1,x_2) = \frac{\partial T_1}{\partial x_1}\dot{x}_1 + \frac{\partial T_1}{\partial x_2}\dot{x}_2 = <dT_1,f> + <dT_1,g>u = T_2(x_1,x_2) \quad (2.83)$$

$$\dot{y}_2 = \dot{T}_2(x_1,x_2) = \frac{\partial T_2}{\partial x_1}\dot{x}_1 + \frac{\partial T_2}{\partial x_2}\dot{x}_2 = <dT_2,f> + <dT_2,g>u = T_3(x_1,x_2,u) \quad (2.84)$$

with

$$<dT, f> = \frac{\partial T}{\partial x_1} f_1 + \frac{\partial T}{\partial x_2} f_2 \quad (2.85)$$

From (2.83) and (2.84), one has

$$<dT_1, f> = T_2, \ <dT_1, g> = 0 \quad (2.86)$$

$$<dT_2,g> \neq 0 \quad (2.87)$$

Using Frobenius Theorem [54], i.e.,

$$<dh,[f,g]> = <d<dh,g>,f> - <d<dh,f>,g> \quad (2.88)$$

one can get a following relation

$$<dT_1,[f,g]> = <d<dT_1,g>,f> - <d<dT_1,f>,g> = 0 - <dT_2,g> \neq 0 \quad (2.89)$$

Therefore, from (2.86) and (2.89)

$$\frac{\partial T_1}{\partial x_2} = 0 \quad (2.90)$$

$$<dT_1,[f,g]> = -\frac{\partial T_1}{\partial x_1} \neq 0 \quad (2.91)$$

The simplest solution is

$$y_1 = T_1 = x_1 \quad (2.92)$$

and from (2.86)

$$y_2 = T_2 = <dT_1,f> = x_2 \tag{2.93}$$

The feedback linearization control u can be obtained from (2.84) as follows:

$$u = \frac{v - <dT_2,f>}{<dT_2,g>} = \frac{v + G + Kx_2^2}{1} = v + G + Kx_2^2 \tag{2.94}$$

Second, consider Meyer's approach. Since the motion is single degree of motion, change coordinate by setting

$$Y = x \tag{2.95}$$

After differentiating until control term u appears, the system can be expressed as follows:

$$\dot{Y} = \dot{x} \tag{2.96}$$

$$\ddot{Y} = \ddot{x}_2 = - G - Kx_2^2 + u \tag{2.97}$$

Define

$$\ddot{Y} = v \tag{2.98}$$

The Brunovsky controller form is

$$\begin{bmatrix} \dot{y}_1 \\ \dot{y}_2 \end{bmatrix} = \begin{bmatrix} 0 & 1 \\ 0 & 0 \end{bmatrix} \begin{bmatrix} y_1 \\ y_2 \end{bmatrix} + \begin{bmatrix} 0 \\ 1 \end{bmatrix} v \tag{2.99}$$

with the feedback linearization control

$$u = v + G + Kx_2^2 \tag{2.100}$$

2.6.2.4 Applications

References 55, 56, and 57 designed an automatic flight controller for UH-1H helicopter applying nonlinear transformation techniques and showed that the controller exhibits good performance in all flight modes. As discussed in previous section, nonlinear transformation technique based on Meyer approach needs to successively differentiate the controlled states to get transformation map from nonlinear system to linear system. Meyer presented a numerical approach for calculating these derivatives. A successive numerical differentiation, however, requires formidable calculation, with attending numerical difficulties.

To reduce the amount of computations, Menon [58] introduced singular perturbation technique to simplify the nonlinear mapping for a flight test trajectory controller of high performance airplane. The slow time scale controller follows path command and generates steady state values for the body attitude. The fast time scale controller is designed to track the commanded values for the body attitude. In Reference 18, the nonlinear transformations have been used to derive pursuit-evasion guidance laws for high performance aircraft.

Heiges [59] applied the above mentioned techniques to design a helicopter trajectory controller and implemented it on the TMAN program. This controller has demonstrated excellent performance in various tactical flight modes.

CHAPTER III

TRAJECTORY PLANNING AS A ONE-SIDED OPTIMAL CONTROL PROBLEM

3.1 Introduction

This chapter discusses the problem formulation and optimal trajectory synthesis using two different performance indices. Candidate trajectories are generated and their optimality is tested using second-variation analysis. Numerical effort involved in the computations are analyzed.

For the first Optimal Route Planning problem, the terrain constraint is embedded into state equations via a coordinate transformation. The performance index is a linear combination of flight time and terrain altitude. In this problem, the computational algorithm requires the first and second partial derivatives of the terrain profile.

The second Optimal Route Planning problem uses a performance index consisting of a quadratic form in the terrain altitude, lateral deviation from the nominal trajectory, and heading angle. By changing the independent variable from time to down-range, the order of the problem is reduced. Each of these trajectory planning schemes will be discussed in greater detail in the ensuing.

3.2 Optimal Route Planning Problem No.1

3.2.1 Problem Formulation

A kinematic model of the helicopter will be employed in the ensuing analysis. Let the terrain profile be specified by a function

$$h_t = f(x,y) \tag{3.1}$$

where h_t is the altitude above a preselected datum at any specified position (x,y), x and y being the down-range and cross-range measured in a chosen inertial frame. It is assumed here that $h_t > 0$ and that the terrain f(x,y) has continuous first and second partial derivatives. This fact is important to ensure that the trajectories emerging from this optimal trajectory planning problem are implementable. Additionally, this is consistent with the proposed cubic spline parameterization of the digital terrain data. While executing nap-of-the-earth flight, the helicopter altitude motion will follow the terrain profile (3.1) with a specified altitude clearance. As a result, the helicopter altitude at any location (x,y) is given by the equation

$$h = f(x,y) + h_c \tag{3.2}$$

In (3.2), h is the helicopter altitude and h_c is the specified terrain clearance. For NOE flight, the clearance is between 5 and 120 feet [1].

A sample terrain profile with the x, y, h coordinate system is shown in Figure 3.1. The local coordinate system x_ℓ, y_ℓ, z_ℓ used in subsequent analysis is also defined in this figure. This moving coordinate system has its origin on the terrain surface at the current x, y position with x_ℓ-y_ℓ plane being the tangent plane. The principal direction of this system is along the intersection of the x_ℓ-y_ℓ plane with the x-h plane. Accordingly, z_ℓ points in the

direction of the normal vector to the local tangent plane. The transformation of vectorial quantities from one system to the other can be accomplished using the terrain gradients: see Appendix A for details. Since the helicopter is constrained to move on the surface defined by equation (3.2), the velocity vector lies in the instantaneous x_ℓ-y_ℓ plane, with the angle χ defining its orientation on this plane. The helicopter velocity components in the local frame can be resolved as:

$$\dot{x}_\ell = V \cos \chi \tag{3.3}$$

$$\dot{y}_\ell = V \sin \chi \tag{3.4}$$

The local heading angle χ and the airspeed V are assumed to be the control variables in the present trajectory planning problem.

Note that it is important to include velocity as a control variable in the present problem to ensure hodograph convexity required for the existence of optimal controls [60]. In order to ensure that the control emerging from this formulation are implementable, the helicopter speed is next bounded as

$$0 < V_{min} \leq V \leq V_{max} \tag{3.5}$$

Because a simple kinematic system is considered here, V_{max} corresponds to the speed at which sufficient excess power is available for avoiding unknown obstacles.

The velocity components (3.3) and (3.4) may next be transformed to the down-range, cross-range, altitude frame using the relations

$$\dot{x} = \frac{V \cos \chi}{\sqrt{1+f_x^2}} + \frac{V f_x f_y \sin \chi}{\sqrt{1+f_x^2}\sqrt{1+f_x^2+f_y^2}} \tag{3.6}$$

$$\dot{y} = \frac{-V\sqrt{1+f_x^2}\sin\chi}{\sqrt{1+f_x^2+f_y^2}} \tag{3.7}$$

The altitude rate on the terrain is given by:

$$\dot{h} = f_x \dot{x} + f_y \dot{y} \tag{3.8}$$

These relations are derived in Appendix A. In the expressions (3.6)-(3.8), f_x and f_y are local terrain gradients, assumed to be calculated from the given terrain profile (3.1).
In equations (3.6) and (3.7), the quantity $1/\sqrt{1+f_x^2+f_y^2}$ denotes the cosine of the angle between the vertical z-axis in the inertial coordinate system and the direction of the normal in the local tangent plane. And the quantity $1/\sqrt{1+f_x^2}$ denotes the cosine of angle between the down-range x-axis in the inertial coordinate system and the x_l axis in the local tangent plane.

It is sometimes desirable to include ambient winds in the trajectory planning problem. If the winds aloft along down-range and cross-range directions are given by

$$u = Q(x,y), \quad v = R(x,y) \tag{3.9}$$

these may be added to the right-hand side of (3.6) and (3.7) to obtain the equations of motion as

$$\dot{x} = \frac{V\cos\chi}{\sqrt{1+f_x^2}} + \frac{V f_x f_y \sin\chi}{\sqrt{1+f_x^2}\sqrt{1+f_x^2+f_y^2}} + u \tag{3.10}$$

$$\dot{y} = \frac{-V\sqrt{1+f_x^2}\sin\chi}{\sqrt{1+f_x^2+f_y^2}} + v \tag{3.11}$$

The equations of motion (3.8), (3.10), (3.11) may be used whenever the helicopter is flying in a terrain-following/terrain-avoidance mode.

Known threats and obstacles may be incorporated in the trajectory planning problem by defining threat overlays of the form

$$\Delta h = P(x,y) \tag{3.12}$$

and adding them to the basic terrain profile given by equation (3.1). The composite profile may then be used to define the equations of motion (3.10) and (3.11). In that case, the resulting trajectories will exhibit automatic threat and obstacle avoidance characteristics.

Additionally, it is possible to consider a formulation in which the specific energy of the helicopter is maintained constant. This will occur whenever the throttle is set to maintain thrust equal to drag while executing the nap-of-the-earth flight. In this case, the airspeed will depend on the terrain profile as:

$$V = \sqrt{2g\,[E - f(x,y) - h_c]} \tag{3.13}$$

In (3.13), g is the acceleration due to gravity and $E = h + V^2/2g$ is the specific energy.

3.2.2 Optimal Route Planning

The performance index considered in this problem is a linear combination of flight time and a terrain masking function. Following the existing literature [7], trajectory masking will be assumed to be accomplished if an integral proportional to the helicopter altitude is minimized. Admittedly, this masking function is crude since it is based on the contention that depressed terrain tends to provide a better masking. If improved terrain masking functions given as a function of down-range x and cross-range y were available, they can be included in the following analysis without difficulty. For simplicity, in all that follows,

the terrain masking will be assumed to be accomplished if the integral of helicopter altitude is minimized. A relative weighting factor is next introduced between the flight time and the terrain masking function to control the trade-off between these two, often conflicting requirements. Thus, a composite performance index of the form

$$J = \int_0^{t_f} [\ (1-K) + K\, f\,(x,y)\ ]\ dt \tag{3.14}$$

with

$$0 \leq K \leq 1 \tag{3.15}$$

will be used in the following.

The initial conditions

$$x(t_0) = x_0,\ y(t_0) = y_0 : \text{given} \tag{3.16}$$

and the terminal conditions

$$x(t_f) = x_f,\ y(t_f) = y_f : \text{given} \tag{3.17}$$

The variational Hamiltonian [12] may next be formed by adjoining the differential constraints (3.6), (3.7) to the performance index (3.14) to yield:

$$H = 1 - K + K\, f(x,y) + \lambda_x \left(\frac{V\cos\chi}{\sqrt{1+f_x^2}} + \frac{V\, f_x f_y \sin\chi}{\sqrt{1+f_x^2}\sqrt{1+f_x^2+f_y^2}}\right)$$

$$+ \lambda_y \left(\frac{-V\sqrt{1+f_x^2}\,\sin\chi}{\sqrt{1+f_x^2+f_y^2}}\right) \tag{3.18}$$

Note that the wind components have been dropped from (3.18).

The Euler-Lagrange equations for this optimal control problem are:

$$\dot{\lambda}_x = - Kf_x - \frac{B_1 \sin\chi\,\lambda_y + (B_2 \sin\chi + B_3 \cos\chi)\,\lambda_x}{A_1^3 A_2^3} V \tag{3.19}$$

$$\dot{\lambda}_y = - Kf_y - \frac{B_4 \sin\chi\,\lambda_y + (B_5 \sin\chi + B_6 \cos\chi)\,\lambda_x}{A_1^3 A_2^3} V \tag{3.20}$$

where

$$A_1 = \sqrt{1+ f_x^2}$$

$$A_2 = \sqrt{1+ f_x^2 + f_y^2}$$

$$B_1 = \{- A_2^2 f_x f_{xx} + A_1^2 (f_y f_{xy} + f_x f_{xx})\}\, A_1^2$$

$$B_2 = - \{f_x f_{xx} A_2^2 + A_1^2 (f_y f_{xy} + f_x f_{xx})\} f_x f_y + A_1^2\, A_2^2\, (f_x f_{xy} + f_y f_{xx})$$

$$B_3 = - A_2^3\, f_x f_{xx}$$

$$B_4 = \{- A_2^2 f_x f_{xy} + A_1^2 (f_x f_{xy} + f_y f_{yy})\}\, A_1^2$$

$$B_5 = - \{f_x f_{xy} A_2^2 + A_1^2 (f_x f_{xy} + f_y f_{yy})\} f_x f_y + A_1^2\, A_2^2\, (f_y f_{xy} + f_x f_{yy})$$

$$B_6 = - A_2^3\, f_x f_{xy}$$

with the optimality condition

$$\tan\chi = \frac{\lambda_x f_x f_y - \lambda_y (1+f_x^2)}{\lambda_x \sqrt{1+f_x^2+f_y^2}} \tag{3.21}$$

The equations (3.6), (3.7), (3.19), and (3.20) together with (3.21) constitute a nonlinear two point boundary value problem, which can be solved if the initial conditions on the two

costates λ_x and λ_y were known. However, since the variational Hamiltonian is not explicitly dependent on time and the final time is free, this optimal control problem has a constant of motion, viz.,

$$H(t) = 0, \quad 0 \le t \le t_f \tag{3.22}$$

i.e.,

$$0 = 1 - K + K\, f(x,y) + \lambda_x \left(\frac{V \cos\chi}{\sqrt{1+f_x^2}} + \frac{V\, f_x f_y \sin\chi}{\sqrt{1+f_x^2}\sqrt{1+f_x^2+f_y^2}}\right) + \lambda_y \left(\frac{-V\sqrt{1+f_x^2}\,\sin\chi}{\sqrt{1+f_x^2+f_y^2}}\right) \tag{3.23}$$

This constant of motion may be employed to eliminate one of the costates in the problem. Using (3.21) and (3.23), one may solve for the costates λ_x and λ_y as

$$\lambda_x = \frac{-\{1 - K + K\, f(x,y)\}\sqrt{1+f_x^2}}{V}\cos\chi \tag{3.24}$$

$$\lambda_y = \frac{\{1 - K + K\, f(x,y)\}(\sqrt{1+f_x^2+f_y^2}\,\sin\chi - f_x f_y \cos\chi)}{V\sqrt{1+f_x^2}} \tag{3.25}$$

Additionally, the costates can be completely eliminated from this problem by employing an adjoint-control transformation as illustrated in the following.

The expressions (3.24) and (3.25) are next differentiated with respect to time and equated to the right hand sides of the equations (3.19) or (3.20). This process yields a differential equation for χ as:

$$\dot{\chi} = \frac{\{(A_1 K + A_2)\cos\chi + A_3(A_4 K + A_5)\sin\chi\}\, V}{A_6(A_7 K + 1)} \tag{3.26}$$

where,

$$B_1 = (f-1)f_{xx} - (1+f_x^2),$$

$$B_2 = (1-f)(1+f_x^2),$$

$$B_3 = f_x(1+f_x^2)^2,$$

$$A_1 = B_1 A_3 f_y,$$

$$A_2 = f_{xx} f_y A_3,$$

$$A_3 = \sqrt{1 + f_x^2 + f_y^2},$$

$$A_4 = B_1 f_x f_y^2 + B_2 f_{xy} f_y - B_3,$$

$$A_5 = f_x f_{xx} f_y^2 - (1+f_x^2) f_{xy} f_y,$$

$$A_6 = \{(1+f_x^2)(1+f_x^2+f_y^2)\}^{3/2},$$

$$A_7 = (f-1).$$

An implicit assumption made in deriving (3.26) is that $\dot{\chi}$ exists everywhere on the terrain. This aspect will be verified while discussing the second variation analysis for this problem. The expression (3.26) was obtained using the MACSYMA program [61].

With the foregoing analysis, the optimal route planning problem has been reduced to that of solving a set of three nonlinear differential equations (3.6), (3.7), and (3.26) with one unknown boundary condition $\chi(0)$. The solution of this problem requires the determination of the initial value of heading angle χ. Since x(0) and y(0) are known, $\chi(0)$ must be selected such that the final conditions on x and y are the desired values $x(t_f)$ and

$y(t_f)$. A simple iterative technique such as the method of bisections [62] may be set up to solve this problem. Flow chart of such an iterative scheme is illustrated in Figure 3.2. If a solution for the system (3.6), (3.7) and (3.26) satisfying the given boundary conditions exists within the given $\chi(0)$ range, then it can be shown that the scheme given in Figure 2 will find it in finite number of iterations [62]. Moreover, enforcing the conditions for the existence of optimal controls can yield further guarantees on the convergence of this numerical algorithm.

Consider next, the second control variable in this problem, viz., the helicopter speed. Since the second control variable V appears linearly in the variational Hamiltonian and is bounded, the optimal control is given by

$$V = V_{max}, \text{ if } S < 0$$

$$V = V_{min}, \text{ if } S > 0$$

$$V = \text{Singular}, S \equiv 0 \tag{3.27}$$

where S is the switching function obtained from

$$S = \frac{\partial H}{\partial V} \tag{3.28}$$

namely,

$$S = \frac{\lambda_x \left(\sqrt{1 + f_x^2 + f_y^2} \cos \chi + f_x f_y \sin \chi \right) - \lambda_y (1 + f_x^2) \sin \chi}{\sqrt{1 + f_x^2} \sqrt{1 + f_x^2 + f_y^2}} \tag{3.29}$$

Substituting λ_x and λ_y from (3.23) and (3.24) into (3.29)

$$S = - \frac{\{(1 - K) + K f\}}{V} \tag{3.30}$$

Since V is always positive, the sign of the switch function is determined by the term within the braces. This term is always less than zero by definition ($0 \leq K \leq 1, 0 < f$). This expression suggests that the maximum speed setting is optimal throughout the trajectory.

Euler solutions for the optimal trajectory planning problem may be generated by numerically integrating the three first order nonlinear differential equations (3.6), (3.7), and (3.26). Starting from arbitrary initial conditions x(0) and y(0), Euler solutions to various end conditions can be generated by changing the initial value of the heading angle. In the present work, a sample terrain data from the U.S. Geological Survey [63] was used. The terrain approximates a part of the Nassau Valley area in California shown in Figure 3.3. The terrain data is stored at 1000 feet intervals and interpolated using Cubic Spline Lattices [64]. This terrain data is given in Table 3.1. First and second gradients of the terrain profile required in subsequent calculations are generated by differentiating the spline polynominals analytically and substituting for down-range and cross-range values. The nonlinear differential equations are integrated using a fixed-step fifth-order Runge-Kutta-Merson technique and the method of bisections is used to carry out the one-dimensional search. All computations were carried out on a VAX 11/750 computer system with double precision arithmetic.

Figure 3.4 illustrates time-optimal trajectories starting at the point O and terminating at several end points. These trajectories were obtained by setting K= 0 and varying the initial value of the heading angle. This value of K corresponds to the case of time-optimal control. The trajectories appear to be close to straight lines except in regions of large terrain curvature. A family of Euler solutions starting at the point O with a large weight on the terrain masking (K = 0.99) is given in Figure 3.5. These trajectories exhibit a more significant curvature. An interesting feature of this solution family is that some of the trajectories appear to intersect in certain regions of the given terrain. This implies the

existence of more than one trajectory satisfying the stationary and boundary conditions. In this situation, the selection of a particular path has to be based on second order necessary conditions. Such an analysis will be presented in the Section 3.4. For a typical set of boundary conditions, Figure 3.6 illustrates the difference between time optimal and maximum terrain masking trajectories with initial heading angles 50 and 68 degrees, respectively. It may be observed from this figure that the terrain masking trajectory tends to seek out lower elevations while time optimal trajectories appear to minimize the arc length.

3.3 Optimal Route Planning Problem No.2

In the trajectory planning scheme discussed in the foregoing, the computation of extremals required first and second partial derivatives of the terrain profile. In some situations, it may not be desirable to compute these derivatives due to the nature of terrain data. A formulation of the trajectory problem that does not require these partial derivatives will be discussed next.

3.3.1 Problem Formulation

Assuming that the helicopter has a speed of V, the flight path angle γ and the heading angle ψ, the velocity components in the defined inertial reference frame is given by

$$\dot{x} = V \cos\gamma \cos\psi \tag{3.31}$$

$$\dot{y} = V \cos\gamma \sin\psi \tag{3.32}$$

The heading angle is the control variable in the this problem, while the flight path angle is defined by the terrain profile. This is due to the fact that the helicopter is executing terrain

following flight. Thus, the kinematic model of the helicopter flight is given by the differential equations (3.31), (3.32) and a nonlinear algebraic equation (3.2). In addition to this, one can define three differential equations describing the point mass dynamics of the helicopter. While it is desirable to include this in the formulation, the resulting trajectory optimization problem becomes intractable. Note that it is possible to correct the present results for neglected dynamics using singular perturbation theory [65 - 67]. The present research will not address this aspect of the optimal trajectory synthesis problem.

In the ensuing formulation, time is not included in the performance index. Moreover, since time does not appear explicitly on the right-hand side of equations (3.31) and (3.32), the independent variable is next changed from time to down-range. This yields a dynamic equation of the form

$$y' = \tan \psi \tag{3.33}$$

Here, a prime over the variables represents differentiation with respect to down-range, the independent variable in this problem. Note that this formulation is independent of the vehicle velocity V. As a consequence, it is possible to impose an additional acceleration constraint on the problem. It needs to be underscored that the vehicle velocity cannot be permitted to be zero along the trajectory. Otherwise, the present modelling will lose its validity.

3.3.2 Optimal Trajectory Planning

Assuming that the nominal trajectory to be flown by the helicopter is given by the function $y_c(x)$, the objective of the second trajectory planning scheme is to maximize terrain masking while minimizing deviations from the nominal trajectory. With this point of view, the equation (3.33) may be modified as:

$$\delta y' \equiv \tan \psi - y_c'(x) \tag{3.34}$$

Here, $y_c'(x)$ is the derivative of the command $y_c(x)$ with respect to down-range x. The heading angle ψ is the control variable in this problem. The second optimal control problem is then defined as:

$$\min_{\psi(t)} \quad \frac{1}{2}\int_{x_0}^{x_f} (f^2 + \varepsilon \delta y^2 + \alpha \psi^2)\, dx \tag{3.35}$$

subject to the differential constraint (3.34). The quantities ε and α are factors that control the relative weight between deviations from the specified path and lateral acceleration. For mathematical convenience, we next replace the term corresponding to ψ^2 with $\tan^2\psi$. Moreover, the nominal trajectory is often specified by straight line segments. In this case, one can redefine the origin of the coordinate system at the initial point with the abscissa pointing in the direction of the down-range direction without any loss of generality. In this case, the quantity δy can be set equal to y.

With these modifications, the optimal control problem is redefined as

$$\min_{y'} \quad \frac{1}{2}\int_{x_0}^{x_f} (f^2 + \varepsilon y^2 + \alpha y'^2)\, dx \tag{3.36}$$

The Euler's necessary condition for this problem can be obtained [12]:

$$y'' = \frac{(\varepsilon y + f f_y)}{\alpha} \tag{3.37}$$

Equation (3.37) is a nonlinear second order differential equation with a varying coefficient. The initial condition $y(x_0)$ and the final condition $y(x_f)$ are specified. As in the previous section, the quantity f_y is the gradient of the terrain profile in the cross-range direction. The Euler's necessary conditions can be obtained via two distinct, although equivalent

approaches. First, one may use the classical calculus of variations to derive (3.37). Alternative approach is to let y" = U and proceed via modern optimal control theory [12]. Here, U is the control variable.

Numerical solutions to the differential equation (3.37) yield the extremals. To construct an extremal joining a pair of x,y boundary conditions, the unknown initial condition y'(0) needs to be determined.

Since just one unknown parameter is involved, it is possible to employ the method of bisections to find the solution. Moreover, linear interpolation may be employed for terrain interpolation since the method outlined here requires just the first gradient of the terrain profile.

Figure 3.14 shows a typical set of Euler solutions starting at the point O for $\alpha = 10^5$, $\varepsilon = 0.001$. These trajectories were generated by changing the initial value of y' and integrating the Euler's necessary condition forward. Note that the effect of increasing α is to produce trajectories that are closer to straight lines, while the influence of increasing ε is to introduce more features into the solution.

Figure 3.15 illustrates two trajectories with same boundary conditions, one being a straight line joining the initial and final points and another being the extremal generated by integrating equation (3.37). This trajectory corresponds to $\alpha = 10^6$, $\varepsilon = 0.01$, and initial heading angle = -45 deg. Nature of the extremal agrees with general intuition that helicopter should fly at lower altitudes and its path may zigzag around hills. Altitude profiles along two trajectories in Figure 3.16 further illustrate this fact.

3.4 Second-Variation Analysis

It can be shown that a sufficient condition for the extremals obtained in the foregoing to provide a weak local minimum for an optimal control problem is that the second variation be strongly positive [68]. The second variation will be strongly positive if the Legendre-Clebsch necessary condition is met in the strengthened form and the no-conjugate point test is satisfied. In optimal control problems with unbounded controls, it can be shown that the variational Hamiltonian is equivalent to the Weierstrass excess function [68]. As a result if the second variation tests are satisfied, then the extremals provide a strong local minimum. In addition to this, it is known [69] that if the integrand of the performance index satisfies a convexity condition, the extremals affording strong local minimum also provide a global minimum. In the following, each of these conditions will be examined for the two previous problems.

3.4.1 Second-Variation Analysis for O.R.P. #1

3.4.1.1 Legendre-Clebsch Necessary Condition

In an earlier section, it was shown that the optimal value of airspeed $V = V_{max}$. Since this control variable appears linearly in the Hamiltonian, the Legendre-Clebsch condition reduces to the scalar form

$$H_{\chi\chi} \geq 0 \tag{3.38}$$

Taking second partial derivative of the Hamiltonian (3.18) with respect to control χ,

$$H_{\chi\chi} = \frac{-\lambda_x \left(\sqrt{1 + f_x^2 + f_y^2}\cos\chi + f_x f_y \sin\chi\right) + \lambda_y (1 + f_x^2)\sin\chi}{\sqrt{1 + f_x^2}\,\sqrt{1 + f_x^2 + f_y^2}}\, V \tag{3.39}$$

Next, substituting λ_x and λ_y from (3.24) and (3.25) into (3.39), one obtains

$$H_{\chi\chi} = (1-K) + K\, f\,(x,y) \tag{3.40}$$

The right-hand side of (3.40) is strictly positive by definition. Thus, the Legendre-Clebsch condition is satisfied in the strengthened form at every point on the terrain. The implication of this is that the problem is regular. As a result, the extremals will be smooth and provide a weak local minimum for sufficiently short intervals.

3.4.1.2 Weierstrass Test

In the Calculus of Variations, strong variations only bound the magnitude of δx, while weak variations bound both the magnitude of δx and the magnitude of the time derivative of δx [35]. Weierstrass gave a test for verifying strong local minimum characteristics of extremals. It can be shown that the Weierstrass's excess function [68] is equivalent to the Variational Hamiltonian in optimal control theory [12].

$$H(x,\lambda,\chi,t) = 1-K+Kf+\lambda_x V\left\{\frac{\cos\chi}{\sqrt{1+f_x^2}}+\frac{f_x f_y \sin\chi}{\sqrt{1+f_x^2}\sqrt{1+f_x^2+f_y^2}}\right\}-\lambda_y V\frac{\sqrt{1+f_x^2}\sin\chi}{\sqrt{1+f_x^2+f_y^2}} \tag{3.41}$$

Substituting λ_x and λ_y from (3.24) and (3.25) into (3.41), one has

$$H(x,\lambda,\chi,t) = (1 - K + K\, f)\ \{1- \cos\,(\chi^\circ - \chi)\} \tag{3.42}$$

Here, χ° is the value of χ satisfying the optimal condition $H_\chi=0$.

and

$$H(x,\lambda,\chi,t) \ > \ H(x,\lambda,\chi^\circ,t) = 0 \tag{3.43}$$

In the foregoing it has been shown that the Weierstrass necessary condition is satisfied along the extremal. Thus, the performance along the extremal is lower than along any other trajectory.

3.4.1.3 Jacobi Test

For extremals of finite length, the task of ensuring that the second variation is nonnegative for admissible variations leads to the accessory-minimum problem in the calculus of variations. This problem attempts to produce a system of admissible variations, not identically zero, which offer the most severe competition in the sense of minimizing the second variation. If a system of nonzero variations making the second variation zero can be found, then a neighboring trajectory is competitive. In this case, the test extremal furnishes at best an improper minimum and at worst a merely stationary value [70]. First value of the independent variable for which such a nontrivial system of variations can be found defines a conjugate-point.

It has been shown in the references [12][71][72] that the accessory minimum problem leads to the analysis of the nature of solutions to linearized Euler-Lagrange equations. We note here that this problem may be cast in the standard linear-quadratic format using the backward sweep method [12]. However, algebraic linearization of the Euler-Lagrange equations (3.6), (3.7), (3.19), (3.20) can become excessively involved. As an alternative, a numerical conjugate point test will be employed in the present research. Reference 73 discusses several numerical methods available for conjugate-point testing. A direct approach for conjugate point testing will be pursued in the following. This approach is based on Theorem 12.1 -12.3 in Reference 70. This theorem is discussed in detail in Appendix B.

From the existance theory of linear ordinary differential equations [74], it is known that the solutions to the linearized Euler-Lagrange equations should be linearly independent. More concisely, the Wronskian determinant should not be zero on an open interval. For these fundamental solutions to be unique, they should be nontrivial and satisfy initial conditions.

In the present problem, the fundamental solutions are obtained by using the finite-difference approximation

$$\begin{aligned} \delta x_1(t) &= x^*(t) - x^i(t), \quad \delta y_1(t) = y^*(t) - y^i(t) \\ dx_2(t) &= x^*(t) - x^j(t), \quad dy_2(t) = y^*(t) - y^j(t) \end{aligned} \tag{3.44}$$

where $(x^i(t),y^i(t))$ and $(x^j(t),y^j(t))$ are neighboring extremals generated by perturbing the initial value of heading angle. Note that this is equivalent to perturbing the initial value of costates, while maintaining the appropriate state initial conditions.

The characteristic determinant $\Delta(t)$ is then formed as:

$$\Delta(t) = \begin{vmatrix} \delta x_1(t) & \delta x_2(t) \\ \delta y_1(t) & \delta y_2(t) \end{vmatrix} \tag{3.45}$$

From the theory of differential equations [74] it is known that this determinant cannot be identically zero. If this characteristic determinant (3.45) after being zero at initial $t = 0$, subsequently becomes zero at $t = t^*$, with $t^* < t_f$, then the point t^* is said to be conjugate to the initial point $t = 0$.

This numerical conjugate point test is applied to the maximum masking extremals given in Figure 3.5 with K=0.99. In this figure, the extremals A and B are of particular interest since these are competing extremals satisfying the boundary condition pair (O, F). The characteristic determinant (3.45) evaluated along these extremals is given in Figures

3.8 and 3.9. From these figures it is clear that a conjugate point to point O occurs along the extremal B, while none is encountered along extremal A. Thus, the extremal A affords a strong local minimum if the desired end conditions were points O and F. On the other hand, the extremal B provides merely a stationary value. This fact is confirmed by computing the performance index along these trajectories and given in Figure 3.10. This figure indirectly proves the princple of optimality by showing that the performance index along optimal trajectory A between two points O and F is always lower than neithboring extremal B. The point conjugate to the point O along extremal B is denoted by the point C in Figure 3.5. A rule of thumb given in Reference 75 is that a conjugate point can be expected to exist at point where the tangent to the extremal experiences a sudden change. In the present case, it may be observed that the extremal B experiences a sharp turn at the point C.

In the minimum flight time problem, K = 0, the integrand of the performance index is a constant, and it does satisfy the weak convex condition given in Reference 69. Thus the extremals satisfying three second variation tests also provide a global optimum [69].

In Figure 3.11, two extremals satisfying the boundary condition pair (O, F) are given for the min-time criterion. Following the same procedure as for the maximum masking problem, the characteristic determinant evaluated along these extremals is given in Figures 3.12 and 3.13. From these figures it is clear that a conjugate point to point O occurs along the extremal A, while none is encountered along extremal B. Thus, the extremal B affords a global minimum if the desired end conditions were points O and F. On the other hand, the extremal A provides merely a stationary value.

3.4.2 Second-Variation Analysis for O.R.P. #2

For the second trajectory planning problem, the Legendre-Clebsch condition will be met in strengthened form if $\alpha > 0$, since the Legendre-Clebsch necessary condition [76] is

$$\frac{\partial^2}{\partial \psi^2} \frac{1}{2}(f^2 + \varepsilon \delta y^2 + \alpha \psi^2) = \alpha > 0 \tag{3.46}$$

Defining $F(x,y,y') = f^2 + \varepsilon y^2 + \alpha y'^2$, the Weierstrass excess function for this problem turns out to be

$$E(x,y,y',p) = F(x,y,y') - F(x,y,p) - (y'-p)F_p(x,y,p) = \alpha (y'-p)^2 \tag{3.47}$$

This is positive if y' is not equal to p.

The Jacobi's differential equation [76] for this problem turns out to be:

$$\eta'' = \frac{1}{\alpha}(\varepsilon + f_y^2 + f f_{yy})\eta \tag{3.48}$$

Here η is the solution to the linearized Euler-Lagrange equations or the second-variation. If the coefficient $\frac{1}{\alpha}(\varepsilon + f_y^2 + f f_{yy})$ on the right hand side is a slowly varying quantity with respect to range, additional analytic results may be obtained using the WKB method [16]. Let

$$q(\tau) = \frac{1}{\alpha}(\varepsilon + f_y^2 + f f_{yy}) \tag{3.49}$$

where τ is the stretched range $\tau = \mu x$, $\mu > 0$. Equation (3.48) can be rewritten

$$\eta'' - q(\tau)\eta = 0 \tag{3.50}$$

The various derivatives in the above differential equation can now be written as

$$\frac{d\eta}{dx} = \frac{d\eta}{d\tau}\frac{d\tau}{dx} = \mu\frac{d\eta}{d\tau} \tag{3.51}$$

$$\frac{d^2\eta}{dx^2} = \mu^2\frac{d^2\eta}{d\tau^2} \tag{3.52}$$

$$\mu^2\frac{d^2\eta}{d\tau^2} - q(\tau)\,\eta = 0 \tag{3.53}$$

with change of variable $\mu = \lambda^{-1}$

$$\frac{d^2\eta}{d\tau^2} - \lambda^2 q(\tau)\,\eta = 0 \tag{3.54}$$

The equation (3.54) with a large parameter λ is referred to as Liouville's problem [74]. Its approximate solution can be obtained using WKB method [16].

$$\eta \approx q^{-\frac{1}{4}}\{C_1\cos(\int_{x_0}^{x_f}\sqrt{q}\,dx) + C_2\sin(\int_{x_0}^{x_f}\sqrt{q}\,dx)\},\ \text{when}\ \ q>0 \tag{3.55}$$

$$\eta \approx (-q)^{-\frac{1}{4}}\{C_1\exp(\int_{x_0}^{x_f}\sqrt{-q}\,dx) + C_2\exp(\int_{x_0}^{x_f}\sqrt{-q}\,dx)\},\ \text{when}\ \ q<0 \tag{3.56}$$

where C_1, C_2 are arbitrary constants. It may be observed from the above solutions that if $q > 0$ in the given interval, there are no conjugate points. Since $f > 0$ by definition, this expression implies that q is always positive if $f_{yy} \geq 0$. That is, if the vehicle is traveling in a valley or along a saddle, the resulting extremal will not contain any conjugate points.

In the cases where $q(\tau)$ changes sign along a given extremal, one has to carry out this test numerically. The procedure employed in the previous trajectory planning technique may once again be used. It may be verified that the integrand of the performance index

satisfies the convexity condition given in [69]. As a result, if a given extremal satisfies the second order necessary conditions, it affords a global minimum.

3.5 Computational Effort

3.5.1 Computational Effort for O.R.P. #1

Studies using a VAX 11/750 computer have shown that an extremal requiring about 70 integration steps consumes between 1.5-2.1 seconds of CPU time. Given the desired initial and final conditions on down-range and cross-range, several Euler solutions need to be evaluated to converge on the one satisfying the given boundary conditions. Using the computational flow chart in Figure 3.2, between six and seven iterations were found adequate to reduce the boundary condition error by an order of magnitude. Clearly, this will depend on the given terrain profile. For example, if the terrain gradients f_x and f_y were small such that the boundary condition error depends approximately linearly on the initial heading angle error, the number of iterations and boundary condition error may be related as using the convergence formula for the method of bisections [62] as:

$$r = \frac{\ln (e_{y_1}/e_{y_r})}{\ln 2} \tag{3.57}$$

In the expression (3.57), r is the number of iterations, e_{y_1} is the initial boundary condition error and e_{y_r} is the boundary condition error after r iterations. It is important to stress here that this relationship does not account for nonlinearities due to terrain profile. Its usefulness is limited to generating a first order estimate on the number of iterations required to satisfy a specified boundary condition error tolerance.

In the present research the total computations for one step integration are about 626 multiplications and divisions and 240 additions and substractions.

3.5.2 Computational Effort for O.R.P. #2

Assuming that the stationary condition (3.37) is integrated using the Euler's method, and that a linear interpolation is employed for computing the terrain altitude at various down-range and cross-range locations, one can obtain a formula for the required number of operations. In the following, it is assumed that multiplication, division, addition, and subtraction each count as one operation. Each integration step is found to require 23 operations. The method of bisections requires two mathematical operations and one logical operation per iteration. Thus, if there are n discretization intervals in the down-range direction and r bisections iterations, the present method would require approximately

$$m = 23\ nr \tag{3.58}$$

operations. Assuming that it is desired to decrease the interval of uncertainty by two orders of magnitude, one requires about 7 iterations using the method of bisections. Thus, the number of operations required for the method of bisections is m = 161n. Note that one can reduce the interval of uncertainty by eight orders of magnitude by increasing the number of iterations by about four times.

Next, assuming equal discretization of the down-range and cross-range directions, the dynamic programming scheme is found to require 23 mathematical operations per node to evaluate the performance index. In a typical computing scheme [12], this will have to be evaluated at n^2 - 1 nodes. After these computations, one has to execute 2n -1 logical

operations. Thus, the total number of operations required in a full scale discrete dynamic programming approach for the present route planning problem is approximately

$$m = 23\ n^2 + 2n \tag{3.59}$$

operations. Thus, to first order, the two methods are equal in terms of computational speed whenever n = 7. Whenever the number of discretization intervals exceeds this figure, the present approach provides a faster solution. In any case, note that the computational effort in the present approach is a linear function of the number of discretization interval, while in the dynamic programming approach, the computational effort is quadratic in the number of discretization intervals.

On a rough terrain, one would require a large number of discretization intervals to obtain results with sufficient fidelity. In that situation, the advantage of the present approach will be even more significant. On the other hand, the dynamic programming approach guarantees the optimality of the solution, while in the Euler solution method, this has to be verified through second order necessary conditions .

3.6 Wind Effects

The magnitude and direction of winds are known to have a substantial effect on the performance of most aircraft. This effect is accentuated on a conventional helicopter because of the low flight speeds. As mentioned in Section 3.2, the ambient winds can be incorporated into the trajectory programming scheme with slight increase in complexity. For the purposes of illustration, the effect of constant winds along x-axis in the first trajectory planning problem will be considered. Using equations (3.8), (3.10), and (3.11), and assuming the same performance index (3.14), one can obtain costate equations as

$$\lambda_x = \frac{-\{1 - K + K\, f(x,y)\}\sqrt{1 + f_x^2}\cos\chi}{V + u\sqrt{1 + f_x^2}\cos\chi} \tag{3.60}$$

$$\lambda_y = \frac{\{1 - K + K\, f(x,y)\}(\sqrt{1 + f_x^2 + f_y^2}\sin\chi - f_x f_y \cos\chi)}{\sqrt{1 + f_x^2}\,(V + u\sqrt{1 + f_x^2}\cos\chi)} \tag{3.61}$$

Following the same steps as in Subsection 3.3.1, the differential equation for heading angle χ turns out to be

$$\dot{\chi} = \frac{V\,(C_1 \sin\chi + C_2 \cos\chi) + u\,A_1 \cos\chi\,(D_1 \sin\chi + D_2 \cos\chi)}{(1 - K + K\,f)\,A_1^3\,A_2^3} \tag{3.62}$$

where,

$$A_1 = \sqrt{1 + f_x^2}$$

$$A_2 = \sqrt{1 + f_x^2 + f_y^2}$$

$$B_1 = \{-A_2^2 f_x f_{xx} + A_1^2 (f_y f_{xy} + f_x f_{xx})\}\,A_1$$

$$B_2 = -\{f_x f_{xx} A_2^2 + A_1^2 (f_y f_{xy} + f_x f_{xx})\} f_x f_y + A_1^2 A_2^2 (f_x f_{xy} + f_y f_{xx})$$

$$C_1 = -Kf_x A_1^2 A_2^3 - (1 - K + Kf)\,B_1 A_2$$

$$C_2 = -Kf_y A_1^2 A_2^3 + (1 - K + Kf)\,\{B_1 f_x f_y + B_2 + A_2^2 f_x f_{xx}\,(f_x f_y - f_{xy} A_1^2)\}$$

$$D_1 = -Kf_x A_1^2 A_2^3 + (1 - K + Kf)\,(-B_1 A_2 + A_2^3 f_x f_{xx})$$

$$D_2 = -KA_1^2 A_2^3\,(1 + f_y)^2 + (1 - K + Kf)\,(B_1 f_x f_y + B_2)$$

The accuracy of these expressions may be verified by putting the wind speed u to zero. In this case, the equation (3.62) exactly corresponds to (3.26). Figures 3.17 and 3.18

show several extremals for the minimum flight criterion and the maximum masking criterion when wind to airspeed ratio u/V equals to 0.1 and all conditions being the same as the Figures 3.4 and 3.5. An observation that may be made from these figures is that the winds affect the maximum masking trajectory to a higher degree.

It is possible to include wind effects in the second route planning problem also. However, this will not be pursued in the present research.

3.7 Conclusion

In this chapter, two systematic methodologies for optimal trajectory planning (ORP) useful in the helicopter terrain-following/terrain-avoidance flight was presented.

For the ORP No.1, the terrain constraint was embedded into state equations via a coordinate transformation. The performance index consisted of a linear combination of flight time and terrain masking. Using an adjoint-control transformation, the optimal control problem solution was reduced to a search for the initial value of heading angle. It was shown that the optimal airspeed, a second control variable in the formulation, should be chosen as the maximum permissible value. A simple computational scheme based on the method of bisections and a fifth order Kutta-Merson numerical integration technique was outlined for generating Euler solutions. Families of Euler solutions for minimum flight time and maximum terrain masking were presented.

It was shown that the Legendre-Clebsch necessary condition and Weierstrass excess function are satisfied everywhere in the admissible region. Further, conjugate points have been shown to occur in certain regions of the specified terrain. In the regions where conjugate points do not occur, the Euler solutions for the maximum masking problem provide a strong local minimum. The Euler solutions for the minimum time problem

satisfying the second-order necessary conditions were shown to provide a global minimum.

For the ORP No.2, the performance index consisted of a quadratic form in the terrain altitude, lateral deviation from the nominal trajectory, and heading angle. By changing the independent variable from time to down-range, the order of the problem was reduced.

The Legendre-Clebsch necessary condition and Weierstrass excess function were satisfied everywhere in the admissible region. For this problem, an approximate conjugate point test was developed using the WKB method.

The winds effects on the trajectories were briefly examined for ORP No.1. It is found that the winds affect the terrain masking trajectory to a higher degree.

CHAPTER IV

TRAJECTORY PLANNING AS A TWO-SIDED OPTIMAL CONTROL PROBLEM

4.1 Introduction

Previous chapter dealt with the situation wherein we seek to determine the optimal trajectory for a vehicle to fly from an initial position to a given final position. In this chapter we will examine the same problem involving two vehicles with conflicting objectives.

In such a situation, the trajectory planning problem will turn out to be a differential game. An example is the case where one of the vehicles is attempting to intercept the other while flying in a terrain following mode to avoid detection. Meanwhile, the second vehicle may be executing a terrain following flight with the objective of avoiding capture. Problems of this nature have received scant attention in the previous literature [77].

Next generation military helicopters such as the LHX must have capabilities to automatically engage with ground and air targets. The avionics requirements for the low altitude air combat mission are complex, and reflect the problems brought about by simultaneous air combat and terrain flight [78].

Since the publication of Isaac's famous book [17], the homicidal chauffeur problem has became a model for vehicle pursuit-evasion. The solutions to this problem are very intricate and have been discussed in References 79 and 80. Ciletti [77] indicated that the

assumption of perfect information and role ambiguity [81] are some of the factors that have prevented the application of differential games theory in realistic military situations. Additionally, dynamics of the vehicles are highly nonlinear and of high order. These factors have led to a situation wherein complete results are given only for a very limited class of problems.

In this chapter, two different approaches are proposed for studying the helicopter pursuit-evasion problem. A nonlinear pursuit-evasion game employing helicopter model incorporating the terrain profile is discussed first. This model was used in Chapter III for trajectory planning. This is followed by an approach based on the feedback linearization technique motivated by the research in Reference 91. Each of these approaches will be discussed in the following sections. In the ensuing, it will be assumed that each player has complete information on the helicopter parameters and a noise free measurement of all the state variables.

4.2 A Nonlinear Pursuit-Evasion Game

4.2.1 Problem Formulation

The helicopter pursuit-evasion problem is analyzed here as a deterministic two-person zero-sum differential game. The game begins at a certain set of initial conditions, when the helicopters first become aware of each other. In the present analysis the respective roles of the players are assigned at the outset. It is assumed that this role definition remains unchanged during the entire game. Although this formalism restricts the applicability of the results, it is useful in revealing salient solution features. In real situations, the evader may be a helicopter without offensive capabilities or with limited maneuvering capabilities.

4.2.1.1 Equations of Motion

When compared with high performance aircraft pursuit-evasion, one of the characteristics of helicopter pursuit-evasion [82, 83] is that each participant attempts to reduce its exposure to the opponent by avoiding high altitude flight throughout the engagement. This is due to the fact that the vertical maneuvering above NOE altitudes may make the helicopters more vulnerable to detection by ground and air based surveillance system. The equations of motion developed in Chapter III are used here to model the helicopter flight in terrain-following mode. In the interest of clarity, these equations of motion are repeated here.

$$\dot{x}_e = \frac{V_e \cos\chi_e}{\sqrt{1+f_{x_e}^2}} + \frac{V_e f_{x_e} f_{y_e} \sin\chi_e}{\sqrt{1+f_{x_e}^2}\sqrt{1+f_{x_e}^2+f_{y_e}^2}} \tag{4.1}$$

$$\dot{y}_e = -\frac{V_e \sqrt{1+f_{x_e}^2}\,\sin\chi_e}{\sqrt{1+f_{x_e}^2+f_{y_e}^2}} \tag{4.2}$$

$$\dot{x}_p = \frac{V_p \cos\chi_p}{\sqrt{1+f_{x_p}^2}} + \frac{V_p f_{x_p} f_{y_p} \sin\chi_p}{\sqrt{1+f_{x_p}^2}\sqrt{1+f_{x_p}^2+f_{y_p}^2}} \tag{4.3}$$

$$\dot{y}_p = -\frac{V_p \sqrt{1+f_{x_p}^2}\,\sin\chi_p}{\sqrt{1+f_{x_p}^2+f_{y_p}^2}} \tag{4.4}$$

The subscript e denotes the evader, while the subscript p denotes the pursuer. To make the problem meaningful, it is assumed that the pursuer has a higher speed than the evader, i.e.,

$$V_p > V_e \tag{4.5}$$

Whenever the terrain gradients f_x, f_y are zero, it is possible to show that the condition (4.5) is essential to guarantee capture. The initial conditions at t = 0 are

$$(x_e,y_e)|_{t=0} \text{ specified} \tag{4.6}$$

$$(x_p,y_p)|_{t=0} \text{ specified} \tag{4.7}$$

This problem is a terrain following version of *simple motion* illustrated graphically in Reference 17. The participants select the direction of travel and may change it as fast as desired. Thus, the control variables in this problem are the heading angles, χ_p and χ_e.

Note that this pursuit-evasion game has a very simple solution whenever the terrain gradients are zero. However, the solution becomes quite complex in the general case; as will be apparent in the ensuing.

4.2.1.2 Termination of Game

The game terminates at the first instant the pursuer succeeds in approaching the evader within the firing range of its weapon system. For the case of a circular weapon range envelope, this condition can be expressed by the requiring that

$$(x_e - x_p)^2 + (y_e - y_p)^2 \,|_{t_f} \le d^2 \tag{4.8a}$$

$$\frac{d}{dt}\{(x_e - x_p)^2 + (y_e - y_p)^2\} < 0 \tag{4.8b}$$

The quantity d is a specified number. The condition (4.8b) is required to ensure sufficient time for weapon usage. The time of capture is determined from the requirement that

$$t_f = \min_t \{(x_e - x_p)^2 + (y_e - y_p)^2 - d^2 = 0\} \tag{4.9}$$

i.e., the instance that the condition (4.8a) is met as an equality.

It has been suggested in the literature [17] [84] that a fan-shaped capture set may be more realistic. However, in all that follows, a circular envelope will only be considered.

4.2.1.3 Measure of Effectiveness

In the most planar games reported in the literature [80] [85], the performance index of the game is the time of capture. The objective of the pursuer is to minimize the terminal time t_f, while the evader endeavors to maximize it. Additionally, in the present setting both players also attempt to minimize their flight altitude to ensure adequate terrain masking. In this case, the performance index can be expressed as

$$J = \min_{\chi_p} \max_{\chi_e} \int_{t_0}^{t_f} (1 + W_p f_p - W_e f_e)\, dt \tag{4.10}$$

where, W_p and W_e are weighting factors for the pursuer's altitude and evader's altitude, respectively. The negative sign on the second term explicitly recognizes the fact that the evader is attempting to maximize the performance index. In order to satisfy the terminal constraint (4.8), it may be appended to the performance index in the form of a penalty function [12]. In this case, the augmented performance index is

$$J^a = \min_{\chi_p} \max_{\chi_e} Q(t_f) + \int_{t_0}^{t_f} (1 + W_p f_p - W_e f_e)\, dt \tag{4.11}$$

The terminal penalty function is given by

$$Q(t_f) = \frac{\nu}{2} \{(x_p - x_e)^2 + (y_p - y_e)^2 - d^2\}\Big|_{t_f} \tag{4.12}$$

and ν is an undetermined multiplier in the game.

4.2.2 Derivation of Optimal Strategies

For convenience, define

$$r_1 \equiv \dot{x}_e,\ r_2 \equiv \dot{y}_e,\ r_3 \equiv \dot{x}_p,\ r_4 \equiv \dot{y}_p \tag{4.13}$$

The variational Hamiltonian [12] may be formulated as

$$H = 1 + W_p f_p - W_e f_e + \sum_{i=1}^{4} \lambda_i r_i \tag{4.14}$$

Expression (4.14) may be written in a more succinct form as:

$$H = 1 + H(\chi_p) + H(\chi_e) \tag{4.15}$$

with

$$H(\chi_p) = W_p f_p + \lambda_3 r_3 + \lambda_4 r_4 \tag{4.16}$$

$$H(\chi_e) = - W_e f_e + \lambda_1 r_1 + \lambda_2 r_2 \tag{4.17}$$

Since H is separable in terms of pursuer-evader controls χ_p and χ_e, the saddle point condition [39] is satisfied. As a result, the order of maximization and minimization does not influence the outcome of the game. Thus, one has

$$\min_{\chi_p} \max_{\chi_e} H = \max_{\chi_e} \min_{\chi_p} H \tag{4.18}$$

The integrand of performance index (4.10) and system equations (4.1 - 4.4) are continuous and satisfy the Lipschitz condition. Thus, the sufficient condition for the game to have the value is also satisfied, see Appendix C for more details. Each player's goal is to reach the value, i.e., saddle point of the performance index.

Euler-Lagrange equations for the evader are given by

$$\dot{\lambda}_1 = W_e f_{x_e} - \frac{B_1 \sin\chi_e \lambda_2 + (B_2 \sin\chi_e + B_3 \cos\chi_e)\lambda_1}{A_1^3 A_2^3} V_e \qquad (4.19)$$

$$\dot{\lambda}_2 = W_e f_{y_e} - \frac{B_4 \sin\chi_e \lambda_2 + (B_5 \sin\chi_e + B_6 \cos\chi_e)\lambda_1}{A_1^3 A_2^3} V_e \qquad (4.20)$$

where

$$A_1 = \sqrt{1+ f_{x_e}^2}$$

$$A_2 = \sqrt{1+ f_{x_e}^2 + f_{y_e}^2}$$

$$B_1 = \{- A_2^2 f_{x_e} f_{x_e x_e} + A_1^2 (f_{y_e} f_{x_e y_e} + f_{x_e} f_{x_e x_e})\} A_1^2$$

$$B_2 = - \{f_{x_e} f_{x_e x_e} A_2^2 + A_1^2 (f_{y_e} f_{x_e y_e} + f_{x_e} f_{x_e x_e})\} f_{x_e} f_{y_e}$$

$$+ A_1^2 A_2^2 (f_{x_e} f_{x_e y_e} + f_{y_e} f_{x_e x_e})$$

$$B_3 = - A_2^3 f_{x_e} f_{x_e x_e}$$

$$B_4 = \{- A_2^2 f_{x_e} f_{x_e y_e} + A_1^2 (f_{x_e} f_{x_e y_e} + f_{y_e} f_{y_e y_e})\} A_1^2$$

$$B_5 = - \{f_{x_e} f_{x_e y_e} A_2^2 + A_1^2 (f_{x_e} f_{x_e y_e} + f_{y_e} f_{y_e y_e})\} f_{x_e} f_{y_e}$$

$$+ A_1^2 A_2^2 (f_{y_e} f_{x_e y_e} + f_{x_e} f_{y_e y_e})$$

$$B_6 = - A_2^3 f_{x_e} f_{x_e y_e}$$

The Euler-Lagrange equations for the pursuer can be obtained as

$$\dot{\lambda}_3 = - W_p f_{x_p} - \frac{D_1 \sin\chi_p \lambda_4 + (D_2 \sin\chi_p + D_3 \cos\chi_p)\lambda_3}{C_1^3 C_2^3} V_p \qquad (4.21)$$

$$\dot{\lambda}_4 = - W_p f_{y_p} - \frac{D_4 \sin \chi_p \lambda_4 + (D_5 \sin \chi_p + D_6 \cos \chi_p) \lambda_3}{C_1^3 C_2^3} V_p \qquad (4.22)$$

$$C_1 = \sqrt{1 + f_{x_p}^2}$$

$$C_2 = \sqrt{1 + f_{x_p}^2 + f_{y_p}^2}$$

$$D_1 = \{- C_2^2 f_{x_p} f_{x_p x_p} + C_1^2 (f_{y_p} f_{x_p y_p} + f_{x_p} f_{x_p x_p})\} C_1^2$$

$$D_2 = - \{f_{x_p} f_{x_p x_p} C_2^2 + C_1^2 (f_{y_p} f_{x_p y_p} + f_{x_p} f_{x_p x_p})\} f_{x_p} f_{y_p}$$

$$+ C_1^2 C_2^2 (f_{x_p} f_{x_p y_p} + f_{y_p} f_{x_p x_p})$$

$$D_3 = - C_2^3 f_{x_p} f_{x_p x_p}$$

$$D_4 = \{- C_2^2 f_{x_p} f_{x_p y_p} + C_1^2 (f_{x_p} f_{x_p y_p} + f_{y_p} f_{y_p y_p})\} C_1^2$$

$$D_5 = - \{f_{x_p} f_{x_p y_p} C_2^2 + C_1^2 (f_{x_p} f_{x_p y_p} + f_{y_p} f_{y_p y_p})\} f_{x_p} f_{y_p}$$

$$+ C_1^2 C_2^2 (f_{y_p} f_{x_p y_p} + f_{x_p} f_{y_p y_p})$$

$$D_6 = - C_2^3 f_{x_p} f_{x_p y_p}$$

The optimality conditions for the two participants are given by

$$\tan \chi_e = \frac{\lambda_1 f_{x_e} f_{y_e} - \lambda_2 (1 + f_{x_e}^2)}{\lambda_1 \sqrt{1 + f_{x_e}^2 + f_{y_e}^2}} \qquad (4.23)$$

$$\tan \chi_p = \frac{\lambda_3 f_{x_p} f_{y_p} - \lambda_4 (1 + f_{x_p}^2)}{\lambda_3 \sqrt{1 + f_{x_p}^2 + f_{y_p}^2}} \qquad (4.24)$$

Terminal conditions on costates can be obtained from the terminal penalty function as

$$\lambda_1(t_f) = \frac{\partial Q}{\partial x_e} = -\nu(x_p - x_e) \tag{4.25}$$

$$\lambda_2(t_f) = \frac{\partial Q}{\partial y_e} = -\nu(y_p - y_e) \tag{4.26}$$

$$\lambda_3(t_f) = \frac{\partial Q}{\partial x_p} = \nu(x_p - x_e) \tag{4.27}$$

$$\lambda_4(t_f) = \frac{\partial Q}{\partial y_p} = \nu(y_p - y_e) \tag{4.28}$$

$$H(t_f) = -\frac{\partial Q}{\partial t_f} = 0 \tag{4.29}$$

Since the final time t_f is unspecified and the Hamiltonian does not explicitly depend on t, this problem has a constant of motion, viz.,

$$H(t) = 0\ ,\ 0 \le t \le t_f \tag{4.30}$$

Substituting equations (4.25) - (4.28) into (4.14) and invoking (4.29), it is possible to obtain an expression for the undetermined multiplier ν as:

$$\nu = \frac{1 + W_p f_p - W_e f_e}{(x_p - x_e)r_1 + (y_p - y_e)r_2 - (x_p - x_e)r_3 - (y_p - y_e)r_4} \Bigg|_{t=t_f} \tag{4.31}$$

It may be verified that the denominator of equation (4.31) is simply the negative of the product of range and range rate. Since the final value of the range is positive and the terminal range rate is negative, the parameter ν has a positive sign for the pure pursuit-evasion game in which $W_p = W_e = 0$. Moreover, expression (4.31) implies that at the final time, if one requires the pursuer and evader's positions to match exactly, ν would become infinite.

4.2.3 Numerical Results

Most differential game solutions reported in the literature are obtained using numerical methods. Among them, simple shooting in retrogressive time [86] [87], differential dynamic programming [88], and gradient method [89] have been widely used. In certain situations, the solutions obtained using reduced order modeling can be corrected for neglected dynamics using singular perturbation techniques [90].

In the present research, retrogressive time integration is used to generate the extremals. The trajectories are generated by first selecting the terminal position of the evader. The terminal position of the pursuer is then selected from the specified capture set. This corresponds to the expression (4.8a) being met as an equality. Substituting the final costates into the optimality conditions (4.23) and (4.24) and noting that the unspecified multiplier ν exists in both numerator and denominator of these equations, the final values of pursuer and evader's heading angle can be calculated. The final values of r_1, r_2, r_3, and r_4 can be computed. Substituting these in equation (4.31) yields the unspecified multiplier ν. This enables the evaluation of the final value of the costates. The state-costate system is then integrated backwards in time to obtain the pusuer-evader trajectories.

Figure 4.1 shows the pursuer and evader trajectories with terrain masking weights set to zero. As in the one-sided trajectory optimization problem, the trajectories are nearly straight lines. In Figure 4.2, the pursuit-evasion trajectories with $W_p = 1$, $W_e = 1$ are illustrated. The value of the parameter ν is computed as ν = 5.79E-3. With nonzero W_p and W_e, the trajectories exhibit significant terrain masking features. Figure 4.3 illustrates the altitude evolution as a function of time-to-go. Note that $t_{go} = 0$ corresponds to the game termination instant. Pursuit-evasion trajectories for another set of initial and final conditions with $W_p = 1$, $W_e = 1$ are given in Figure 4.4. The value of the parameter ν is

computed in this case as ν = 2.03E-3. The corresponding altitude history is given in Figure 4.5. Figure 4.6 illustrates trajectories for the pursuer and evader with $W_p = 0.0$, $W_e = 1.0$. Note that in this case, the pursuer does not attempt any terrain masking. As a result, its trajectory is nearly a straight line joining the initial and final conditions. The value of the parameter ν is computed as ν = -.747E-3. For $W_p = 0.5$ and $W_e = 1.0$, Figure 4.7 shows the pursuit-evasion trajectories with ν = -.375E-3. For the same weighting W_e, the trajectories become more curved as the weighting W_p is increased.

Legendre-Clebsch Condition

The optimality conditions (4.23-4.24) do not guarantee that the players maximize or minimize the performance index according to their role. To determine the correct optimal controls that make the pursuer minimize the performance index, while making the evader maximize, the verification of Legendre-Clebsch condition is necessary .

For the present differential game, the Legendre-Clebsch condition requires that

$$H_{\chi_e\chi_e} \leq 0 \tag{4.32}$$

$$H_{\chi_p\chi_p} \geq 0 \tag{4.33}$$

where

$$H_{\chi_e\chi_e} = \frac{-\lambda_1 \sqrt{1 + f_{x_e}^2 + f_{y_e}^2}\ \cos\chi_e + \{\lambda_2 (1 + f_{x_e}^2) - \lambda_1 f_{x_e} f_{y_e}\} \sin\chi_e}{\sqrt{1 + f_{x_e}^2}\ \sqrt{1 + f_{x_e}^2 + f_{y_e}^2}} V_e \quad . \tag{4.34}$$

$$H_{\chi_p\chi_p} = \frac{-\lambda_3 \sqrt{1 + f_{x_p}^2 + f_{y_p}^2}\ \cos\chi_p + \{\lambda_4 (1 + f_{x_p}^2) - \lambda_3 f_{x_p} f_{y_p}\} \sin\chi_p}{\sqrt{1 + f_{x_p}^2}\ \sqrt{1 + f_{x_p}^2 + f_{y_p}^2}} V_p \tag{4.35}$$

The conditions (4.32),(4.33) may be strengthened by requiring strict inequality.

Since these expressions are too difficult for hand computations, they are numerically evaluated along the extremals. Figure 4.8 shows these quantities evaluated along the trajectories in Figure 4.2. It may be seen that the Legendre-Clebsch necessary conditions are satisfied in the strengthened form. Figure 4.9 illustrates the L-C test along the extremals in Figure 4.4. In this case, it appears that this test is satisfied in the strengthened form every where except a small region near the final region. It is important to emphasize that the Jacobi test needs to be carried out along these trajectories before concluding the optimality. This will not be pursued any further in this thesis.

4.3 Feedback Linearized Solution to a Pursuit-Evasion Game

As illustrated in the previous section, the numerical solution of even simple differential games requires a tremendous amount of computational effort. An approach proposed recently for solving a class of differential games [18] is to transform a nonlinear model into linear time-invariant form. A linear differential game is then solved and the results are transformed back to original coordinates to obtain a nonlinear feedback law suitable for real time implementation. The advantage of this approach is that it can handle high-order nonlinear vehicle models in the analysis. In the following, such a differential game will be formulated and solved. The ensuing formulation will employ a high order model of the helicopter.

4.3.1 Vehicle Model

The point-mass model for a high performance helicopter can be expressed by the following nonlinear differential equations:

$$\dot{x} = V \cos\gamma \cos\psi \tag{4.36}$$

$$\dot{y} = V \cos\gamma \sin\psi \tag{4.37}$$

$$\dot{h} = V \sin\gamma \tag{4.38}$$

$$\dot{V} = \frac{T \sin\theta}{m} - g \sin\gamma \tag{4.39}$$

$$\dot{\gamma} = \frac{g}{V}\left(\frac{T \cos\theta \cos\phi}{mg} - \cos\gamma\right) \tag{4.40}$$

$$\dot{\psi} = \frac{T \cos\theta \sin\phi}{mV \cos\gamma} \tag{4.41}$$

Here, x is the down-range, y the cross-range, h altitude, V the speed, γ the flight path angle, ψ the heading angle, T the main rotor thrust, m the vehicle mass and g is the acceleration due to gravity. Figure 4.10 shows the definition of the axis system. The control variables are the pitch attitude of the helicopter θ, roll attitude of the helicopter ϕ, and the main rotor thrust T. If desired, one may model T in terms of two components. The first depending only on the vehicle states T_o and the second component δT that depends purely on the collective control, i.e., $T = T_o + \delta T$. The assumptions involved in this model are stationary atmosphere and uniform gravitational acceleration. It is important to note that this highly simplified helicopter model does not permit hovering.

4.3.2 Problem Formulation

The point mass helicopter model (4.36) - (4.41) will be transformed to a linear, time-invariant form in this section. Various steps involved in this transformation will be discussed in detail.

In order to execute the terrain flight mode, admissible trajectories should satisfy the terrain profile constraint. i.e., the vehicle altitude h should be:

$$h = h_c + f(x,y) \tag{4.42}$$

This equality constraint can be absorbed into the state equations as will be shown in the following. Differentiating the equation (4.42) with respect to time and noting that h_c is a constant, one has

$$\dot{h} = f_x\dot{x} + f_y\dot{y} \tag{4.43}$$

Equating (4.43) to (4.38), and substituting (4.36) and (4.37) for $\dot{x}$ and $\dot{y}$ results in

$$\tan\gamma = f_x \cos\psi + f_y \sin\psi \tag{4.44}$$

Differentiating once again with respect to time results in,

$$\sec^2\gamma\,\dot{\gamma} = f_{xx}\dot{x}\cos\psi + f_{xy}\dot{y}\cos\psi + f_{yx}\dot{x}\sin\psi + f_{yy}\dot{y}\sin\psi - f_x\sin\psi\,\dot{\psi} + f_y\cos\psi\,\dot{\psi} \tag{4.45}$$

Next, substituting from (4.36), (4.37), (4.40), and (4.41) for $\dot{x}$, $\dot{y}$, $\dot{\gamma}$ and $\dot{\psi}$, and rearranging yields the following relation

$$T\cos\theta\cos\phi = mV^2\cos^3\gamma\,\{(f_{xx}\cos\psi + f_{xy}\sin\psi)\cos\psi + (f_{xy}\cos\psi + f_{yy}\sin\psi)\sin\psi\}$$
$$+ (-f_x\sin\psi + f_y\cos\psi)\cos\gamma\, T\cos\theta\sin\phi + mg\cos\gamma \tag{4.46}$$

The expression (4.46) relates the vehicle states and control variables to the terrain profile.

It specifies the vertical force required to ensure that the vehicle trajectory satisfies the terrain profile constraint. As a result, this expression dictates the altitude dynamics for the two vehicles.

Following Reference 18, the remaining components of the nonlinear helicopter models for the pursuer and evader may be transformed into the Brunovsky canonical form by differentiating the expressions (4.36) and (4.37) with respect to time and substituting for $\dot{V}$, $\dot{\gamma}$, $\dot{\psi}$ from the expressions (4.39) - (4.41). Defining four pseudo control variables, the helicopter models can be put in the form

$$\ddot{x}_p = \bar{a}_{p1} \qquad \ddot{y}_p = \bar{a}_{p2} \tag{4.47}$$

$$\ddot{x}_e = \bar{a}_{e1} \qquad \ddot{y}_e = \bar{a}_{e2} \tag{4.48}$$

where, $\bar{a}_{p1}$, $\bar{a}_{p2}$, $\bar{a}_{e1}$ and $\bar{a}_{e2}$ are the vehicle acceleration components in the earth-fixed frame. These quantities may be related to the pursuer-evader states and controls as

$$\bar{a}_{p1} = \left(\frac{T_p \sin\theta_p}{m_p} - g \sin\gamma_p\right) \cos\gamma_p \cos\psi_p - \frac{T_p \cos\theta_p \sin\phi_p \sin\psi_p}{m_p}$$

$$- g \left(\frac{T_p \cos\theta_p \cos\phi_p}{m_p g} - \cos\gamma_p\right) \sin\gamma_p \cos\psi_p \tag{4.49}$$

$$\bar{a}_{p2} = \left(\frac{T_p \sin\theta_p}{m_p} - g \sin\gamma_p\right) \cos\gamma_p \sin\psi_p + \frac{T_p \cos\theta_p \sin\phi_p \cos\psi_p}{m_p}$$

$$- g \left(\frac{T_p \cos\theta_p \cos\phi_p}{m_p g} - \cos\gamma_p\right) \sin\gamma_p \sin\psi_p \tag{4.50}$$

$$\bar{a}_{e1} = \left(\frac{T_e \sin\theta_e}{m_e} - g \sin\gamma_e\right) \cos\gamma_e \cos\psi_e - \frac{T_e \cos\theta_e \sin\phi_e \sin\psi_e}{m_e}$$

$$- g \left(\frac{T_e \cos\theta_e \cos\phi_e}{m_e g} - \cos\gamma_e\right) \sin\gamma_e \cos\psi_e \tag{4.51}$$

$$\bar{a}_{e2} = \left(\frac{T_e \sin\theta_e}{m_e} - g \sin\gamma_e\right) \cos\gamma_e \sin\psi_e + \frac{T_e \cos\theta_e \sin\phi_e \cos\psi_e}{m_e}$$

$$- g \left(\frac{T_e \cos\theta_e \cos\phi_e}{m_e g} - \cos\gamma_e\right) \sin\gamma_e \sin\psi_e \tag{4.52}$$

Equations (4.47) and (4.48) are linear time-invariant form. If the pseudo control variables $\bar{a}_{p1}$, $\bar{a}_{p2}$, $\bar{a}_{e1}$ and $\bar{a}_{e2}$ were known, the actual helicopter controls can be obtained using the following equations:

$$\phi_p = \tan^{-1}\left(\frac{\bar{a}_{p2}\cos\psi_p - \bar{a}_{p1}\sin\psi_p}{F_p}\right) \tag{4.53}$$

$$\theta_p = \tan^{-1}\left(\frac{\sin\phi_p\,(\bar{a}_{p1}\cos\psi_p + \bar{a}_{p2}\sin\psi_p + F_p\sin\gamma_p)}{(\bar{a}_{p2}\cos\psi_p - \bar{a}_{p1}\sin\psi_p)\cos\gamma_p}\right) \tag{4.54}$$

$$T_p = \frac{\bar{a}_{p2}\cos\psi_p - \bar{a}_{p1}\sin\psi_p}{\cos\theta_p\sin\phi_p}\,m_p \tag{4.55}$$

where, $F_p = (\bar{a}_{p2}\cos\psi_p - \bar{a}_{p1}\sin\psi_p)\cos\gamma_p\,(-f_{x_p}\sin\psi_p + f_{y_p}\cos\psi_p) + g\cos\gamma_p$

$$+ V_p^2\cos^3\gamma_p\;(f_{xx_p}\cos^2\psi_p + 2\,f_{yx_p}\sin\psi_p\cos\psi_p + f_{yy_p}\sin^2\psi_p)$$

Note that the equations (4.53) - (4.55) used the vertical force component constraint expressed in (4.46). A similar set of expressions may be obtained for the evader also.

4.3.3 Linear Quadratic Pursuit-Evasion Game

With the definition of position vector

$$r_p = \begin{pmatrix} x_p \\ y_p \end{pmatrix} \tag{4.56}$$

the feedback linearized vehicle models (4.47), (4.48) may be expressed in the standard state variable form as:

$$\dot{r}_p = v_p\,,\; r_p(t_0) \text{ given} \tag{4.57a}$$

$$\dot{r}_e = v_e\,,\; r_e(t_0) \text{ given} \tag{4.57b}$$

$$\dot{v}_p = a_p\ ,\ v_p(t_0) \text{ given} \tag{4.57c}$$

$$\dot{v}_e = a_e\ ,\ v_e(t_0) \text{ given} \tag{4.57d}$$

Next, introducing the relative coordinates, one has

$$r = r_p - r_e \tag{4.58a}$$

$$v = v_p - v_e \tag{4.58b}$$

These dynamic equations can be written in a more succinct form as

$$\begin{bmatrix} \dot{r} \\ \dot{v} \end{bmatrix} = \begin{bmatrix} 0 & I \\ 0 & 0 \end{bmatrix} \begin{bmatrix} r \\ v \end{bmatrix} + \begin{bmatrix} 0 \\ I \end{bmatrix} (a_p - a_e) \tag{4.59}$$

Where 0 is a 2 x 2 zero matrix and I is a 2 x 2 identity matrix. The control variables in the model are the acceleration components in the earth fixed coordinate system. The pursuer uses the control a_p to attempt to capture the evader, while the evader uses the control a_e to avoid capture.

To further simplify notation, write the above equation as

$$\dot{\xi} = F\xi + Gu \tag{4.60}$$

with

$$F = \begin{bmatrix} 0 & I \\ 0 & 0 \end{bmatrix} \quad G = \begin{bmatrix} 0 \\ I \end{bmatrix} \quad \xi = \begin{bmatrix} r \\ v \end{bmatrix} \quad u = a_p - a_e$$

The objective of the pursuer is to minimize the terminal miss, which the pursuer attempts to maximize. The terminal miss is defined here as

$$\frac{1}{2} r^T(t_f) S_f r(t_f) \tag{4.61}$$

The superscript T denotes the transpose of the vector and S_f is a positive semidefinite matrix. Integral quadratic acceleration constraints are next imposed on both the pursuer and the evader to make this game meaningful, and also to enable the application of the well known Linear-Quadratic game results [12]. These constraints are included using two positive definite weighting matrices W_p and W_e.

Adjoining these constraints to the performance index, one has

$$J = \min_{a_p} \max_{a_e} \frac{1}{2} r^T(t_f) S_f r(t_f) + \frac{1}{2} \int_{t_0}^{t_f} (a_p^T W_p a_p - a_e^T W_e a_e) dt \quad (4.62)$$

The saddle-point solution to this problem is given by [12]

$$a_p = - W_p^{-1} G^T S \begin{bmatrix} r \\ v \end{bmatrix} \quad (4.63)$$

$$a_e = - W_e^{-1} G^T S \begin{bmatrix} r \\ v \end{bmatrix} \quad (4.64)$$

The matrix S is the solution of the matrix Riccati equation

$$\dot{S} = -SF - F^T S + SG(W_p^{-1} - W_e^{-1})G^T S \quad (4.65)$$

with the terminal condition

$$S(t_f) = \begin{bmatrix} S_f & 0 \\ 0 & 0 \end{bmatrix}$$

In order to obtain solutions in the general case, the matrix Riccati equation (4.65) has to be integrated backwards in time. To illustrate the present solution further, simplifications will be introduced in this problem.

If S_f, W_p, and W_e were constant diagonal matrices with $S_f(i,i) = \sigma_i$, $W_p(i,i) = 1/\alpha_i$ and $W_e(i,i) = 1/\beta_i$, i = 1, 2, the saddle point solution can be expressed in the form

$$a_p = k_1 r + k_2 v \tag{4.66}$$

$$a_e = k_3 \; a_p \tag{4.67}$$

In the expressions (4.66) and (4.67), k_1, k_2 and k_3 are 2 x 2 diagonal feedback gain matrices with

$$k_1(i,i) = \frac{-\alpha_i \, t_{go}}{\frac{1}{\sigma_i} + (\alpha_i - \beta_i)\frac{t_{go}^3}{3}} \;, \; i = 1, 2 \tag{4.68}$$

$$k_2(i,i) = k_1(i,i) \, t_{go} \;, \; i = 1, 2 \tag{4.69}$$

$$k_3(i,i) = \frac{\beta_i}{\alpha_i} \;, \; i = 1, 2 \tag{4.70}$$

The time-to-go required for the computation of feedback gains is defined as

$$t_{go} = t_f - t \tag{4.71}$$

While implementing this guidance law, it is preferable to compute t_{go} using feedback information. This is because the vehicle model is approximate. Consequently, the specified final time will not be equal to the actual time for capture. In the following, a method for computing the time-to-go will be discussed.

4.3.4 Terminal Time Estimation

Guidance scheme discussed in the foregoing requires an accurate estimate of time-to-go for satisfactory operation. Several methods for calculating this quantity are available in the missile guidance literature [91, 92]. However, most of the reported time-to-go calculation methods neglect the two-player nature of an engagement scenario. In Reference

93, an exact method for calculating time-to-go was outlined. This approach is developed for the present differential game in the ensuing.

Since the transformed min-max problem in Subsection 4.3.2 does not explicitly depend on time, the variational Hamiltonian is constant, i.e.,

$$H(t_0) = H(t) = H(t_f) = \text{constant} \tag{4.72}$$

If the desired conditions at the termination of the differential game can be defined in terms of the final differential position and velocity components, it is possible to evaluate the variational Hamiltonian at the final time. This is feasible in the present problem since the control variables are available in state feedback form with time-to-go as the only unknown parameter. Next, equating the numerical value of the corresponding expression at the initial time results in a polynomial in time-to-go. A positive real solution of this polynomial is then the exact value of time-to-go. In case of multiple solutions, the smallest value may be selected. For further details on the calculation of time-to-go, refer to Reference 93.

For the present application, assuming that the weighting matrices S_f, W_p, and W_e are identity matrices multiplied by scalars σ, $1/\alpha$, and $1/\beta$, respectively, the polynomial equation for the terminal time is as follows [93]:

$$R^2 \{\frac{1}{\sigma} + \frac{(\alpha - \beta)t_f^3}{3}\}^2 = (\Delta x + \Delta \dot{x}\, t_f)^2 + (\Delta y + \Delta \dot{y}\, t_f)^2 \tag{4.73}$$

where

$$R^2 = \{(x_p - x_e)^2 + (y_p - y_e)^2\}|_{t_f}$$

$$\Delta x = (x_p - x_e)|_{t_0}\,, \quad \Delta \dot{x} = (\dot{x}_p - \dot{x}_e)|_{t_0}$$

$$\Delta y = (y_p - y_e)|_{t_0}\,, \quad \Delta \dot{y} = (\dot{y}_p - \dot{y}_e)|_{t_0}$$

Note that the quantity R defines the capture radius.

If the current time is assumed to be the initial time and set to zero, $t_{go} = t_f$. The roots of this sixth order polynomial are the values of time-to-go. Since there are six possible values, the smallest real positive value needs to be used. In the present work, the roots were found using the method of golden section.

4.3.5 Numerical Results

Two scenarios are examined for the pursuer and evader starting at the coordinates (4000, 4000) and (5000, 5000), respectively. In both engagements, the weighting factors are chosen as follows: $\sigma = 1.0$, $\alpha = 0.0007$, and $\beta = 0.00001$.

Figure 4.11 shows the trajectories for the pursuer and evader both with zero initial heading angles. The corresponding velocity histories are shown in Figure 4.12. The speed variations occurring due to the terrain profile can be seen to affect the pursuer to a higher degree. This is because the pursuer is assumed to have a higher acceleration capability when compared with the evader. Load factor histories for two helicopters are given in Figure 4.13. The load factor is defined here as the ratio of main rotor thrust and the helicopter weight. Evader's thrust appears to be smoother than the pursuer's. Figures 4.14 and 4.15 illustrate roll and pitch attitudes of helicopters. Various features appearing in these figures arise from the terrain profiles. Altitude histories for two helicopters are shown in Figure 4.16.

In the the second scenario the pursuer has an initial heading angle 90 angles and the evader is at a 0 degree heading angle. The resulting trajectories are shown in Figure 4.17. As may be observed in Figure 4.18, this game involves the typical turn-and-dash strategy. To turn quickly, the pursuer first decelerates and then accelerates to catch the evader. Figure 4.19 shows load factor histories. Figures 4.20 and 4.21 show the corresponding

roll and pitch attitude histories. Altitude histories for two helicopters are given in Figure 4.22.

4.4 Conclusion

The helicopter pursuit-evasion problem while executing the terrain-following/terrain-avoidance mode was studied in this chapter. Numerical methods for obtaining solutions to these problems were outlined. As an alternative to numerical method, feedback linearizing transformations were combined with the linear quadratic game results to synthesize explicit nonlinear feedback strategies for helicopter pursuit-evasion. Further investigation of these solutions will be of future interest.

CHAPTER V

PERFORMANCE VERIFICATION

5.1 Introduction

The one-sided optimal trajectory planning schemes of the helicopter discussed in Chapter III considered only the kinematic equations. The objective there was to make the optimal control problem analytically tractable. To verify whether the generated trajectories satisfy the physical constraints, these need to be evaluated on a detailed simulation of a helicopter .

In this report, a six degree of freedom helicopter simulation program called the "TMAN" [21] is used for evaluating the generated trajectory. This program was developed from a more general helicopter simulation program called ARMCOP [94]. This computer code is being used in the Vertical Motion Simulator to conduct piloted simulation of helicopter flight including air combat at NOE flight levels. Previously, a path planning scheme using dynamic programming [8] has been tested at the NASA Ames Research Center using this program.

The TMAN program incorporates a six-degree-of-freedom rigid body vehicle model, a first order engine lag response, a simple closed form trim solution, and linearized quasi-static aerodynamic force and moment equations. Originally, this program was designed to

simulate a generic helicopter motion in response to a joy stick. As a result, a coarse stability augmentation system is incorporated in the simulation. Recently, Heiges [19, 59] developed a trajectory controller for this helicopter model using feedback linearization. The TMAN program together with the controller developed in [59] is used in this report to evaluate some of the trajectories generated in Chapter III.

5.2 Simulation Results

Trajectories given in Figure 3.6 are used for evaluating the helicopter performance. Note that these trajectories were generated with the constant airspeed assumption. The airspeed employed in the present investigation is extracted from the available helicopter performance data. For example, Reference 82 has presented AH-1S data for both maximum rate of climb and rate of descent over its entire speed regime. This data is summarized in Table 5.1. It may be observed from this table that over the density altitude 1000 to 3000 feet range, the maximum rate of climb varies between 8 ft/sec to 36 ft/sec. The best rate of climb appears to occur at an airspeed about 100 ft/sec. Since the TMAN program uses an AH-1S type helicopter data, all simulations were carried out at this speed.

Figures 5.1 through 5.8 illustrate the helicopter responses for the maximum terrain masking trajectory while Figures 5.9 - 5.16 give the simulation results along the minimum flight time trajectory. Figures 5.1 and 5.9 show the altitude rate for both trajectories. The maximum altitude rates are about 35 ft/sec. The nonlinear controller [19] was designed on an assumption that the cyclic stick and pedals are primarily moment generating controls and do not make a significant contribution to the body forces. The collective is the only direct force control. Since airspeed is constant in these simulations, altitude change primarily

affects the collective control. Figures 5.5 and 5.13 give collective control histories for both trajectories.

As pointed out in Reference 2, the flight along the maximum terrain masking requires frequent and severe rolling and yawing motion than the flight along the minimum time trajectory. This is because the helicopter seeks to fly at low altitudes to maximize terrain masking. The maximum bank angles for the terrain masking and minimum time trajectories are about 12 and 6 degrees as shown in Figures 5.7 and 5.15, respectively. The maximum heading angle change in the case of maximum masking trajectory is nearly 40 degrees as depicted in Figure 5.8. The maximum heading change in the case of minimum time is only 15 degrees (see Figure 5.16). From Figures 5.6 and 5.14, it is evident that the minimum pitch angle is approximately -6.0 for both cases.

These simulations indicate that the synthesized trajectories are implementable in helicopter simulations provided that the airspeeds along these paths are chosen carefully. It may be necessary to synthesize an acceleration control loop in the helicopter model to ensure adequate ride quality. Clearly, the man-machine interface issues have to be sufficiently addressed before attempting a full scale piloted simulation. These issues will be of future research interest.

CHAPTER VI

CONCLUSIONS AND FUTURE RESEARCH

This report systematically analyzed trajectory planning schemes for the helicopter terrain-following/terrain-avoidance flight by employing optimal control theory and differential game theory. Numerical algorithms for trajectory synthesis have been developed and validated through simulation. With adequate computing resources, trajectory planning methods developed here appear to be implementable on-board the helicopter.

6.1 Concluding Remarks

For the first optimal route planning method, the terrain constraint was embedded into state equations via a coordinate transformation. The performance index here consisted of a linear combination of flight time and terrain masking. Using an adjoint-control transformation, the optimal control problem solution was reduced to a search for the initial value of heading angle. It was shown that the optimal airspeed, a second control variable in the formulation, should be chosen as the maximum permissible value. A simple computational scheme based on the method of bisections and a fifth order Kutta-Merson numerical integration technique was outlined for generating Euler solutions. Families of Euler solutions for minimum flight time and maximum terrain masking were presented.

It was shown that the Legendre-Clebsch necessary condition and Weierstrass excess function are satisfied everywhere in the admissible region. Further, conjugate points have been shown to occur in certain regions of the specified terrain. In the regions where conjugate points do not occur, the Euler solutions for the maximum masking problem provide a strong local minimum. The Euler solutions for the minimum time problem satisfying the second-order necessary conditions were shown to provide a global minimum.

For the second optimal route planning scheme, the performance index consisted of a quadratic form in the terrain altitude, lateral deviation from a nominal trajectory, and the heading angle. By changing the independent variable from time to down-range, the order of the problem was reduced. Once again, the Euler solutions for this problem was shown to require a one dimensional search. The numerical flow chart developed for the previous trajectory planning scheme was shown to be useful for this problem.

The Legendre-Clebsch necessary condition and Weierstrass excess function were shown to be satisfied everywhere in the admissible region. For this problem, an approximate conjugate point test was developed using the WKB method.

The wind effects on the trajectories were briefly examined for the first optimal route planning problem. It was found that the winds affect the terrain masking trajectory to a higher degree than the time optimal path.

Trajectory planning problem was next formulated as a differential game to synthesize optimal trajectories in the presence of an actively maneuvering adversary. Numerical methods for obtaining solutions to these problems were outlined. As an alternative to numerical method, feedback linearizing transformations were combined with the linear quadratic game results to synthesize explicit nonlinear feedback strategies for helicopter pursuit-evasion.

The one-sided trajectory planning schemes were based on the kinematic equations of the helicopter. To verify whether the generated trajectories satisfy the physical constraints, these trajectories were tested on a 6 DOF helicopter simulation using a currently available flight path controller. The results indicate that the synthesized trajectories are implementable provided the airspeed along these paths is chosen carefully.

6.2 Future Research

Based on the results of this study, the following research areas are recommended for further research into the NOE guidance problem.

Real Time Simulation and Flight Testing

As mentioned in Chapter V, NASA Ames Research Center is testing a path planning scheme based on the dynamic programming method. The present trajectory planning scheme appears to be a viable alternative candidate, thus it needs to be evaluated on the Vertical Motion Simulator. Such an investigation would reveal various issues relating to both man-machine interface and helicopter physical constraints.

Use of Alternative Performance Indices

Use of performance indices other than minimum time and maximum masking need to be investigated. For example, a weighted combination of time, masking, and flight path angle can be considered. Constraining the flight-path angle would have the effect of limiting the helicopter climb/descent rate. Since the rate of climb for a helicopter is related to the excess power, such a limit on the climb rate may be required in real applications.

Helicopter Dynamics in NOE Flight

The NOE operation requires helicopter fly close to the ground to avoid detection and operate at low speeds to avoid collisions with unknown obstacles. This low-altitude/low-airspeed flight regime is unique to the helicopter, and yet the least studied out of all the flight regimes. Operation in the close proximity of ground brings in the need for studying this flight regime in greater detail.

Time-varying Obstacle Avoidance

Known and stationary obstacles may be incorporated into the trajectory planning problem by overlaying the artificial envelope on the terrain map as discussed in Chapter III. However, there exist only few path planning schemes examining the problem of avoiding the time-varying obstacles, such as schemes for thunder-storm avoidance. References 95 and 96 may be useful in understanding how the time-varying obstacle can be included in the analysis.

These and other research items will be of future interest.

APPENDIX A

TANGENT PLANE AND THE COORDINATE TRANSFORMATION

A.1 Introduction

The purpose of this appendix is to define the tangent plane oriented coordinate system used in the development of the route planning problem discussed in Chapters III and IV. Further, the development of a transformation relating vectorial quantities in the tangent plane coordinate system to an inertial frame will be developed.

A.2 Tangent Plane

Referring to Figure 3.1, let $P(x_o, y_o, z_o)$ be any point on the surface $z = f(x,y)$. If $f(x,y)$ is differentiable at (x_o, y_o) then the surface has a tangent plane at P. If f_x and f_y are the gradients of the surface along x and y directions, then the equation describing this plane is given by [74]

$$-f_x(x_o, y_o)\,(x - x_o) - f_y(x_o, y_o)\,(y - y_o) + (z - z_o) = 0 \qquad \text{(A.1)}$$

Moreover, the vector

$$\vec{N} = -f_x \vec{i} - f_y \vec{j} + \vec{k} \qquad \text{(A.2)}$$

is normal to the surface at point P. A line which is normal to the surface at P has

parametric equations

$$x = x_o - f_x((x_o, y_o)\, t$$
$$y = y_o - f_y((x_o, y_o)\, t \qquad (A.3)$$
$$z = z_o + t$$

where t is an arbitrary parameter.

A.3 Coordinate Transformation

The following discusses the transformation of quantities in tangent plane coordinate system to the inertial frame. From (A.2), unit normal vector is given by

$$\vec{n} = \frac{-f_x \vec{i} - f_y \vec{j} + \vec{k}}{\sqrt{1 + f_x^2 + f_y^2}} \qquad (A.4)$$

Select a unit tangent vector as

$$\vec{t_1} = \frac{\vec{i} + f_x \vec{k}}{\sqrt{1 + f_x^2}} \qquad (A.5)$$

This unit tangent vector direction is parallel to the plane containing the inertial coordinates x and z. Next, the cross-product between the tangent and normal vectors may be used to obtain a unit vector orthogonal to these two vectors using the cross-product as follows:

$$\vec{t_2} = \vec{t_1} \times \vec{n} \qquad (A.6)$$

i.e.,

$$\vec{t_2} = \frac{f_x f_y \vec{i} - (1 + f_x^2)\, \vec{j} - f_y \vec{k}}{\sqrt{1 + f_x^2}\sqrt{1 + f_x^2 + f_y^2}} \qquad (A.7)$$

On the tangent plane, the kinematic equations of motion of a particle can be described as

$$\dot{x}_\ell = V \cos \chi$$
$$\dot{y}_\ell = V \sin \chi \tag{A.8}$$

Here, χ is the angle made by the velocity vector V with the tangent vector $\vec{t}_1$. Note that the component of the velocity vector normal to the surface is zero. This is because of the fact that the vehicle is executing a terrain following flight. The subscript ℓ denotes the local coordinate system.

The transformation of the velocity vector in the local coordinates system to the inertial frame may be accomplished using the following:

$$\begin{bmatrix} \dot{x} \\ \dot{y} \\ \dot{z} \end{bmatrix} = \begin{bmatrix} \cos(x_\ell,x) & \cos(y_\ell,x) & \cos(z_\ell,x) \\ \cos(x_\ell,y) & \cos(y_\ell,y) & \cos(z_\ell,y) \\ \cos(x_\ell,h) & \cos(y_\ell,h) & \cos(z_\ell,h) \end{bmatrix} \begin{bmatrix} \dot{x}_\ell \\ \dot{y}_\ell \\ 0 \end{bmatrix} \tag{A.9}$$

The direction cosines can be obtained as

$$\begin{bmatrix} \dot{x} \\ \dot{y} \\ \dot{z} \end{bmatrix} = \begin{bmatrix} \langle \vec{t}_1, \vec{i} \rangle & \langle \vec{t}_2, \vec{i} \rangle & \langle \vec{n}, \vec{i} \rangle \\ \langle \vec{t}_1, \vec{j} \rangle & \langle \vec{t}_2, \vec{j} \rangle & \langle \vec{n}, \vec{j} \rangle \\ \langle \vec{t}_1, \vec{k} \rangle & \langle \vec{t}_2, \vec{k} \rangle & \langle \vec{n}, \vec{k} \rangle \end{bmatrix} \begin{bmatrix} \dot{x}_\ell \\ \dot{y}_\ell \\ 0 \end{bmatrix} \tag{A.10}$$

where $\langle \cdot, \cdot \rangle$ denotes the inner product.

Thus, the kinematic equations of motion over the terrain profile becomes

$$\dot{x} = \frac{V \cos \chi}{\sqrt{1 + f_x^2}} + \frac{f_x f_y V \sin \chi}{\sqrt{1 + f_x^2}\sqrt{1 + f_x^2 + f_y^2}} \tag{A.11}$$

$$\dot{y} = -\frac{\sqrt{1+f_x^2}\ V \sin\chi}{\sqrt{1+f_x^2+f_y^2}} \tag{A.12}$$

$$z = f(x,y) \tag{A.13}$$

These equations were used in the trajectory planning schemes discussed in Chapters III and IV.

APPENDIX B

NUMERICAL CONJUGATE POINT TESTING FOR FIXED END-POINTS PROBLEMS

B.1 Introduction

The need for conjugate point test in the calculus of variations arise from the requirement that the second variation evaluated along an optimal path must be greater than zero for all admissible variations of states and costates. A pointwise test for the sign of second variation is the well known Legendre-Clebsch necessary condition. For extremals of finite length, however, the task of ensuring that the second variation is positive for all admissible neighboring paths is more involved [73]. The proposed Jacobi test [97] seeks the minimum value of the second variation. This problem is called the accessory minimum problem. The objective here is to find a system of variations which gives the value of zero to the second variation. If this is possible, it implies that a neighboring path is competitive and that the extremal furnishes at best an improper minimum of performance index and at worst merely a stationary value.

Analytical conjugate point test is impossible in all but very simple optimal control problems. However, a family of numerical methods are available in the literature. This appendix examines three of these techniques. The first two are very general, while the third approach is useful in more classical situations such as the optimal trajectory planning

problem discussed in Chapter III. All these methods are equivalent, although some are numerically more efficient than others.

B.2 Second Variation

Consider the general optimal control problem described in Chapter II.

$$\dot{x} = f(x,u,t) \ , \qquad x(t_0) = x_0 \tag{B.1}$$

$$\dot{\lambda} = - H_x \tag{B.2}$$

$$H_u = 0 \tag{B.3}$$

$$H\ (x,u,\lambda,t) = L\ (x,u,t) + \lambda^T\ f\ (x,u,t) \tag{B.4}$$

$$P\ (x(t_f),t_f) = 0 \tag{B.5}$$

$$Q(x(t_f),t_f) \ = \ g(x(t_f),t_f) + \nu^T P(x(t_f),t_f) \tag{B.6}$$

$$\lambda^T(t_f) = \frac{\partial Q}{\partial x}\Big|_{t_f} \tag{B.7}$$

The augmented performance index is given by:

$$J^a = Q(x(t_f),t_f) + \int_{t_0}^{t_f} \{H(x,u,\lambda,t) - \lambda^T \dot{x}\}\ dt \tag{B.8}$$

Expanding the augmented performance index (B.8) to second order [12], one has

$$\Delta J^a = \delta J^a + \frac{1}{2}\delta^2 J^a + \text{higher order terms}$$

$$= Q\delta x(t_f) - \lambda^T(t_f)\delta x(t_f) + \int_{t_0}^{t_f} [(\lambda+H_x)\,\delta x+H_u\,\delta u]\;dt + \frac{1}{2}\delta x^T(t_f)\frac{\partial^2 Q}{\partial x^2}\delta x(t_f)$$

$$+\frac{1}{2}\int_{t_0}^{t_f}\begin{bmatrix}\delta x^T & \delta u^T\end{bmatrix}\begin{bmatrix}H_{xx} & H_{xu}\\ H_{ux} & H_{uu}\end{bmatrix}\begin{bmatrix}\delta x\\ \delta u\end{bmatrix} dt + \text{h.o.t.} \qquad \text{(B.9)}$$

Since the first variation terms vanish along every stationary trajectory, second-variation becomes

$$\delta^2 J^a = \delta x^T(t_f)\frac{\partial^2 Q}{\partial x^2}\delta x(t_f) + \int_{t_0}^{t_f}\begin{bmatrix}\delta x^T & \delta u^T\end{bmatrix}\begin{bmatrix}H_{xx} & H_{xu}\\ H_{ux} & H_{uu}\end{bmatrix}\begin{bmatrix}\delta x\\ \delta u\end{bmatrix} dt \qquad \text{(B.10)}$$

The differential constraints and boundary conditions in this problem are

$$\dot{\delta x} = f_x\delta x + f_u\delta u, \qquad \text{(B.11)}$$

$$\delta x(0) = 0, \qquad \text{(B.12)}$$

$$\delta P = [\,P_x\,\delta x]_{t_f} = 0 \qquad \text{(B.13)}$$

The accessory minimum problem attempts to find the minimum value of the second variation (B.10) subject to the differential constraints (B.11) and boundary conditions (B.12), (B.13). The Euler-Lagrange equations for this accessary minimum problem are given by

$$\dot{\delta\lambda} = -\,H_{xx}\delta x - f_x^T\delta\lambda - H_{xu}\delta u \qquad \text{(B.14)}$$

$$H_{ux}\,\delta x + f_u^T\delta\lambda + H_{uu}\,\delta u = 0 \qquad \text{(B.15)}$$

$$\delta\lambda(t_f) = \{g_{xx} + (\nu^T P_x)_x\}\delta x\,\Big|_{t_f} \qquad \text{(B.16)}$$

If one assumes that control is nonsingular (i.e., $H_{uu} \neq 0$), the expression (B.15) may be put in the form

$$\delta u = -H_{uu}^{-1}(H_{ux}\delta x + f_u^T \delta\lambda) \tag{B.17}$$

In this case, one may substitute for δu in (B.14) and (B.11) resulting in

$$\begin{bmatrix} \dot{\delta x} \\ \dot{\delta\lambda} \end{bmatrix} = \begin{bmatrix} A(t) & -B(t) \\ -C(t) & -A^T(t) \end{bmatrix} \begin{bmatrix} \delta x \\ \delta\lambda \end{bmatrix} \tag{B.18}$$

where,

$$A(t) = f_x - f_u H_{uu}^{-1} H_{ux},$$

$$B(t) = f_u H_{uu}^{-1} f_u^T,$$

$$C(t) = H_{xx} - H_{xu} H_{uu}^{-1} H_{ux}.$$

This set of linear differential equations must satisfy the boundary conditions (B.12), (B.13), and (B.16).

B.3 The Riccati Equation Method

Since the accessary minimum problem (B.18) is linear and the differential equations and the terminal boundary conditions are homogeneous, both $\delta x(t)$ and $\delta\lambda(t)$ are proportional to $\delta x(t_0)$, or proportional to $\delta\lambda(t_f)$. Using the backward sweep [41], where in one assumes a solution of the form

$$\delta\lambda(t) = S(t)\, \delta x(t), \quad S(t_f) = Q_{xx} \tag{B.19}$$

a matrix Riccati equation can be obtained as follows [71]:

$$\dot{S} = - SA - A^T S + SBS - C, \; S(t_f) = Q_{xx} \tag{B.20}$$

Existence of a bounded symmetric-matrix S to the matrix Riccati equation (B.20) determines the existence of a conjugate point. In other words, if S becomes infinite at any point $\hat{t}$ along a test extremal, then the second variation is zero in the interval $[t_0, \hat{t}]$. In such a case, a neighboring extremal may furnish a lower value of the performance index.

B.4 The Kelly-Moyer Method

Regarding the linearized Euler equations (B.18) as a mapping between the variations of unspecified initial costates, $\delta\lambda_i(0)$ (i = 1, 2, 3,···, n), and the variations of states, $\delta x_i(t)$ (i = 1, 2, 3,···, n), the following can be written

$$\begin{bmatrix} \delta x_1(t) \\ \delta x_2(t) \\ \vdots \\ \delta x_n(t) \end{bmatrix} = \begin{bmatrix} \frac{\partial x_1}{\partial \lambda_{1_0}} & \frac{\partial x_1}{\partial \lambda_{2_0}} & \cdots & \frac{\partial x_1}{\partial \lambda_{n_0}} \\ \vdots & \vdots & \vdots & \vdots \\ \frac{\partial x_n}{\partial \lambda_{1_0}} & \frac{\partial x_n}{\partial \lambda_{2_0}} & \cdots & \frac{\partial x_n}{\partial \lambda_{n_0}} \end{bmatrix} \begin{bmatrix} \delta\lambda_1(0) \\ \delta\lambda_2(0) \\ \vdots \\ \delta\lambda_n(0) \end{bmatrix} \tag{B.21}$$

where $\lambda_{i_0} \equiv \lambda_i(0)$, i = 1, 2,..., n .

Setting

$$M(t) = \begin{bmatrix} \frac{\partial x_1}{\partial \lambda_{1_0}} & \frac{\partial x_1}{\partial \lambda_{2_0}} & \cdots & \frac{\partial x_1}{\partial \lambda_{n_0}} \\ \vdots & \vdots & \vdots & \vdots \\ \frac{\partial x_n}{\partial \lambda_{1_0}} & \frac{\partial x_n}{\partial \lambda_{2_0}} & & \frac{\partial x_n}{\partial \lambda_{n_0}} \end{bmatrix} \tag{B.22}$$

Kelly [73], Cicala [75], and Moyer [98] showed that the rank of the matrix M(t) provides the criterion for the existence of a conjugate point. If the rank of the matrix M(t) drops at any point along the extremal, it indicates the existence of a conjugate point. In other words, neighboring extremals starting at t_0 in n-dimensional state space must collapse into a smaller dimension at a conjugate point.

B.5 The Bliss Method

In Reference 70, a numerical method for conjugate point testing was suggested. For a two dimensional system, if four fundamental solutions (x_i, y_i) $(i = 1,2,3,4)$ to the linearized Euler-Lagrange equations can be obtained, then the determinant of the matrix

$$d(t) = \begin{bmatrix} x_1 & x_2 & x_3 & x_4 \\ y_1 & y_2 & y_3 & y_4 \\ \dot{x}_1 & \dot{x}_2 & \dot{x}_3 & \dot{x}_4 \\ \dot{y}_1 & \dot{y}_2 & \dot{y}_3 & \dot{y}_4 \end{bmatrix} \tag{B.23}$$

will be non-zero. Since (x_i,y_i) (i = 1,2,3,4) are the solutions of the two dimensional accessory minimum problem, their linear combination is also a solution of the accessory system. Thus,

$$x = c_1x_1 + c_2x_2 + c_3x_3 + c_4x_4$$
$$y = c_1y_1 + c_2y_2 + c_3y_3 + c_4y_4 \tag{B.24}$$

This fact is exploited in the following theorem. In (B.23), note that (x_i,y_i) (i = 1,2,3,4) can be computed from the linearized costate equations.

Theorem *In a two dimensional variational problem, if four solutions (x_i,y_i) (i = 1,2,3,4) of the accessory equations of a nonsingular extremal arc are formed as a matrix and if the determinant of matrix*

$$D(t,t_0) = \begin{bmatrix} x_1(t) & x_2(t) & x_3(t) & x_4(t) \\ y_1(t) & y_2(t) & y_3(t) & y_4(t) \\ x_1(t_0) & x_2(t_0) & x_3(t_0) & x_4(t_0) \\ y_1(t_0) & y_2(t_0) & y_3(t_0) & y_4(t_0) \end{bmatrix} \tag{B.25}$$

is not identically zero, then the conjugate point to point$(x(t_0),y(t_0))$ is the $(x(t),y(t))$ which makes determinant of matrix $D(t,t_0)$ zero.

Since the initial conditions on x_1, x_2, y_1, y_2 are arbitrary, matrix $D(t,t_0)$ can be re-expressed as

$$D(t,t_0) = \begin{bmatrix} x_1(t) & x_2(t) & x_3(t) & x_4(t) \\ y_1(t) & y_2(t) & y_3(t) & y_4(t) \\ 0 & 0 & x_3(t_0) & x_4(t_0) \\ 0 & 0 & y_3(t_0) & y_4(t_0) \end{bmatrix} \tag{B.26}$$

The determinant of this matrix D can be changed using Laplace Expansion as follows:

$$\Delta(t,t_0) = \begin{vmatrix} x_1(t) & x_2(t) \\ y_1(t) & y_2(t) \end{vmatrix} \begin{vmatrix} x_3(t_0) & x_4(t_0) \\ y_3(t_0) & y_4(t_0) \end{vmatrix} \tag{B.27}$$

The second determinant of right-hand side in above equation (B.27) is arbitrary. Hence, for $\Delta(t,t_0)$ to be zero, the characteristic determinant

$$\Delta(t) = \begin{vmatrix} x_1(t) & x_2(t) \\ y_1(t) & y_2(t) \end{vmatrix} \tag{B.28}$$

should be zero at conjugate point $t = t^*$, $t_0 < t^* \leq t_f$.

B.6 Relationship

Jacobi's differential equations, or accessory system of differential equations, are linear and homogeneous. There exist two well-known methods for solving linear two-point boundary-value problems [12]: the backward sweep method and the transition matrix method. The backward sweep method results in the Riccati equations. On the other hand, Kelly-Moyer and Bliss Methods are based on the state transition matrix.

Relationship of Riccati Equation Method and Kelly-Moyer Method

To test conjugate point by Kelly-Moyer method, the sign of determinant of matrix M(t) should be evaluated along the extremal. Equation (B.18) can be rewritten in terms of the partitioned transition matrix $\Phi(t,t_0)$ as

$$\begin{bmatrix} \delta x(t) \\ \delta\lambda(t) \end{bmatrix} = \begin{bmatrix} \Phi_{xx}(t,t_0) & \Phi_{x\lambda}(t,t_0) \\ \Phi_{\lambda x}(t,t_0) & \Phi_{\lambda\lambda}(t,t_0) \end{bmatrix} \begin{bmatrix} \delta x(t_0) \\ \delta\lambda(t_0) \end{bmatrix} \tag{B.29}$$

Using the expression (B.21), one can find out that

$$M(t) = \Phi_{x\lambda}(t,t_0) \tag{B.30}$$

From the forward sweep equation, one has [12]

$$\delta\lambda(t_0) = S(t_0)\,\delta x(t_0) \tag{B.31}$$

From this,

$$M^{-1}(t) = S(t,t_0) \tag{B.32}$$

Relationship of Kelly-Moyer Method and Bliss Method

The following corollary given by Bliss illustrates the relationship between the Kelly-Moyer method and Bliss method.

Corollary *In a two dimensional variational problem, if the accessory equations of a nonsingular extremal arc are a trajectory of a four-parameter family*

$$x(t,a,b,c,d), \qquad y(t,a,b,c,d) \tag{B.33}$$

then the conjugate point to a point t_0 is determined by the zeros t of the determinant of matrix

$$D(t,t_0) = \begin{bmatrix} x_a(t) & x_b(t) & x_c(t) & x_d(t) \\ y_a(t) & y_b(t) & y_c(t) & y_d(t) \\ x_a(t_0) & x_b(t_0) & x_c(t_0) & x_d(t_0) \\ y_a(t_0) & y_b(t_0) & y_c(t_0) & y_d(t_0) \end{bmatrix} \tag{B.34}$$

provided that the determinant of matrix D is not identically zero along trajectory.

B.7 Numerical Effort

All matrices mentioned in the foregoing are n by n. Thus, there is no difference in the size of matrix. To find the existence of conjugate point, however, the first method based on backward sweep checks the boundedness of a matrix, but the methods based on the transition matrix, Kelly-Moyer method and Bliss method, check the sign of determinant of the matrix. The latter approach is numerically better conditioned.

The matrix Riccati method requires the integration of $n \times n$ equations and thus demands a formidable amount of calculations. Primary difficulty here is the requirement for various partial derivatives. In the present case, this would mean the computation of higher order terrain gradients.

The numerical evaluation of the elements of Kelly-Moyer method evidently requires computer codes considerably more complex than those required for the calculation of Euler solutions. As an alternative to partial derivatives, Menon [99] used a scheme in which the partial derivatives with respect to the λ_{i_0} are calculated approximately in terms of difference quotients. Thus, small increments in the λ_{i_0} are employed in the evaluation of neighboring solutions of the extremal.

The numerical Bliss method is similar to the Kelly-Moyer method. Instead of partial derivatives, fundamental solutions are obtained numerically. As an alternative to fundamental solutions, in the present work a computer code was assembled based on the finite differences. This code generates three trajectories corresponding to each heading angle, the first being the nominal and next two, the neighboring trajectories obtained by perturbing the initial value of the heading angle by a small amount in the positive and negative sense. This is equivalent to perturbing the initial values of costates while

enforcing the constant of motion. The required fundamental solutions are then computed using a finite difference scheme.

The main difficulty encountered in both finite difference quotients computations [99] and finite difference method is the errors arising from higher order effects. These errors can be controlled to a certain extent by verifying the linearity of the x(t) and y(t) differences versus the magnitude of the corresponding increment in the initial heading angle. This check can be incorporated in the computer program.

If the final end-point is not fixed, the matrix Riccati method requires additional matrix calculation, see Reference 12 for further details.

APPENDIX C

SEPARABILITY OF THE HAMILTONIAN AND ITS CONSEQUENCE ON DIFFERENTIAL GAME SOLUTIONS

C.1 Introduction

While discussing the trajectory planning schemes in Chapter IV, it was pointed out that in order to ensure that the outcome of the game is not influenced by the order of action, the value of the game should exist. The value exists only when the final performance index has a saddle point. The conditions for the existence of the saddle point are the separability of the variational Hamiltonian and continuous mapping. In the following, each of these issues will be elaborated.

C.2 Separability of The Hamiltonian

Consider a system of differential equations written in vector form

$$\dot{x} = f(x,\phi,\psi,t), \qquad x(t_0)=x_0 \qquad (C.1)$$

where, $x(t)$: = state vector of dimension n, $x \in X$

$\phi(t)$: = control of Player 1 of dimension ℓ, $\phi \in \Phi$

$\psi(t)$: = control of Player 2 of dimension m, $\psi \in \Psi$

with terminal constraints:

$$P\,(x(t_f),t_f) = 0,\ t_f \text{ is free} \tag{C.2}$$

and the performance index being defined as

$$J[x,\phi,\psi,t] = g(x(t_f),t_f) + \int_{t_0}^{t_f} L(x,\phi,\psi,t)\,dt \tag{C.3}$$

The variational Hamiltonian for this problem is given by

$$H = L + \lambda^T f + \mu_1{}^T P + \mu_2{}^T g \tag{C.4}$$

If the right-hand side of system dynamics (C.1) and the integral part of payoff (C.3) are in the form

$$f\,(x,\phi,\psi,t) = f_1\,(x,\phi,t) + f_2\,(x,\psi,t) \tag{C.5}$$

$$L\,(x,\phi,\psi,t) = L_1\,(x,\phi,t) + L_2\,(x,\psi,t) \tag{C.6}$$

then the Hamiltonian is separable in the space of controls ψ and ϕ as follows:

$$H = H_1 + H_2 + \mu_1{}^T P + \mu_2{}^T g \tag{C.7}$$

$$H_1 = L_1\,(x,\phi,t) + \lambda^T f_1\,(x,\phi,t) \tag{C.8}$$

$$H_2 = L_2\,(x,\psi,t) + \lambda^T f_2\,(x,\psi,t) \tag{C.9}$$

In this case, Friedman [39] showed that there exists a saddle point for the Hamiltonian. The order of action is immaterial in this case, i.e.,

$$\max_{\psi}\ \min_{\phi}\ H(x,\phi,\psi,\lambda,t) = \min_{\phi}\ \max_{\psi}\ H(x,\phi,\psi,\lambda,t) = H(x,\phi^o,\psi^o,\lambda,t) \tag{C.10}$$

Equation (C.10) is known as the Isaacs condition in differential game [39]. This condition is also known as the saddle point condition.

C.3 Sufficient Condition for a Game to have Value

As discussed in the previous section, the Isaacs condition guarantees the existence of the pointwise saddle point. If the final performance index in the game has a saddle point, then one is guaranteed that the order of action is immaterial. This section treats how the pointwise saddle point can be transformed to the global saddle point. The chief requirement here is that the game must have a value.

Friedman [39] [100] proved that a sufficient condition for the game to have a value is the Isaacs condition and the following requirements.:

(i) $f(x,\phi,\psi,t)$ is continuous and satisfies the Lipschitz condition,

(ii) $g(x(t_f), t_f)$ and $L(x,\phi,\psi,t)$ are continuous.

Here, condition (i) is required so that the trajectory generated by integrating equations of motion (C.1) is unique and continuous, while condition (ii) is required to ensure that the performance index is continuous. Under these conditions, if the variational Hamiltonian is separable, the performance index will be a unique quantity regardless of the player's order of action.

To show the existence of the value, Friedman [39] and Fleming [101] considered an approximating upper and lower game for every partition of the time interval $[t_0, t_f]$ into K equal sub-intervals. Using the requirement (i), the trajectory evolves according to

$$x(t_{j+1}) = x(t_j) + \int_{t_j}^{t_{j+1}} f(x,\phi_j,\psi_j,\tau)d\tau \qquad (C.11)$$

Two possibilities are next considered. The first one in which the minimizing player plays first. In the second case, the maximizing player plays first. The performance index in each case is

$$V_K^{+} = \inf_{\psi_0} \sup_{\phi_0} \cdots \inf_{\phi_{K-1}} \sup_{\psi_{K-1}} J[x,\phi_j,\psi_j,t] \qquad j = 0,1,2,\cdots,K-1 \qquad (C.12)$$

$$V_K^{-} = \sup_{\phi_0} \inf_{\psi_0} \cdots \sup_{\psi_{K-1}} \inf_{\phi_{K-1}} J[x,\phi_j,\psi_j,t] \qquad j = 0,1,2,\cdots,K-1 \qquad (C.13)$$

With the increment of K,

$$\lim_{K\to\infty} V_K^{+} = V^{+}, \quad \lim_{K\to\infty} V_K^{-} = V^{-} \qquad (C.14)$$

It can be shown [39] that in the general case,

$$V^{+} \geq V^{-} \qquad (C.15)$$

Note that the above expression will be an equality if the Isaac's condition is satisfied. In such a case,

$$\max_{\psi} \min_{\phi} J[x,\phi,\psi,t] = \min_{\phi} \max_{\psi} J[x,\phi,\psi,t] = J[x,\phi^{\circ},\psi^{\circ},t] \qquad (C.16)$$

APPENDIX D

CONVEXITY CONDITION FOR GLOBAL MINIMUM

Convex functionals play a special role in optimal control theory because most of the theory of local extrema for general nonlinear functionals can be strengthened to become global theory when applied to convex functionals [69].

By definition in Reference 35, a real-valued functional J: $\boldsymbol{Y} \rightarrow \mathfrak{R}$ is convex if

$$J[\alpha\, y_1 + (1 - \alpha)\, y_2] \leq \alpha\, J[y_1] + (1 - \alpha)\, J[y_2],\ \forall\ y_1, y_2 \in Y\ ,\ 0 < \alpha < 1 \qquad (D.1)$$

The following theorem [35] asserts the global nature of results for minimization problems with convex functionals such as those defined in (D.1).

Theorem *If $J(y_0)$ is a weak local minimum of $J(y)$ on $\boldsymbol{Y}$ and J is convex at y_0 relative to $\boldsymbol{Y}$, then $J(y_0)$ is a global minimum.*

A sufficient condition for convexity of functionals is that the integrand be convex for the integral interval. Thus the test of convexity for a functional can be reduced to a test of the convexity of the integrand. Typical integrands that are convex appear in Linear Quadratic Regulator theory and in the accessory minimum problem related to the Jacobi condition in nonsingular cases.

BIBLIOGRAPHY

[1] Sheridan, P. F., and Wiesner, W., "Aerodynamics of Helicopter Flight Near the Ground," *The 33rd Annual National Forum of the American Helicopter Society,* Washington, D.C., May, 1977, Preprint No. 77.33-04.

[2] Dooley, L. W., "Handling Qualities Considerations for NOE Flight," *Journal of the American Helicopter Society,* Vol. 22, No. 4, October, 1977, pp. 20-27.

[3] Landis, K. H., and Aiken, E. W., "Simulator Investigation of Side-Stick Controller/Stability and Control Augmentation Systems for Night Nap-of-Earth Flight," *Journal of the American Helicopter Society*, Vol. 29, No. 1, January, 1984, pp. 56-65.

[4] Sridhar, B., and Phatak, A. V., "Simulation and Analysis of Image-Based Navigation System for Rotorcraft Low-Altitude Flight," *The AHS National Specialists' Meeting Automation Applications of Rotorcraft,* Atlanta, GA, April 4-6, 1988.

[5] Cheng, V. H. L., and Sridhar, B., "Considerations for Automated Nap-of-the-Earth Rotorcraft Flight," Proceedings of American Control Conference, Vol. 2, Atlanta, GA, June 15-17, 1988, pp. 967-976.

[6] Cheng, V. H. L., "Obstacle-Avoidance Automatic Guidance," Proceedings of AIAA Guidance, Navigation and Control Conference, Minneapolis, Minnesota, August 15-17, 1988.

[7] Denton, R. V., Jones, J. E., and Froberg, P. L., "A New Technique for Terrain Following/Terrain Avoidance Guidance Command Generation," AGARD-CP-387, 1985.

[8] Dorr, D. W., "Rotary Wing Aircraft Terrain-Following/Terrain-Avoidance System Development," Proceedings of AIAA Guidance, Navigation and Control Conference, Williamsburg, VA, August 18-20, 1986, Paper No. 86-2147.

[9] Hoffman, J. D., "Terrain Following/Terrain Avoidance/Threat Avoidance for Helicopter Applications," *American Helicopter Society Mideast Region Proceeding National Specialists' Meeting*, CherryHill, New Jersey, October 13-15, 1987.

[10] Gilmore, J. F., and Semeco, A. C., "Knowledge-Based Approach Toward Developing an Autonomous Helicopter System," *Optical Engineering*, Vol. 25, March, 1986, pp. 415-427.

[11] Olinger, M. D., and Bird, M. W., "Tactical Flight Management: Threat Penetration Algorithm Design," Proceedings of IEEE 1984 National Aerospace Electronics Conference, Dayton, OH, May 21-25, 1984, pp. 510-515.

[12] Bryson, A. E., and Ho, Y. C., Applied Optimal Control, Hemisphere, New York, 1975.

[13] Menon, P. K. A., Kim, E., and Cheng, V. H. L., "Helicopter Trajectory Planning Using Optimal Control Theory," Proceedings of the 1988 American Control Conference, Vol. 2, Atlanta, GA, June 15-17, 1988, pp. 1440-1447.

[14] Zermelo, E., "Über das Navigationsproblem bei ruhender oder veränderlicher Windverteilung," Zeitschrift für angewandte Mathematik und Mechanik, Bd. 11, 1931.

[15] Menon, P. K. A., Kim, E., and Cheng, V. H. L., "Optimal Terrain Masking Trajectories for Helicopters," *AIAA Guidance, Navigation and Control Conference,* Minneapolis, MN, August 15-17, 1988.

[16] Nayfeh, A. H., Introduction to Perturbation Techniques, John Wiley & Sons, Inc., New York, 1981.

[17] Isaacs, R., Differential Games, John Wiley & Sons, New York, 1965.

[18] Menon, P. K. A., "Short-Range Nonlinear Feedback Strategies for Aircraft Pursuit-Evasion," *Journal of Guidance, Control, and Dynamics*, Vol. 12 , No. 1, Jan-Feb, 1989, pp. 27-32.

[19] Heiges, M. W., "A Helicopter Flight Path Controller Design via a Nonlinear Transformation Technique," *Ph.D. Dissertation,* Georgia Institute of Technology , Atlanta, GA, March, 1989.

[20] Lewis, M. S., Mansur, M. H., and Chen, R. T. N., "A Piloted Simulation of Helicopter Air Combat to Investigate Effects of Variations in Selected Performance and Control Response Characteristics," *NASA TM 89438*, August, 1987.

[21] Lewis, M. S., and Aiken, E. W., "Piloted Simulator of One-on-One Helicopter Air Combat at NOE Flight Levels," *NASA TM 86686*, April , 1985.

[22] Pugh, G. E., and Krupp, J. C., "A Value-Driven Control System for the Coordination of Autonomous Cooperating Underwater Vehicles," *Unmanned system*, Vol. 6, No. 2, 1988, pp. 24-35.

[23] Crowley, J. L., "Navigation for an Intelligent Mobile Robot," *IEEE Journal of Robotics and Automation,* Vol. RA-1, No. 1, March , 1985, pp. 31-41.

[24] Reed, C. G., and Hogan, J. J., "Range Correlation Guidance for Cruise Missiles," Proceedings of IEEE 1978 National Aerospace Electronics Conference, Dayton, OH, May 16-18, 1978, pp. 1255-1262.

[25] Kupferer, R. A., and Halski, D. J., "Tactical Flight Management-Survival Penetration," Proceedings of IEEE 1984 National Aerospace Electronics Conference, Dayton, OH, May 21-25, 1984, pp. 503-509.

[26] Fleury, P. A., "Covert Penetration Systems-Future Strategic Aircraft Missions Will Require a New Sensor System Approach," Proceedings of IEEE 1986

National Aerospace Electronics Conference, Dayton, OH, May 19-23, 1986, pp. 220-226.

[27] Bellman, R., Dynamic Programming, Princeton University Press, Princeton, N. J., 1957.

[28] Winston, P. H., Artificial Intelligence, Addison-Wesley Pub., Reading, MA, 1984.

[29] Denton, R. V., and Marsh, J. V., "Applications of Autopath Technology to Terrain/Obstacle Avoidance," Proceedings of IEEE 1982 National Aerospace Electronics Conference, Dayton, OH, May 18-20, 1982, pp. 1373-1377.

[30] Chan, Y. K., and Foddy, M., "Real Time Optimal Flight Flight Path Generation by Storage of Massive Data Bases," Proceedings of IEEE 1985 National Aerospace Electronics Conference, Dayton, OH, May 20-24, 1985, pp. 516-521.

[31] Austin, F., et al., "Automated Maneuvering Decisions for Air-to-Air Combat," Proceedings of 1987 AIAA Guidance, Navigation, and Control Conference, Monterey, CA, Paper Preprint 87-2393.

[32] Von Neumann, J., and Morgenstern, O., Theory of Games and Economic Behavior, Princeton University Press, Princeton, 1944.

[33] Pontryagin, L. S., Boltyanskii, V. G., Gamkrelidze, R. V., and Mishchenko, E. F., The Mathematical Theory of Optimal Process, The Macmillan Company, New York, 1964.

[34] Pierre, D. A., Optimization Theory with Applications, Dover Publications, N.Y., 1986.

[35] Ewing, G. M., Calculus of Variation with Applications, Dover Publication, New York, 1969.

[36] Ho, Y. C., "Review of *Differential Games,* by R. Isaacs," *IEEE Trans. on Automatic Control*, Vol. AC-10, No. 4, October, 1965, pp. 501-503.

[37] Berkovitz, L. D., and Fleming, W. H., "On Differential Games With Integral Payoff," *Annals of Math. Study*, No.39, Princeton University Press, Princeton, 1957, pp. 413-435.

[38] Berkovitz, L. D., "A variational Approach to Differential Games," *Annals of Math. Study*, No. 52, Princeton University Press, Princeton, 1964, pp. 127-173.

[39] Friedman, A., Differential Games, Wiley-Interscience, New York, 1971.

[40] Starr, A. W., and Ho, Y. C., "Nonzero-Sum Differential Games," *Journal of Optimization and Applications*, Vol. 3, No. 3, 1969, pp. 184-206.

[41] Simaan, M., and Cruz, J. B., "On the Stackelberg Strategy in Nonlinear-Sum Games," *Journal of Optimization and Applications*, Vol. 11, No. 5, 1973, pp. 533-555.

[42] Berkovitz, L. D., Optimal Control Theory, (Applied Mathematical Sciences, Vol. 12), Springer-Verlag, New York, 1974.

[43] Ho, Y. C., Bryson, A. E., and Baron, S., "Differential Games and Optimal Pursuit-Evasion Strategies," *IEEE Trans. on Automatic Control*, Vol. AC-10, No. 4, October, 1965, pp. 385-389.

[44] Basar, T., and Olsder, G. J., Dynamic Noncooperative Game Theory, Academic Press, New York, 1982.

[45] Kailath, T., Linear Systems, Prentice-Hall Inc., New Jersey, 1980.

[46] Wonham, W. M., Linear Multivarable Control: A Geometric Approach, 2nd Ed., Springer-Verlag, New York, 1979.

[47] Krener, A. J., "On the Equivalence of Control Systems and the Linearization of Nonlinear Systems," *SIAM Journal of Control*, Vol. 11, No. 4, November, 1973, pp. 670-676.

[48] Brockett, R. W., "Feedback Invariants for Nonlinear Systems," *Proceedings of IFAC World Congress*, Helsinki, Finland, 1978, pp. 1115-1120.

[49] Ball, W. W. R., A Short Account of the History of Mathematics, Dover Publications, New York, 1960.

[50] Meyer, G., "The Design of Exact Nonlinear Model Followers," *Joint Automatic Control Conference*, FA-3A, 1981.

[51] Sussmann, H. J., "Lie Brackets, Real Analyticity and Geometric Control," Differential Geometric Control Theory, *Proceedings of the Conference held at Michigan Technological University*, June 28 - July 2, 1982, pp. 1-116.

[52] Hunt, L. R., Su, R., and Meyer, G., "Global Transformations of Nonlinear Systems," *IEEE Transactions on Automatic Control*, Vol. AC-28, No. 1, January, 1983, pp. 24-30.

[53] Hunt, L. R., and Su, R., "Control of Nonlinear Time-Varying systems," Proceedings of IEEE Conference on Decision and Control, San Diego, CA, 1981, pp. 558-563.

[54] Su, R., "On the Linear Equivalents of Nonlinear Systems," *Systems and Control Letters*, Vol. 2, No. 1, July, 1982, pp. 48-52.

[55] Meyer, G., and Cicolani, L., "Application of Nonlinear System Inverses to Automatic Flight Control Design-System Concepts and Flight Evaluations," *AGARDograph 251 on Theory and Applications of Optimal Control in Aerospace Systems*, 1980.

[56] Meyer, G., Hunt, R. L., and Su, R., "Design of Helicopter Autopilot by Means of Linearizing Transformations," *Proceedings of Guidance and Control Panel 35th Symposium*, AGARD-CP -321, 1983, pp. 4.1-4.11.

[57] Meyer, G., Su, R., Hunt, R. L., "Application of Nonlinear Automatic Flight Control," *Automatica*, Vol. 20, No. 1, 1984, pp. 101-107.

[58] Menon, P. K. A., Badgett, M. E., Walker, R. A., and Duke, E. L., "Nonlinear Flight Trajectory Controller for Aircraft," *Journal of Guidance, Control, and Dynamics*, Vol. 10, No. 1, Jan-Feb 1987, pp. 67-82.

[59] Heiges, M. W., Menon, P. K. A., and Schrage, D. P., "Synthesis of a Helicopter Full Authority Controller," Proceedings of the AIAA Guidance, Navigation and Control Conference, Boston, MA, August 14 - 16, 1989, Part 1, pp. 207-213.

[60] Lee, E. B., and Markus, L., Foundations of Optimal Control Theory, Wiley, New York, 1967.

[61] Bogen, R., et al., MACSYMA Reference Manual, Version 10, The Mathlab Group Laboratory for Computer Science, M.I.T., Cambridge, MA, 1983.

[62] Conte, S. D., and de Door, C., Elementary Numerical Analysis, McGraw Hill, N.Y., 1980.

[63] U.S. Geological Survey, San Andreas, California; N3800-W12030/15, AMS 1860II-Series V795, Denver, CO, 1962.

[64] Rogers, D. F., and Adams, J. A., Mathematical Elements for Computer Graphics, McGraw Hill, N.Y., 1976.

[65] Kelley, H. J., "Reduced Order Modelling in Aircraft Mission Analysis", *AIAA J.*, Vol. 9, 1972, pp. 349-350.

[66] Kelley, H. J., "Aircraft Maneuver Optimization by Reduced Order Approximation," *Control and Dynamics*, Vol. 10, edited by C.J. Leondes, Academic Press, N. Y., 1973, pp. 131-178.

[67] Calise, A. J., and Moerder, D. D., "Singular Perturbation Techniques for Real Time Aircraft Trajectory Optimization and Control," *NASA-CR-3597*, 1982.

[68] Gelfand, I. M., and Fomin, S. V., Calculus of Variations with Application, Prentice-Hall, N. J., 1963.

[69] Luenberger, D. G., Optimization by Vector Space Methods, John Wiley & Sons, Inc., New York, 1968.

[70] Bliss, G. A., Lectures on the Calculus of Variations, Univ. of Chicago, 1946.

[71] Breakwell, J. V., and Ho, Y. C., "On the Conjugate Point Condition for the Control Problem," *International Journal Engineering*, Vol. 2, 1965, pp. 565-579.

[72] Breakwell, J. V., Speyer, J. L., and Bryson, A. E., "Optimization and Control of Nonlinear Systems Using the Second Variations," *Journal of SIAM Control* Series A, Vol. 1, No. 2, 1963, pp. 193-223.

[73] Kelley, H. J., and Moyer, H. G., "Computational Jacobi Test Procedure," *JUREMA Workshop*, Dubrovnik, Yugoslvia, June 29-30, 1984.

[74] Hildebrand, F. B., Advanced Calculus for Applications, Prentice-Hall, Inc., New Jersey, 1976.

[75] Cicala, P., An Engineering Approach to the Calculus of Variations, Libreria Editrice Univ., Torino, Italy, 1956.

[76] Bolza, O., Lectures on the Calculus of Variations, Dover Publications, N.Y., 1961.

[77] Ciletti, M. D., and Starr, A. W., "Differential Games: A Critical View," Differential Games: Theory and Applications, *1970 Joint Automatic Control Conference*, Atlanta, GA, June 26, 1970, pp. 1-17.

[78] Lappos, N. D., "The LHX-Evolved for Total Combat Fitness," *VERTIFLITE*, Vol. 35, No. 5, July/August, 1989, pp. 16-17.

[79] Breakwell, J. V., and Merz, A. W., "Toward a Complete Solution of the Homicidal Chauffeur Game," Proceedings of 1st International Conference on the Theory and Application of Differential Games, Amherst, Mass., 1969, pp. III-1 - III-5.

[80] Merz, A. W., "The Homicidal Chauffeur," *AIAA Journal*, Vol. 12, No. 3, March, 1974, pp. 259-260.

[81] Merz, A. W., "To Pursue or to Evade-That is the Question," *Journal of Guidance, Control , and Dynamics*, Vol. 8, No. 2, 1985, pp. 161-165.

[82] Flight Systems, Inc., "Helicopter Effectiveness in Air-to-Air Combat," *U.S. Army Aviation Research and Development Command, Contract No. NAS2-10239*, 1979.

[83] Buresh, J., Parlier, C., and Wilson, W., "Air-to-Air Combat Development of the AH-64A Apache," Proceedings of AIAA 4th Flight Test Conference, San Diego, CA, May 18-20, 1988, pp. 268-277.

[84] Rajan, N., Prasad, U. R., and Rao, N. J., "Pursuit-Evasion of Two Aircraft in a Horizontal Plane," *Journal of Guidance and Control*, No.3, May-June, 1980, pp. 261-267.

[85] Leondes, C. T., ed., *Control and Dynamic Systems: Advances in Theory and Applications,* Vol. 17, 1981.

[86] Prasad, U. R., Rajan, N., and Rao, N. J., "Planar Pursuit-Evasion with Variable Speeds, Part 1, Extremal Trajectory Maps," *J. Optimization Theory and Applications*, Vol. 33, No. 3, March, 1981, pp.401-418.

[87] Rajan, N., and Ardema, M. D., "Barriers and Dispersal Surfaces in Minimum-Time Interception," *J. Optimization Theory and Applications*, Vol. 42, No. 2, February, 1984. pp. 201-228.

[88] Järmark, B. S. A., "Convergence Control in Differential Dynamic Programming Applied to Air-to-Air Combat" *AIAA Journal,* Vol. 14, No. 1, January, 1976, pp. 118-121.

[89] Roberts, D. A., and Montgomery, R. C., "Development and Application of a Gradient Method for Solving Differential Games," *NASA-TN-D-6502*, November, 1971.

[90] Shinar, J., "Validation of Zero-Order Feedback Strategies for Medium-Range Air-to-Air Interception in a Horizontal Plane," *NASA TM-84237*, April, 1982.

[91] Riggs, T. L., "Linear Optimal Guidance for Short Range Air-to-Air Missiles," Proceedings of IEEE 1979 National Aerospace Electronics Conference, Dayton, OH, May 23-27, 1979, pp. 757-764.

[92] Lee, G. K. F., "Estimation of the Time-to-Go Parameter for Air-to-Air Missiles," *Journal of Guidance, Control, and Dynamics*, Vol. 8, No. 2, 1985, pp. 262-266.

[93] Menon, P. K. A., Calise, A. J., and Leung, S. K. M., "Guidance Law for Spacecraft Pursuit-Evasion and Rendezvous," *AIAA Guidance, Navigation and Control Conference,* Minneapolis, MN, August 15-17, 1988.

[94] Talbot, P., Tingling, B., Decker, W., and Chen, R., "A Mathematical Model of a Single Main Rotor Helicopter for Piloted Simulation," *NASA TM 84281*, September, 1982.

[95] Kant, K., and Zucker, S., "Planning Collision-Free Trajectories in Time-Varying Environments: A Two-Level Hierarchy," Proceedings of IEEE Conference on Robotics and Automation, Vol. 3, Philadelphia, Pennsylvania, April 24-29, 1988, pp. 1644-1649.

[96] Khatib, O., "Real-Time Obstacle Avoidance for Manipulators and Mobile Robots," *The International Journal of Robotics Research*, Vol. 5, No. 1, 1986, pp. 90-98.

[97] Fox, C., An Introduction to the Calculus of Variations, Dover Publications, New York, 1987.

[98] Moyer, H. G., "Optimal Control Problems That Test for Envelope Contacts," *Journal of Optimization Theory and Applications*, Vol. 6, No. 4, 1970, pp. 287-299.

[99] Menon, P. K. A., "Optimal Symmetric Flight with an Intermediate Vehicle Model," *Ph. D. Thesis*, Virginia Polytechnic Institute and State University, Blacksburg, VA, September, 1983.

[100] Roxin, E. O., "On Differential Games Without Value," Differential Games: Theory and Applications, *1970 Joint Automatic Control Conference*, Atlanta, GA, June 26, 1970, pp.95-119.

[101] Elliott, R. J., "Introduction to Differential Games," The Theory and Application of Differential Games, (Grote, J. D., ed.) Proceedings of the NATO Advanced Study Institute held at University of Warwick, Coventry, England, August 27-September 6, 1974.

Table 3.1 Digital Terrain Data used for Trajectory Planning

unit: 1000 feet

Cross-Range

Down-Range	0	1	2	3	4	5	6	7	8	9	10	11	12	13	14	15	16	17	18	19
0	1.360	1.280	1.200	1.300	1.250	1.200	1.150	1.120	1.200	1.120	1.120	0.980	1.040	1.040	1.160	1.240	1.240	1.240	1.300	1.428
1	1.280	1.360	1.300	1.300	1.360	1.250	1.200	1.120	1.200	1.240	1.120	1.129	1.040	1.040	1.040	1.160	1.200	1.280	1.300	1.360
2	1.340	1.280	1.360	1.440	1.480	1.360	1.280	1.120	1.120	1.240	1.120	1.129	1.120	1.120	1.120	1.040	1.120	1.200	1.280	1.300
3	1.400	1.340	1.600	1.520	1.520	1.420	1.360	1.200	1.200	1.250	1.240	1.200	1.120	1.120	1.200	1.040	1.040	1.120	1.200	1.280
4	1.400	1.340	1.340	1.732	1.340	1.360	1.360	1.440	1.360	1.240	1.240	1.240	1.120	1.120	1.200	1.200	1.120	1.120	1.120	1.120
5	1.400	1.400	1.340	1.340	1.340	1.400	1.360	1.520	1.520	1.360	1.240	1.240	1.240	1.120	1.120	1.267	1.200	1.200	1.120	1.120
6	1.400	1.400	1.340	1.340	1.340	1.340	1.360	1.520	1.680	1.600	1.440	1.360	1.280	1.240	1.120	1.120	1.120	1.240	1.200	1.200
7	1.450	1.400	1.400	1.400	1.340	1.340	1.340	1.400	1.600	1.828	1.680	1.520	1.280	1.240	1.240	1.240	1.212	1.240	1.280	1.280
8	1.600	1.500	1.400	1.405	1.404	1.403	1.402	1.401	1.440	1.600	1.680	1.760	1.520	1.240	1.240	1.240	1.240	1.240	1.353	1.360
9	1.760	1.600	1.500	1.480	1.400	1.480	1.480	1.400	1.520	1.760	1.520	1.520	1.520	1.440	1.360	1.360	1.361	1.362	1.363	1.440
10	2.000	1.760	1.600	1.480	1.401	1.680	1.520	1.480	1.400	1.520	1.521	1.440	1.360	1.520	1.521	1.522	1.440	1.441	1.362	1.440
11	2.500	2.000	1.760	1.601	1.401	1.680	1.989	1.520	1.402	1.405	1.406	1.604	1.612	1.480	1.484	1.609	1.602	1.520	1.442	1.447
12	2.240	2.603	2.020	1.681	1.481	1.681	1.922	1.623	1.482	1.402	1.406	1.403	1.482	1.485	1.489	1.562	1.682	1.763	1.607	1.621
13	2.160	2.421	2.161	1.764	1.621	1.611	1.761	1.619	1.601	1.401	1.404	1.407	1.521	1.482	1.485	1.489	1.521	1.682	1.801	1.710
14	2.002	2.081	2.019	1.920	1.760	1.610	1.601	1.521	1.525	1.521	1.523	1.405	1.482	1.483	1.480	1.520	1.601	1.610	1.801	2.020
15	1.742	2.102	2.001	1.840	1.761	1.646	1.624	1.601	1.523	1.527	1.528	1.521	1.601	1.681	1.762	1.763	1.767	1.762	1.780	1.750
16	1.841	2.162	2.349	1.921	1.862	1.721	1.681	1.904	1.610	1.520	1.521	1.524	1.521	1.841	2.009	2.180	2.100	2.150	2.200	2.000
17	1.840	1.920	2.160	2.040	1.841	1.701	1.680	1.760	1.682	1.640	1.601	1.442	1.440	1.602	1.842	2.242	2.323	2.321	2.403	2.242
18	1.821	1.882	1.923	2.022	1.840	1.680	1.682	1.841	1.682	1.689	1.641	1.621	1.502	1.522	1.762	2.081	2.241	2.243	2.321	2.499
19	1.841	1.845	1.901	1.922	1.842	1.682	1.680	1.761	1.766	1.682	1.642	1.600	1.521	1.522	1.600	1.920	2.160	2.320	2.161	2.089

Table 5.1 Maximum Rate of Climb (ft/sec) for AH-1S

Speed (ft/sec)	Density Altitude			
	sea level	1000 ft	2000 ft	3000 ft
0	22.2	21.25	20.22	19.1
16.67	25.21	24.65	24.02	23.35
33.33	29.08	28.63	28.13	27.58
50	32.25	31.9	31.52	31.1
66.67	34.43	34.2	33.92	33.6
83.33	35.6	35.43	35.25	35.02
100	35.91	35.82	35.7	35.53
116.67	35.42	35.43	35.37	35.23
133.33	34.23	34.27	34.28	34.25
150	2.27	32.38	32.47	32.5
166.67	29.52	29.7	29.87	29.97
183.33	25.9	26.18	26.43	26.62
200	21.38	21.78	22.12	22.4
216.67	15.9	16.42	16.67	16.32
233.33	8.77	8.72	8.58	8.37
250	0	0	0	0

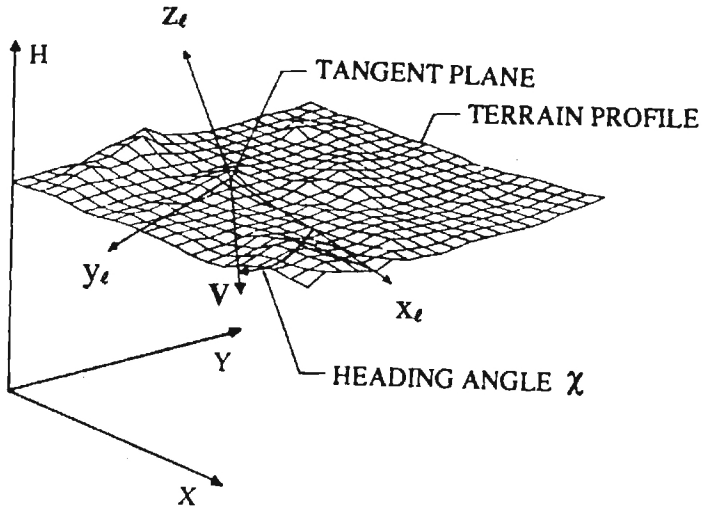

Figure 3.1 The Coordinate System

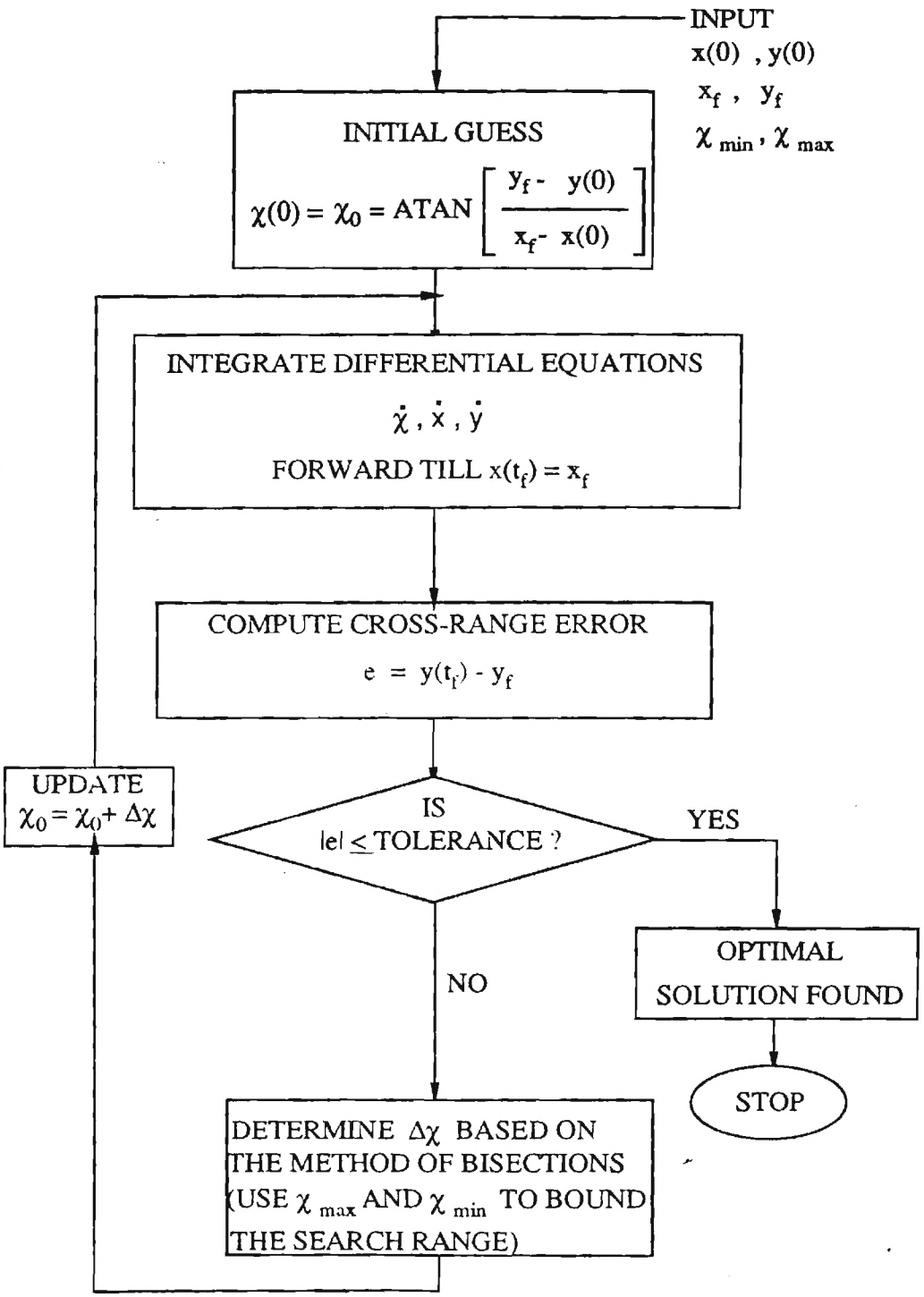

Figure 3.2 Flow Chart for Generating Euler Solutions

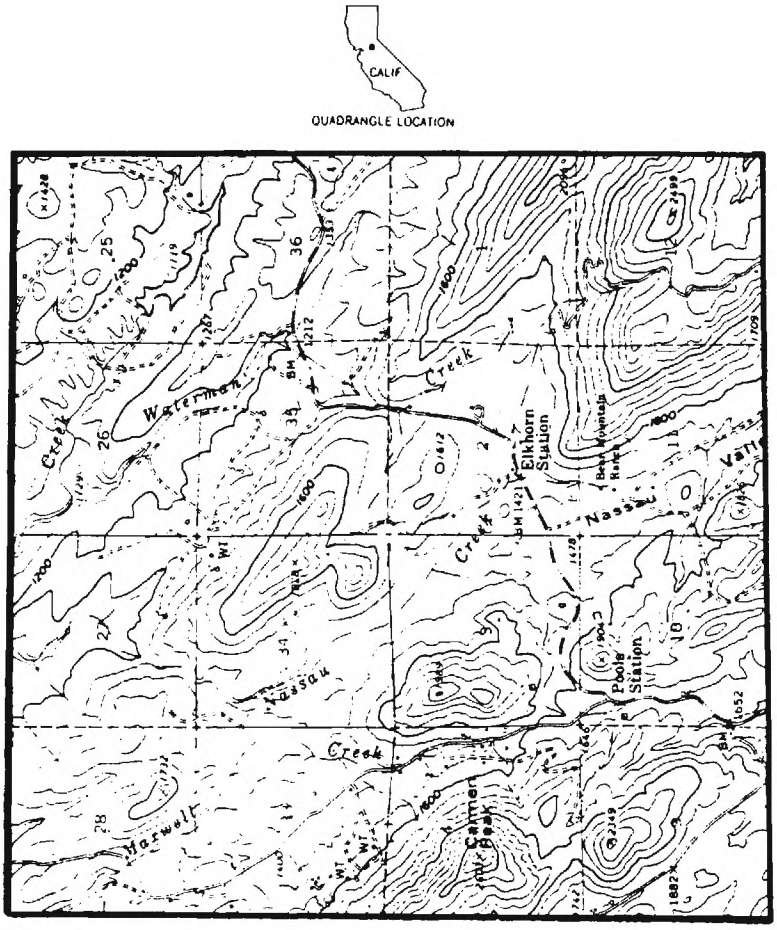

Figure 3.3 Sample Terrain Map of the Nassau Valley, California

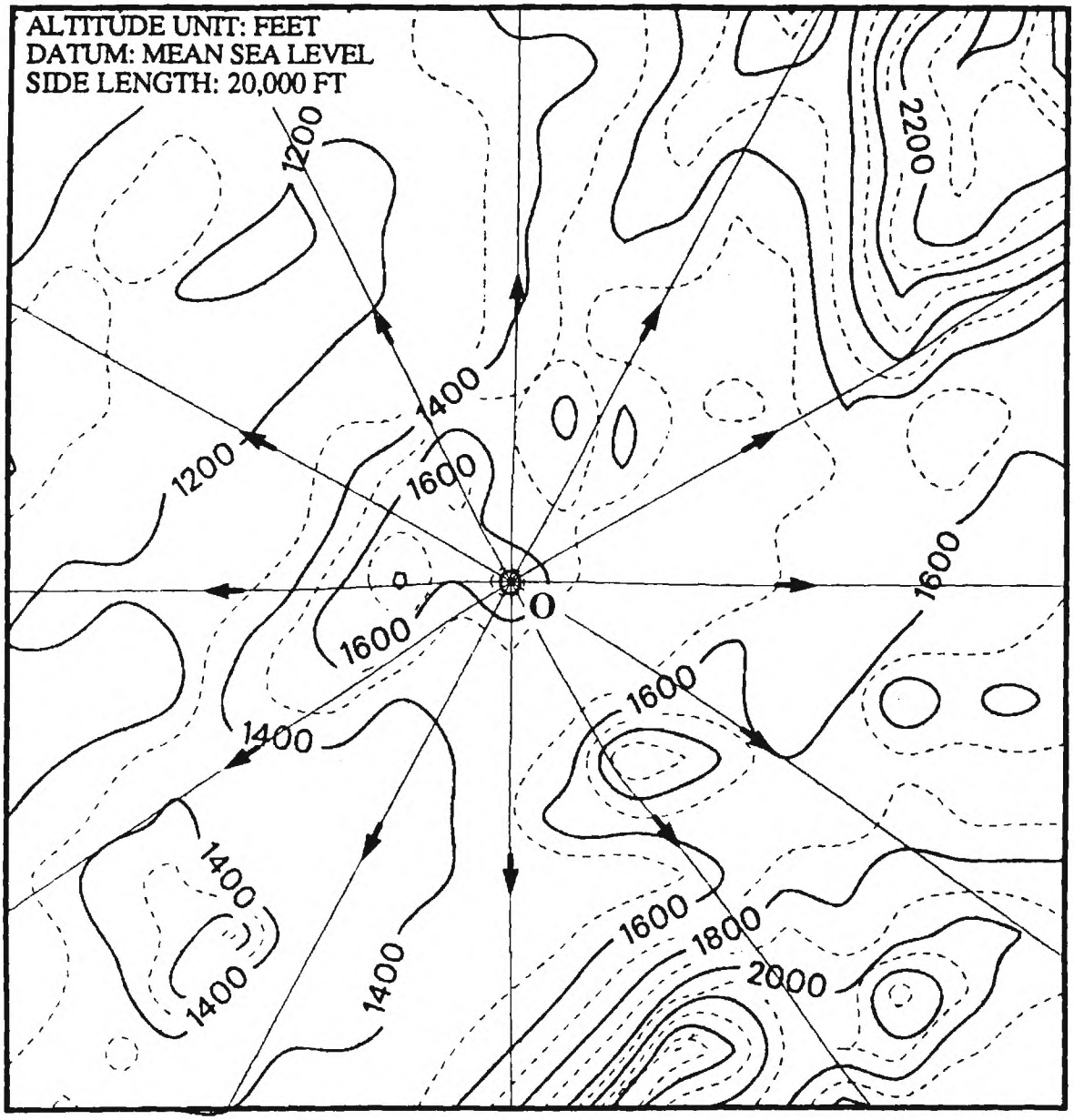

Figure 3.4 Euler Solutions for Minimum Flight Time Criterion (K = 0)

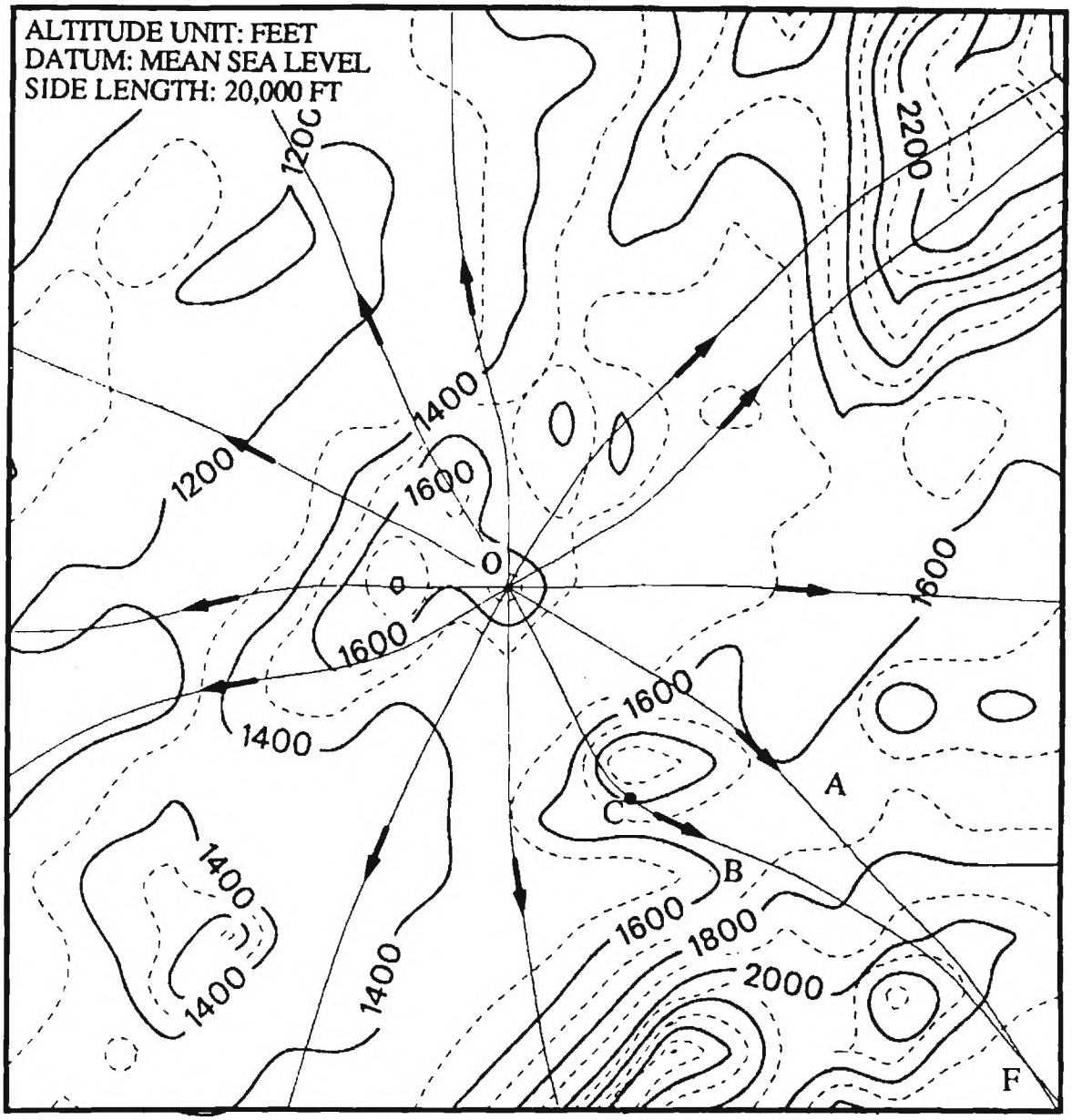

Figure 3.5 Euler Solutions for Maximum Terrain Masking Criterion (K = 0.99)

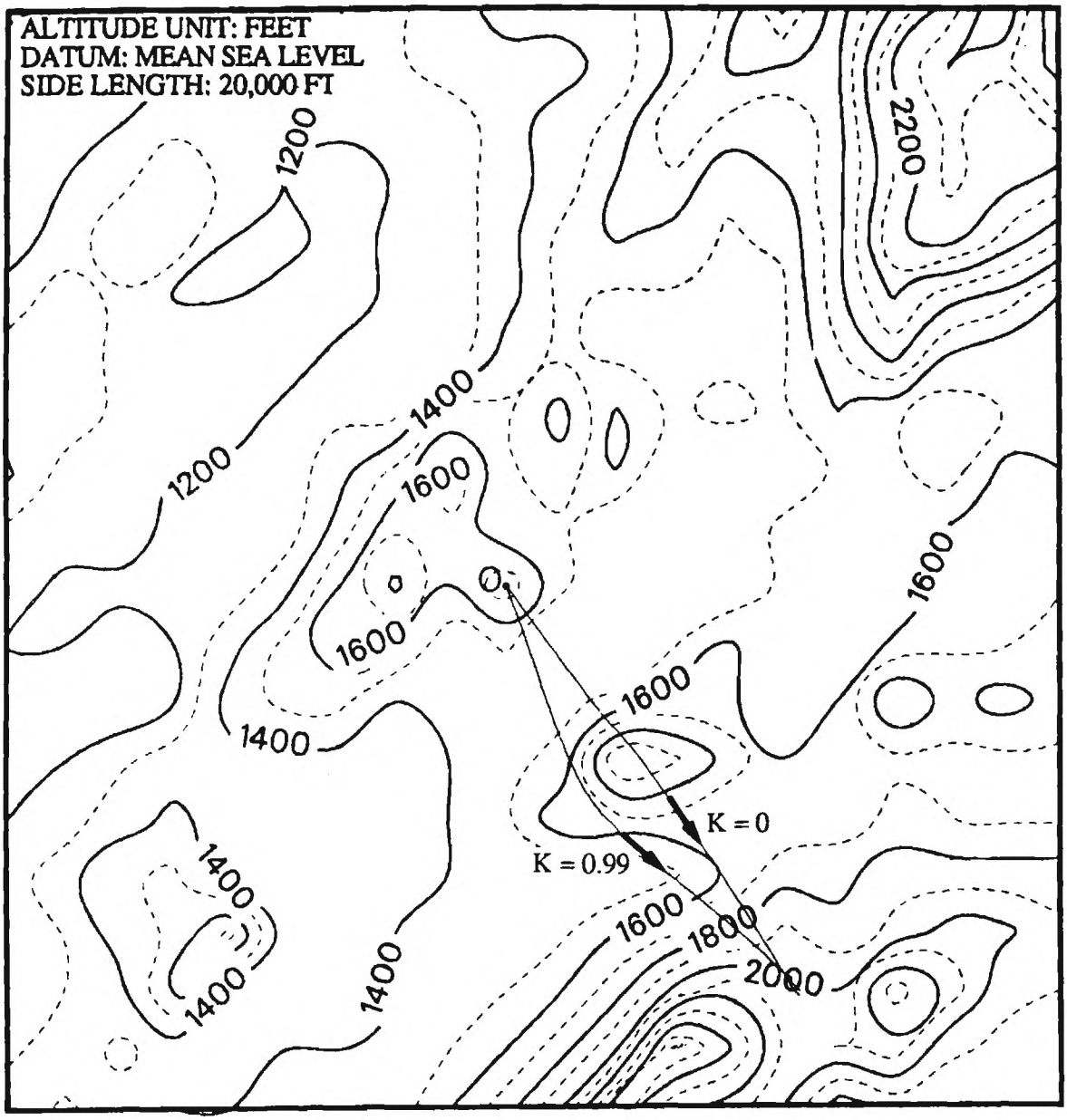

Figure 3.6 Comparison between Minimum Time Trajectory
and Maximum Terrain Masking Trajectory

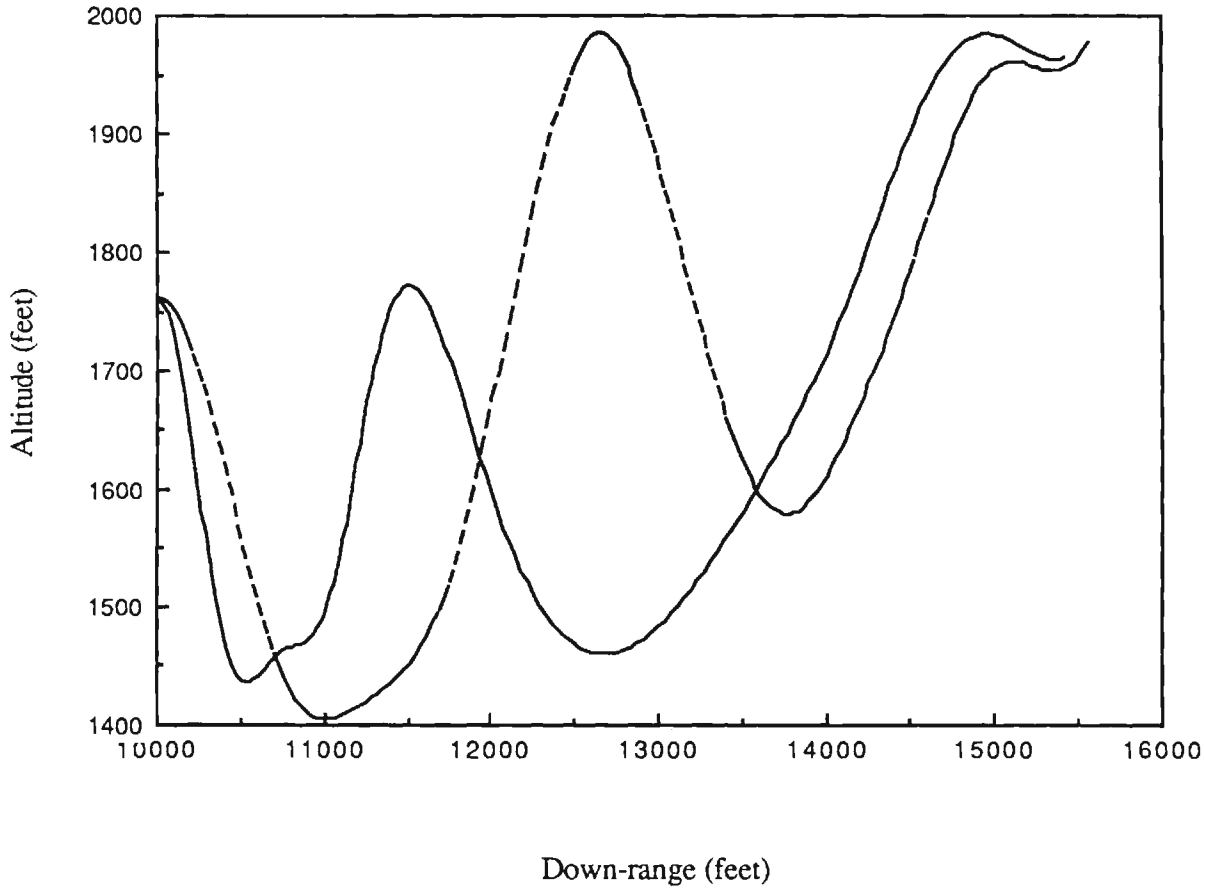

Figure 3.7 Altitude Profiles along Different Criterion Trajectories
Solid line:maximum terrain masking trajectory
Dotted line:minimum flight time trajectory

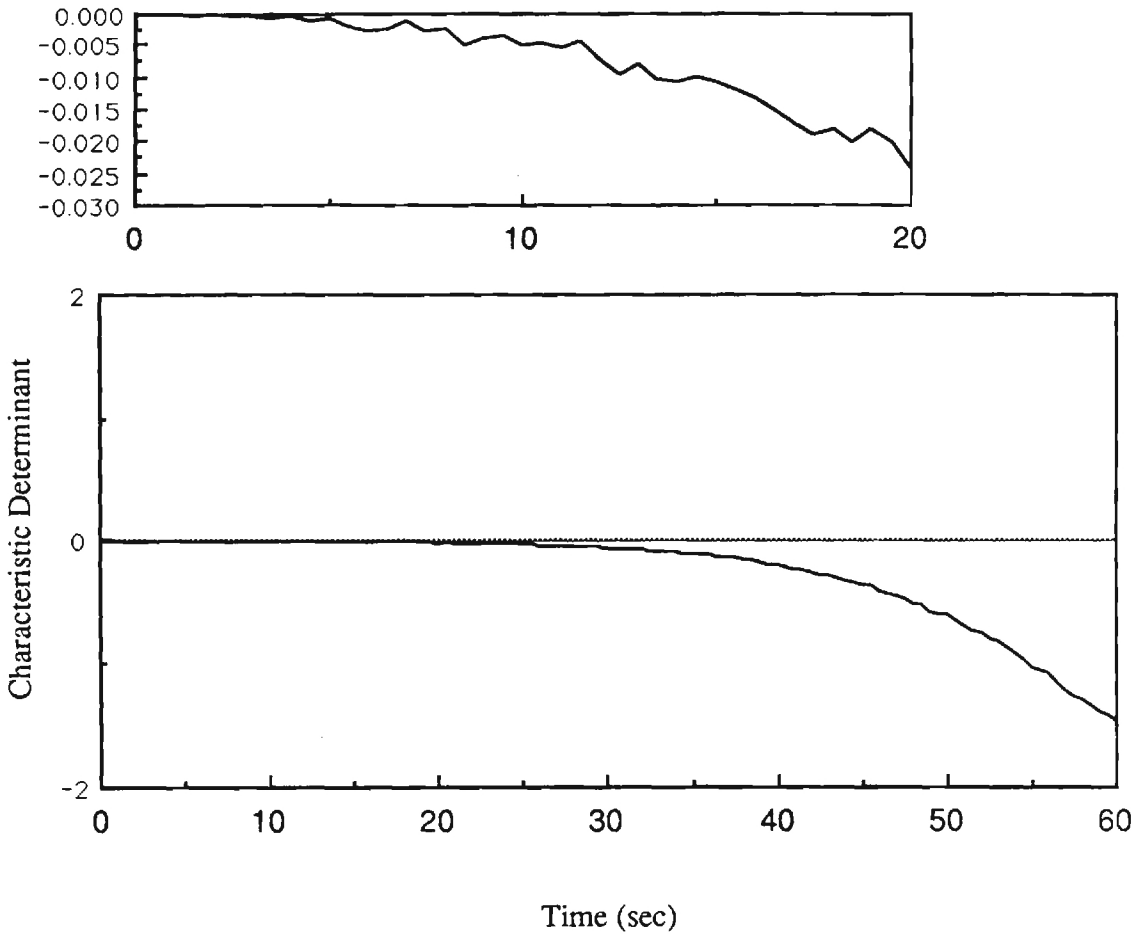

Figure 3.8 Characteristic Determinant Δ(t) along the Trajectory A
for Maximum Terrain Masking (K = 0.99)

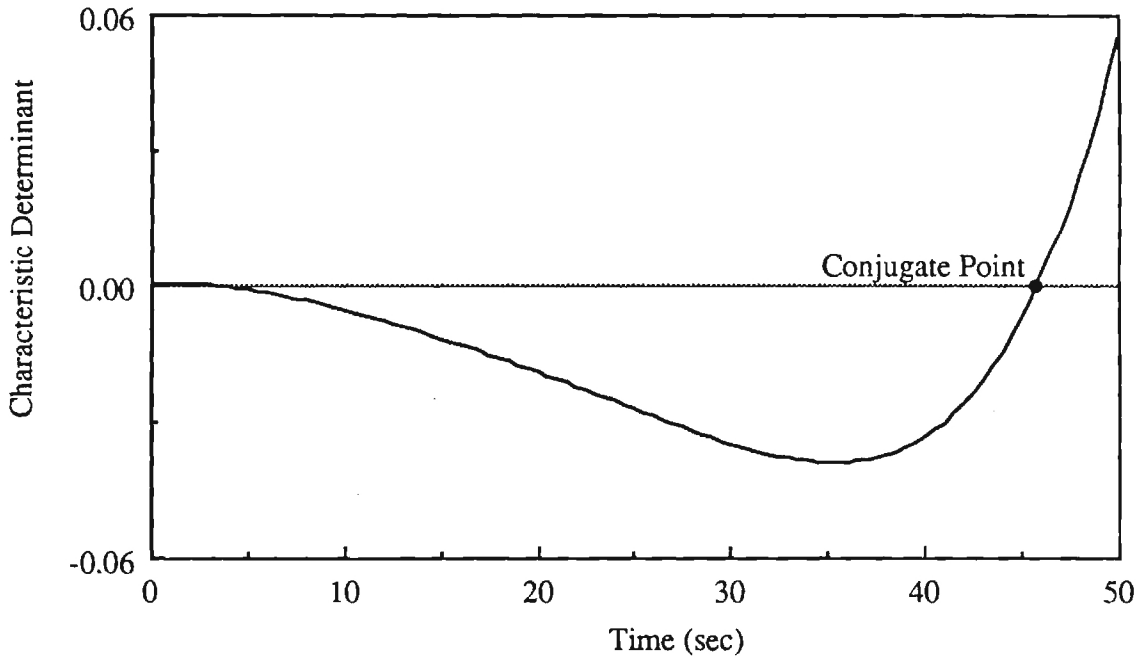

Figure 3.9 Characteristic Determinant $\Delta(t)$ along the Trajectory B for Maximum Terrain Masking (K = 0.99)

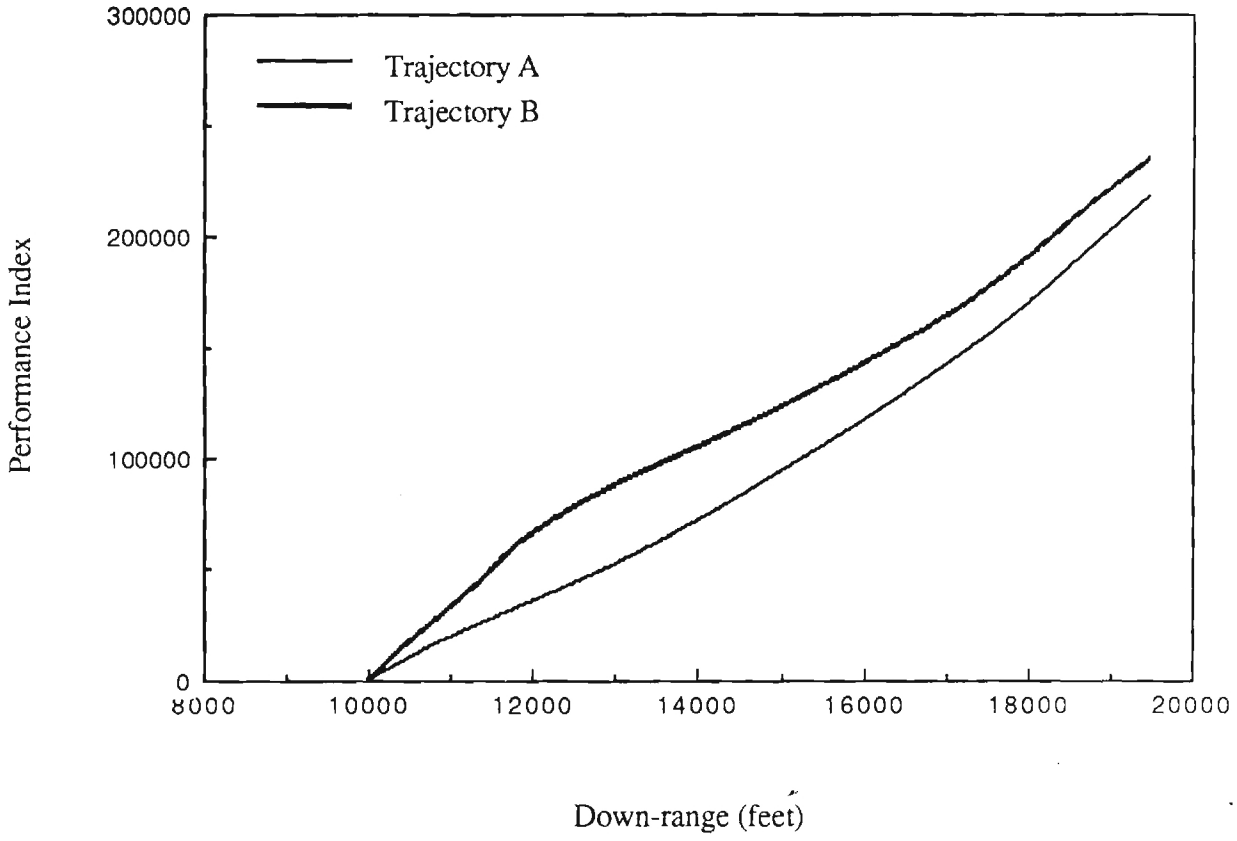

Figure 3.10 Comparison of Performance Index along Trajectories A and B for Maximum Terrain Masking

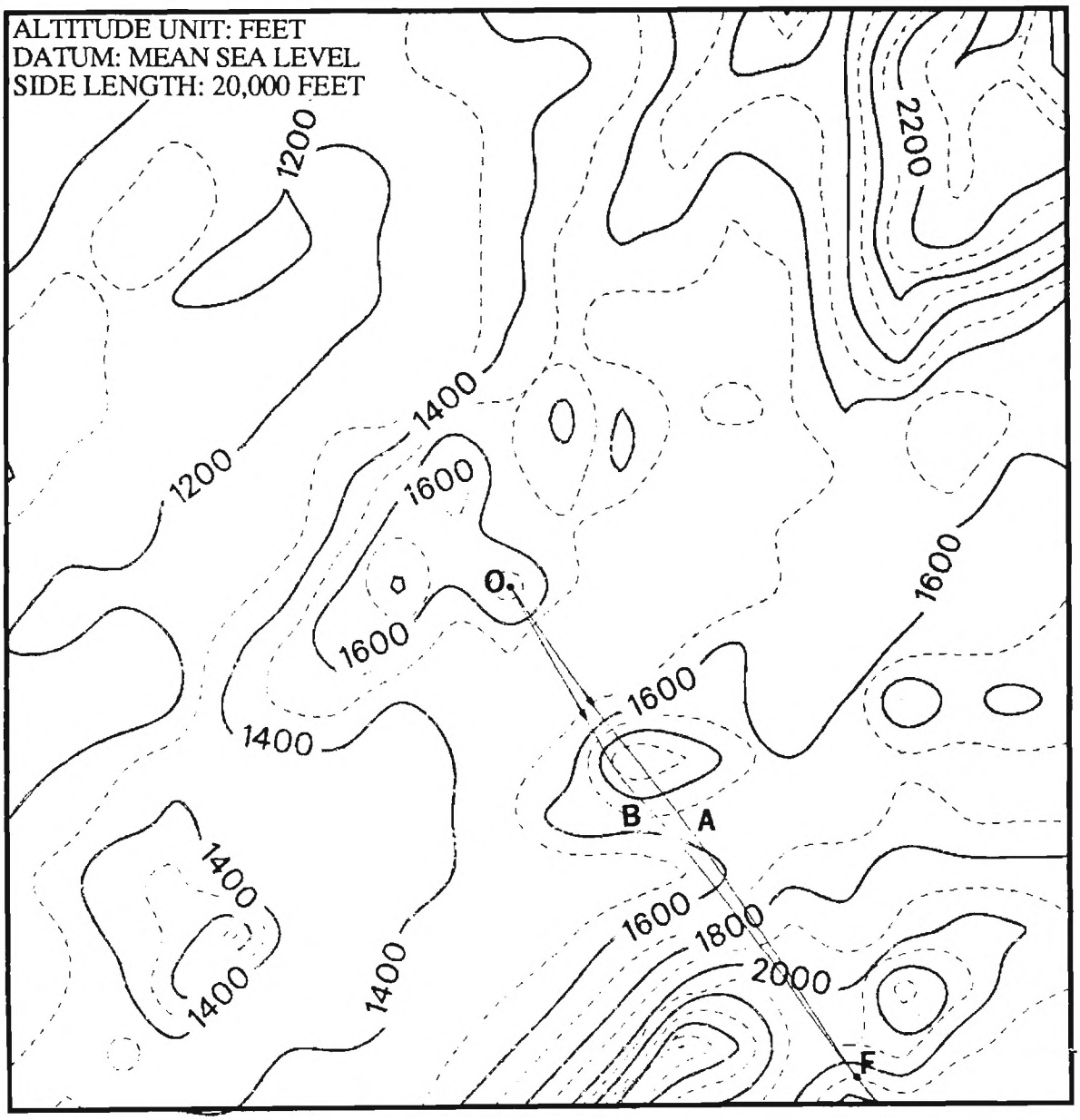

Figure 3.11 Two Extremals for Minimum Flight Time Criterion
having a Same Terminal Position

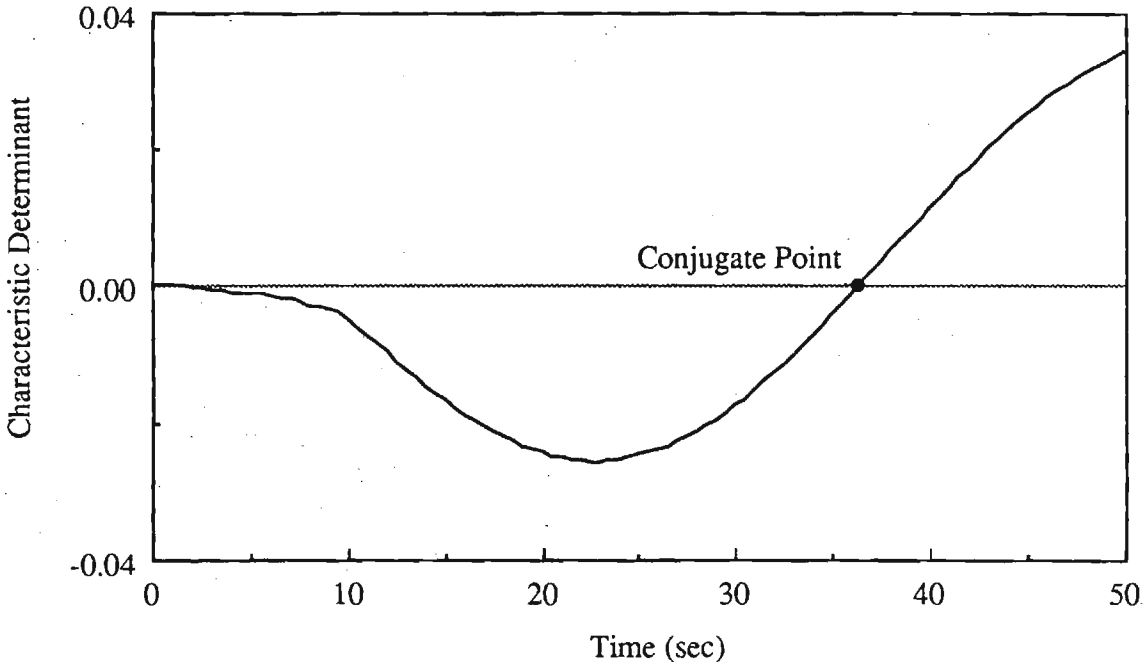

Figure 3.12 Characteristic Determinant Δ(t) along the Trajectory A
for Minimum Flight Time (K = 0.0)

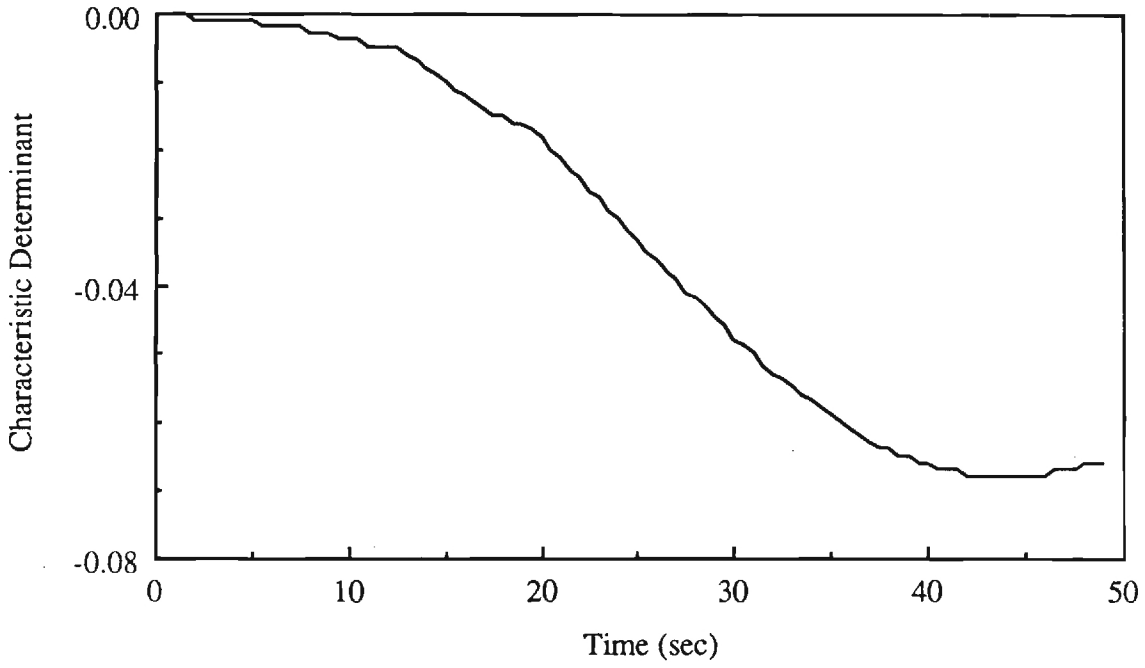

Figure 3.13 Characteristic Determinant Δ(t) along the Trajectory B
for Minimum Flight Time (K = 0.0)

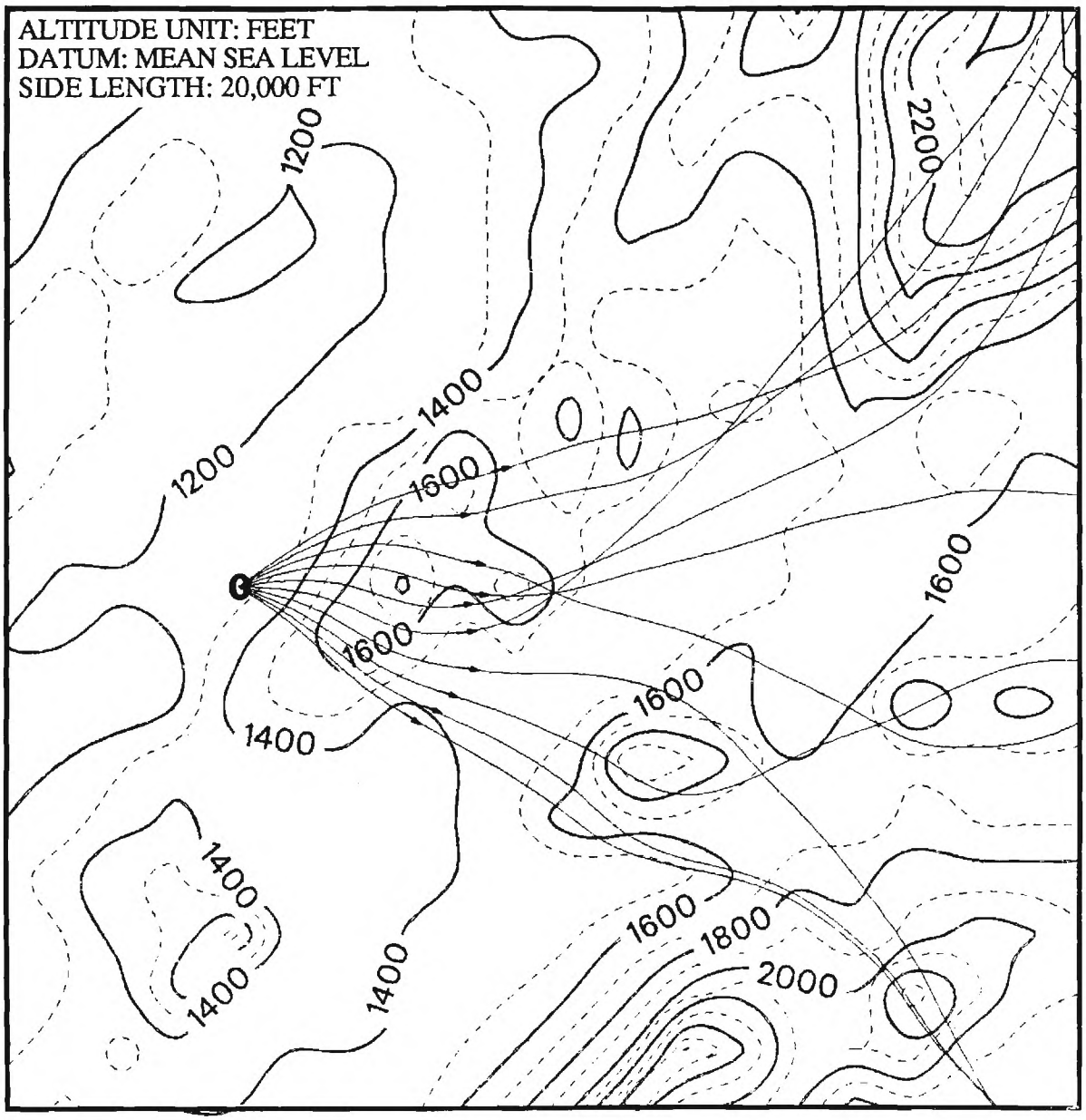

Figure 3.14 Euler Solutions for Optimal Route Planning No.2

(α = 10**5, ε =0.001)

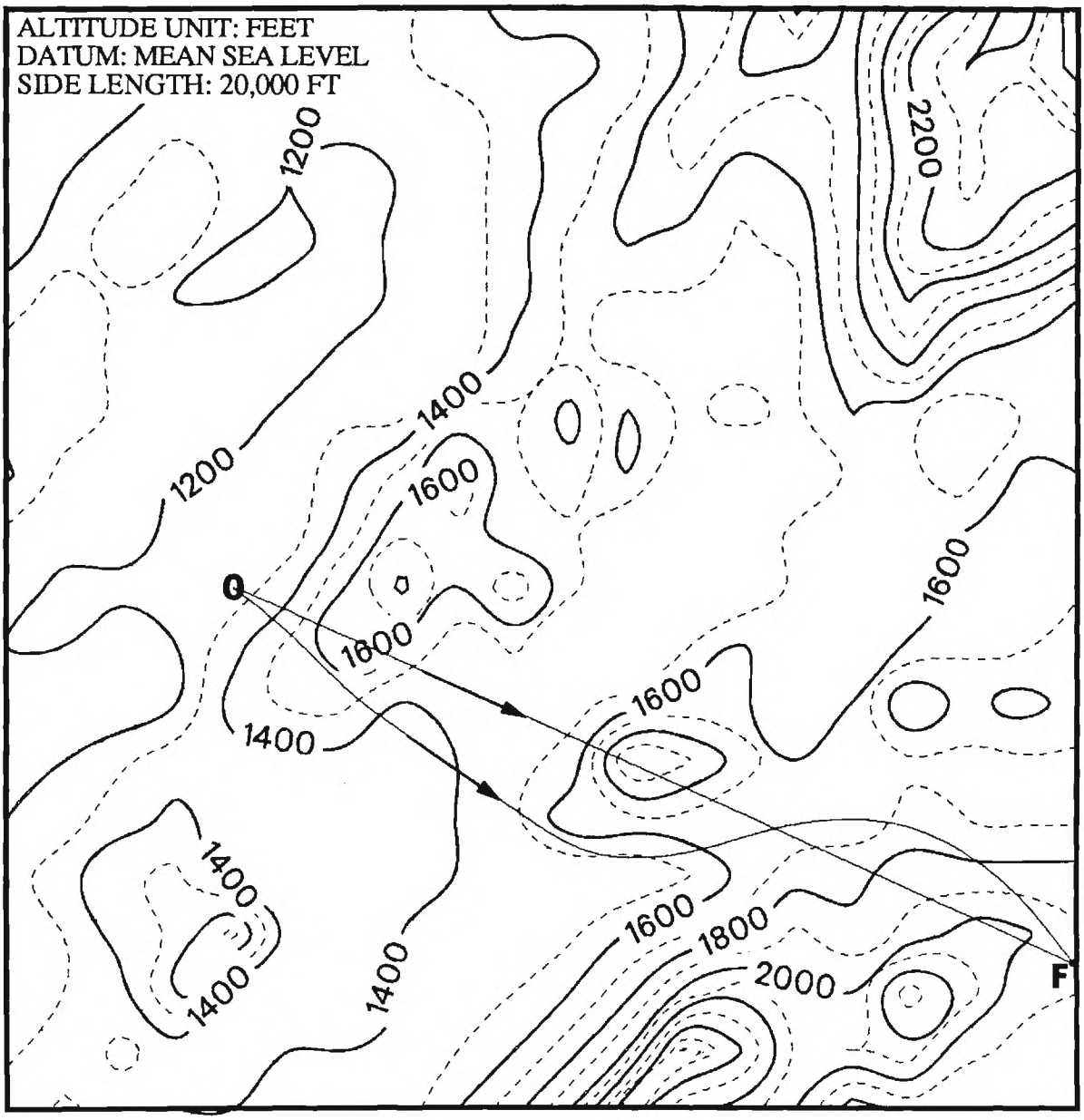

Figure 3.15 Comparison between Straight Trajectory and an Optimal Route Planning No.2 Trajectory (α = 10**6, ε =0.01)

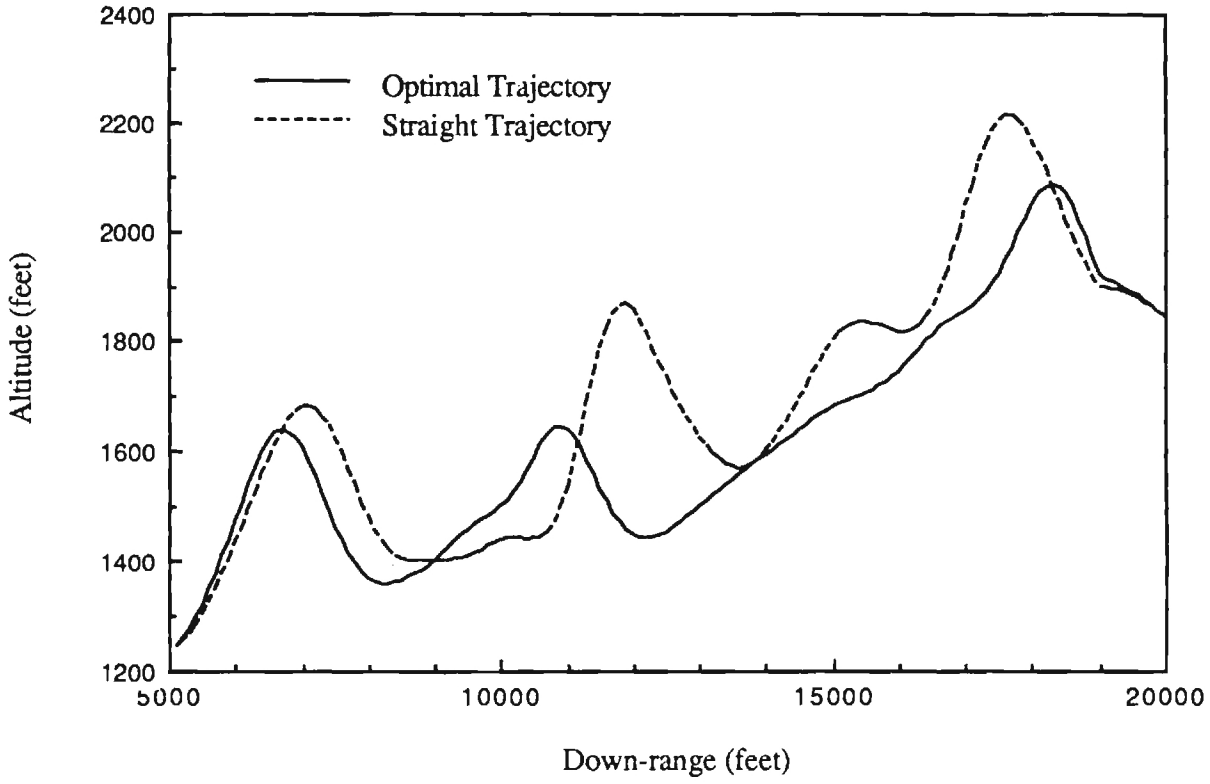

Figure 3.16 Altitude Profiles along Straight Trajectory and Optimal Trajectory

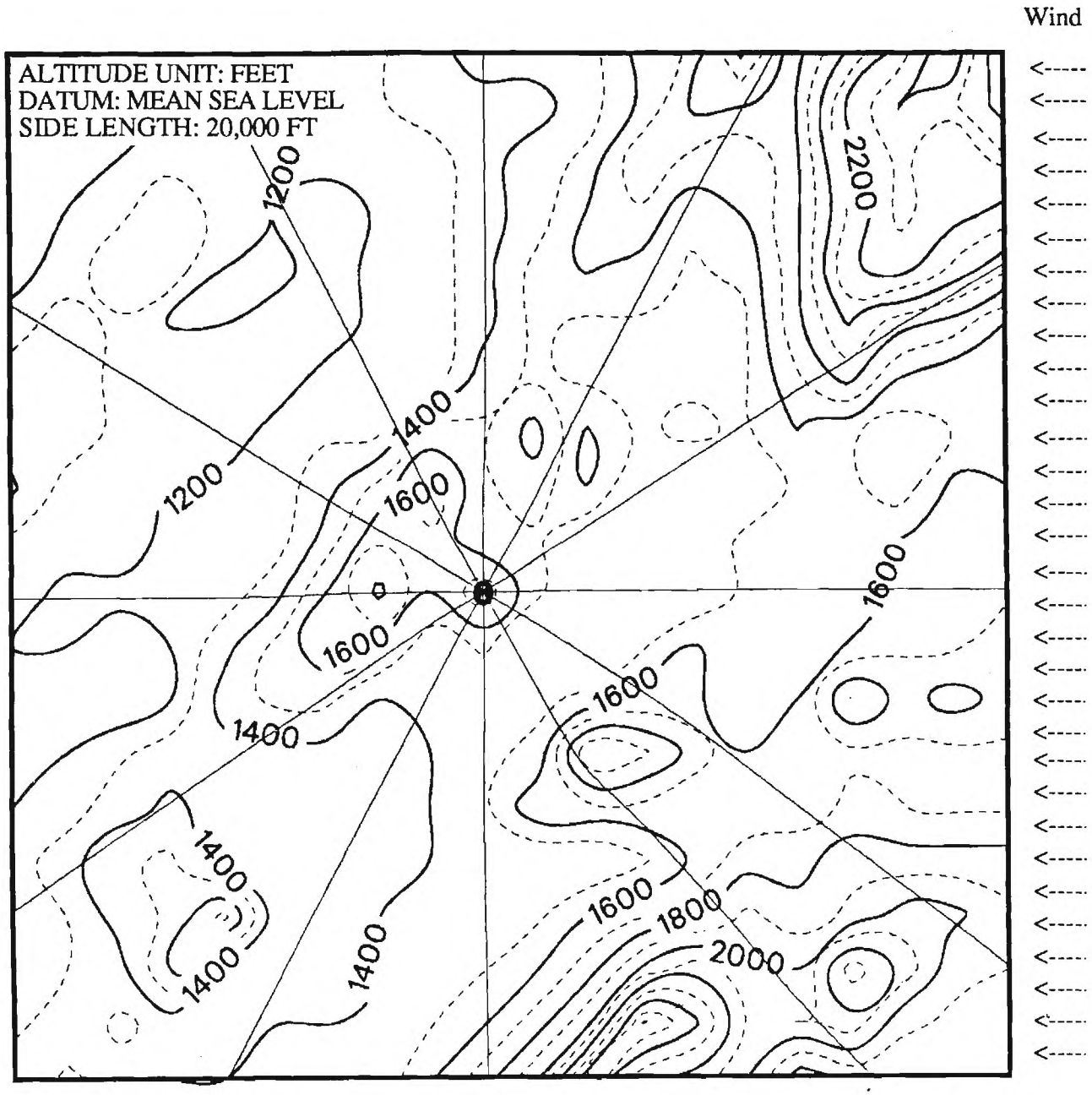

Figure 3.17 Euler Solutions for Minimum Flight Time Criterion
Considering Wind Effects (u/V =0.1)

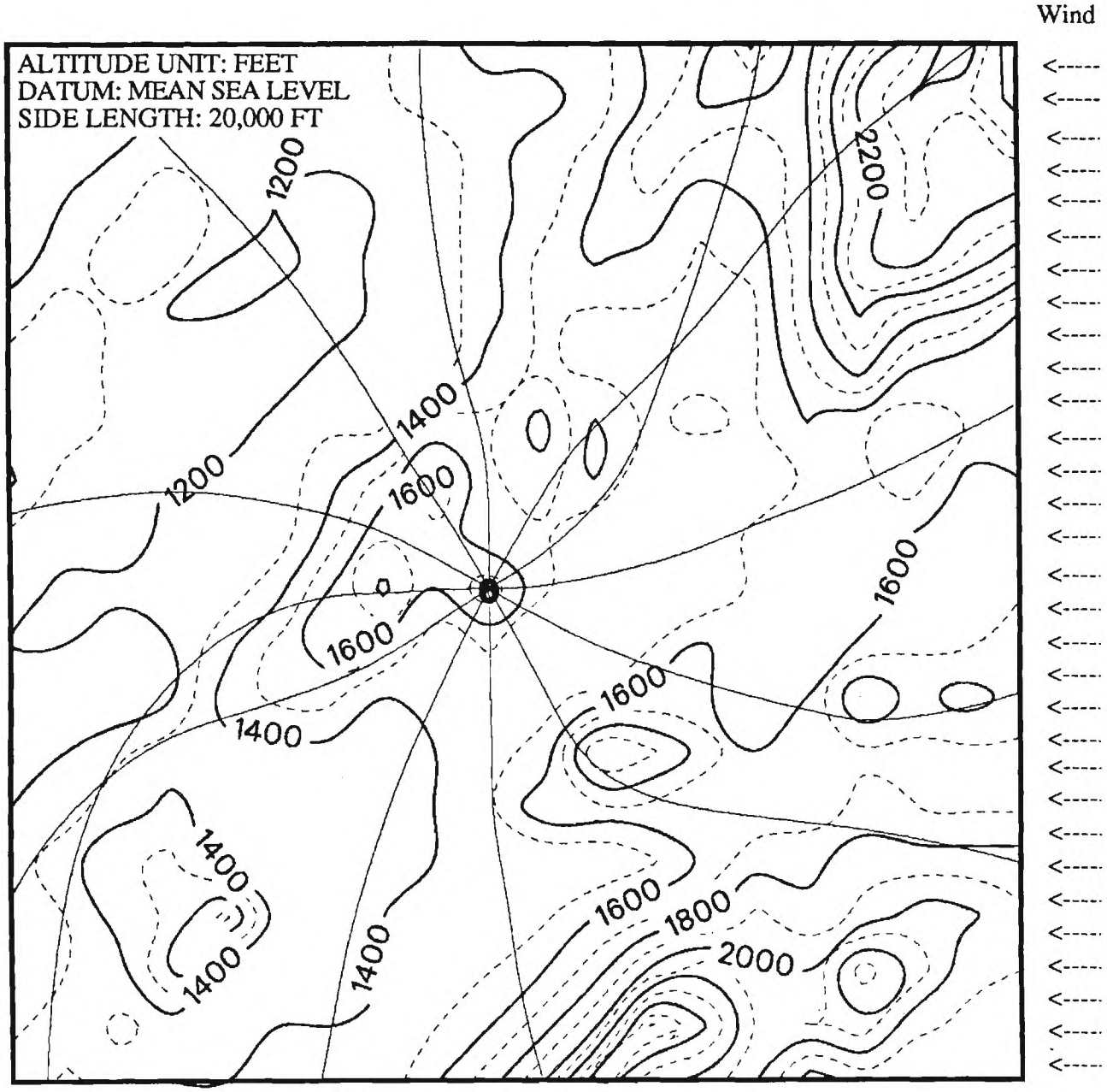

Figure 3.18 Euler Solutions for Maximum Terrain Masking Criterion Considering Wind Effects (u/V =0.1)

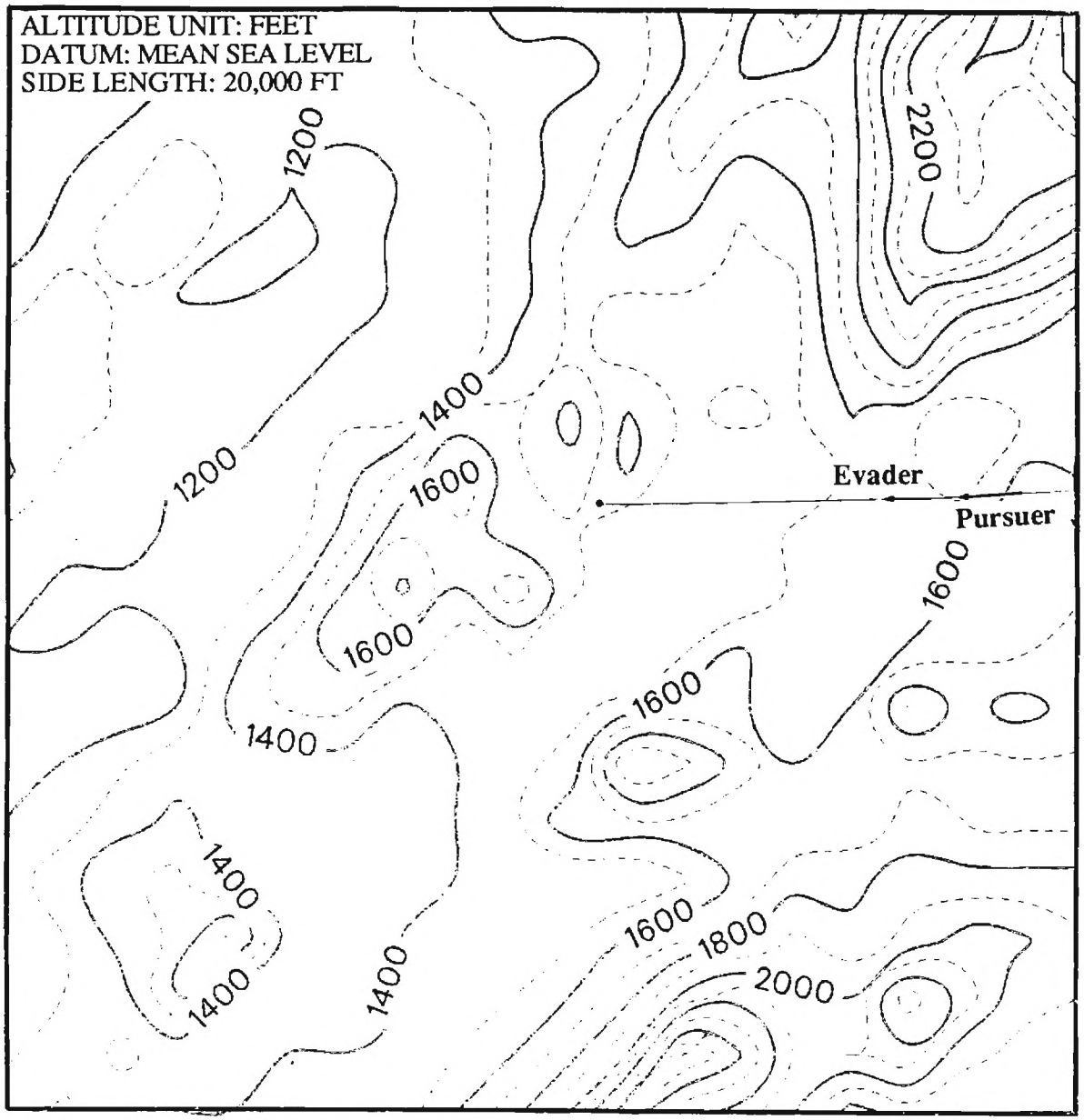

Figure 4.1 Trajectories for the Pursuer and Evader
($W_p = 0.0$, $W_e = 0.0$)

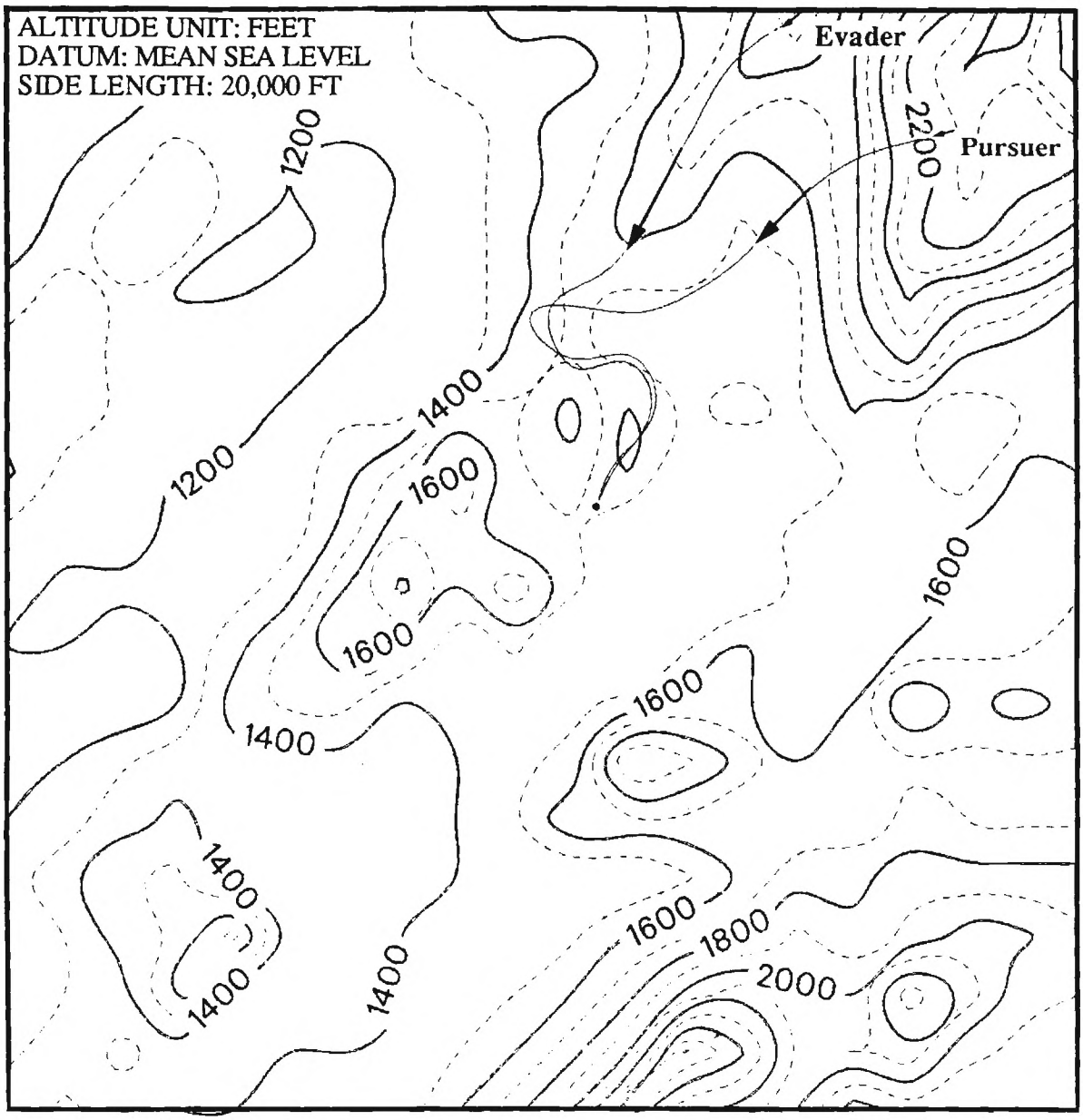

Figure 4.2 Trajectories for the Pursuer and Evader
(W_p = 1.0, W_e = 1.0)

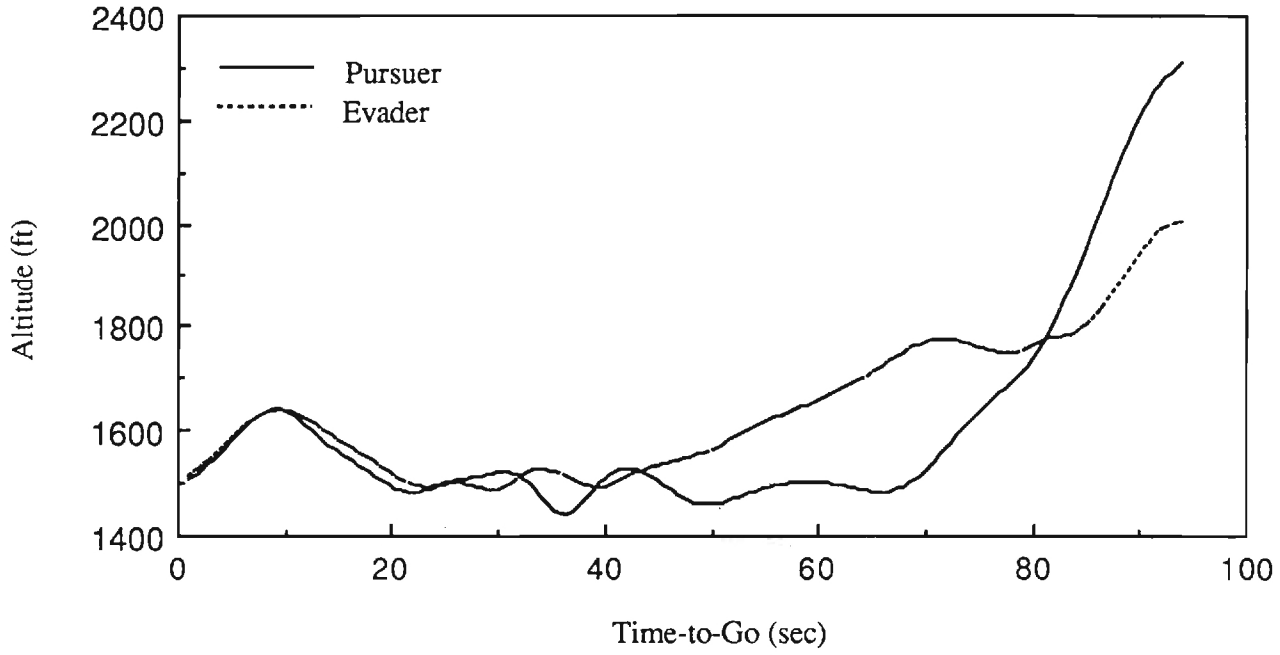

Figure 4.3 Altitude Histories for the Pursuer and Evader

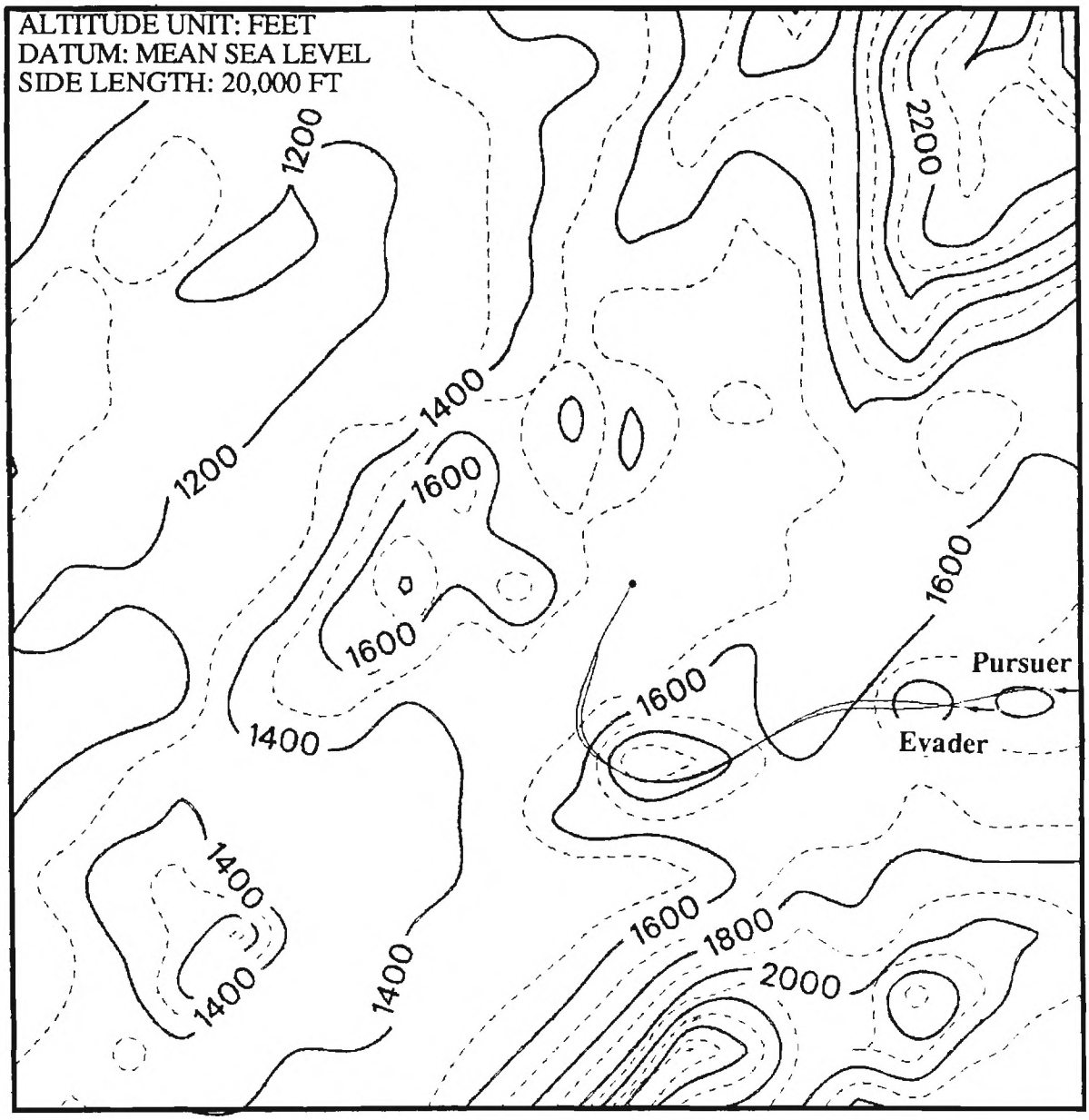

Figure 4.4 Trajectories for the Pursuer and Evader
($W_p = 1.0$, $W_e = 1.0$)

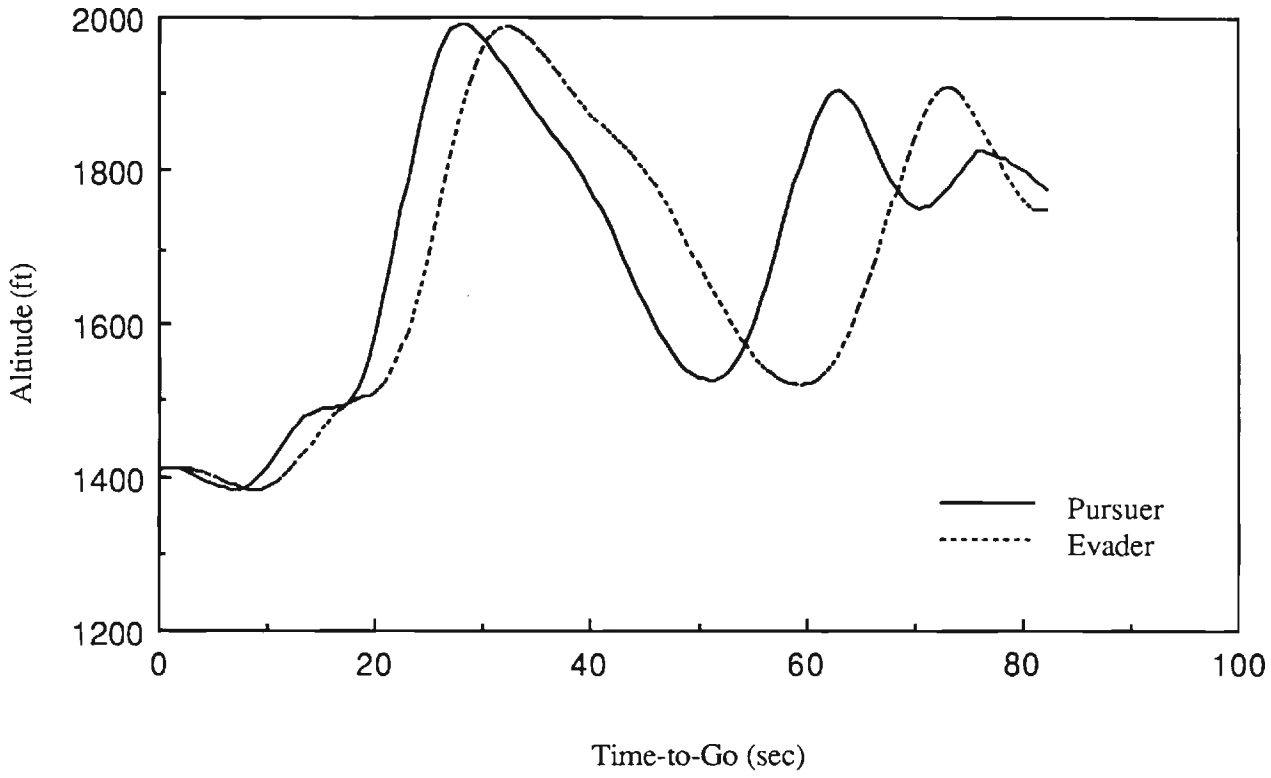

Figure 4.5 Altitude Histories for the Pursuer and Evader

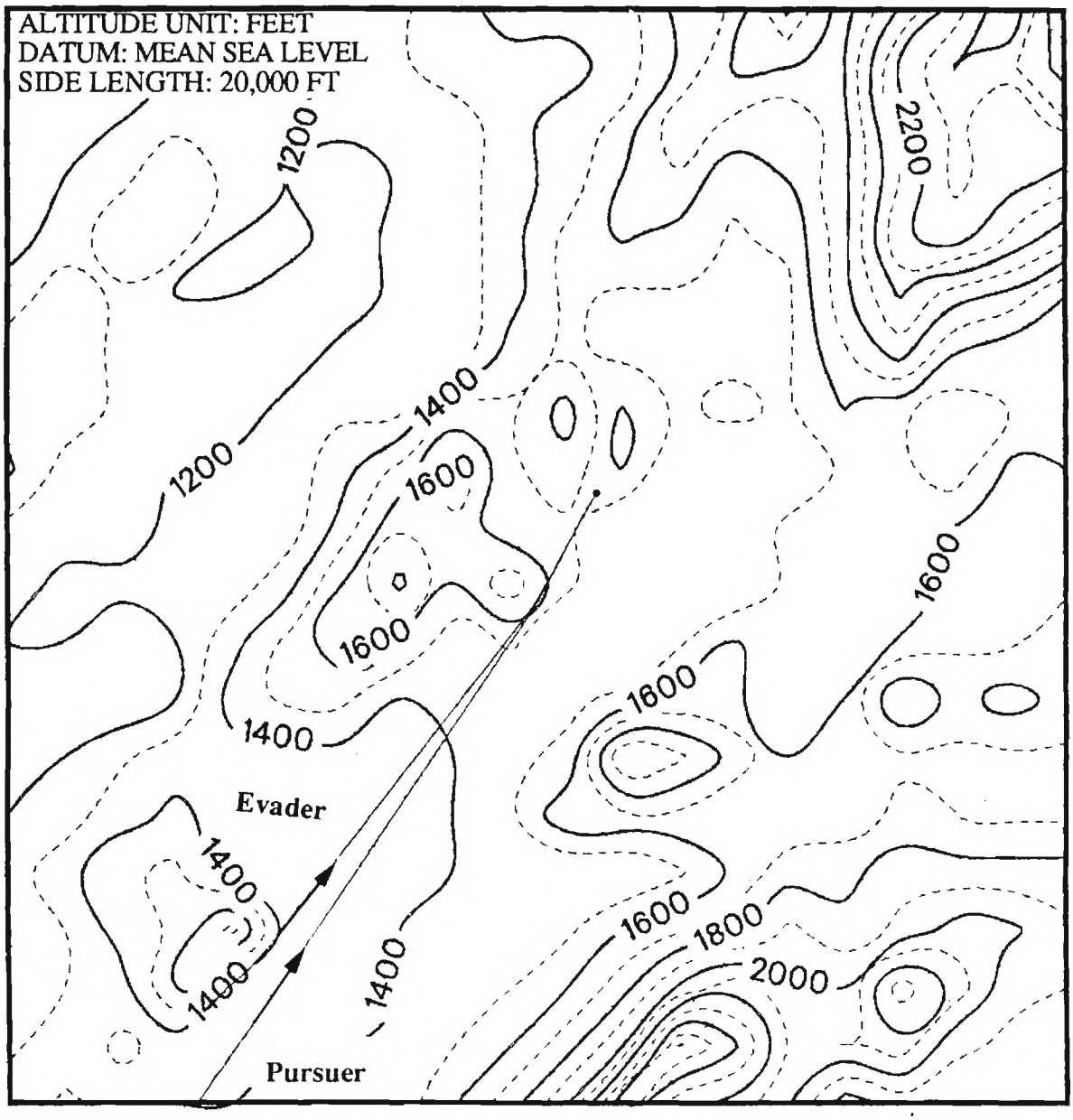

Figure 4.6 Trajectories for the Pursuer and Evader
($W_p = 0.0$, $W_e = 1.0$)

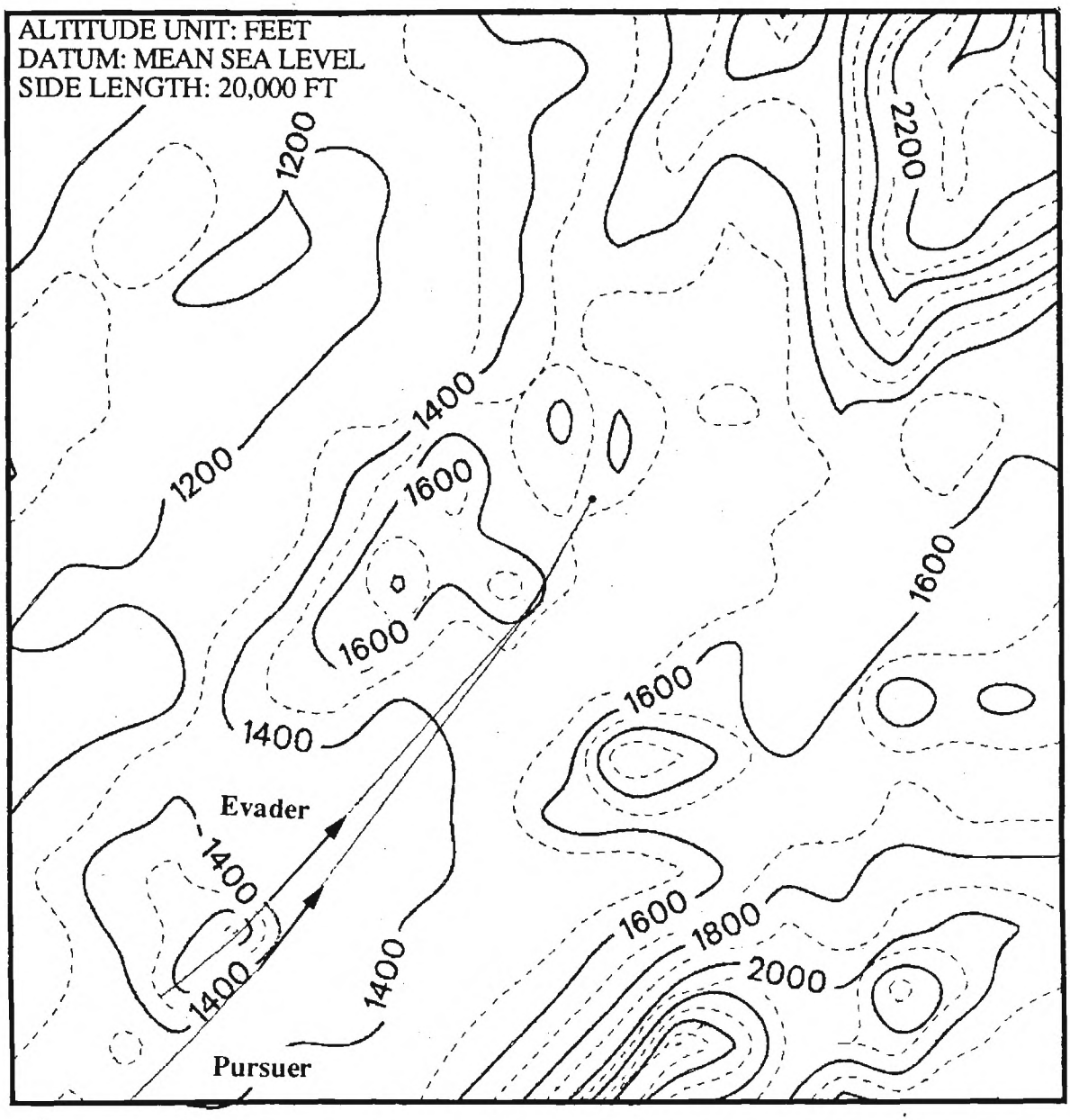

Figure 4.7 Trajectories for the Pursuer and Evader
($W_p = 0.5$, $W_e = 1.0$)

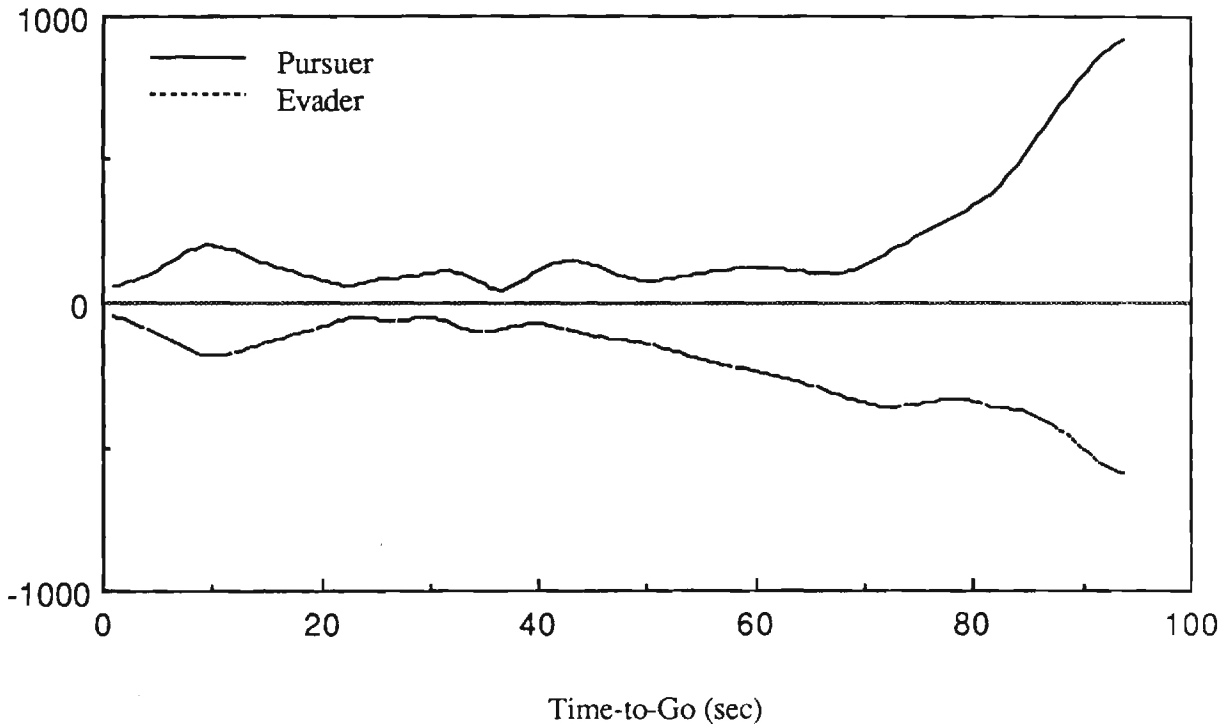

Figure 4.8 Legendre-Clebsch Test for the Pursuer and Evader

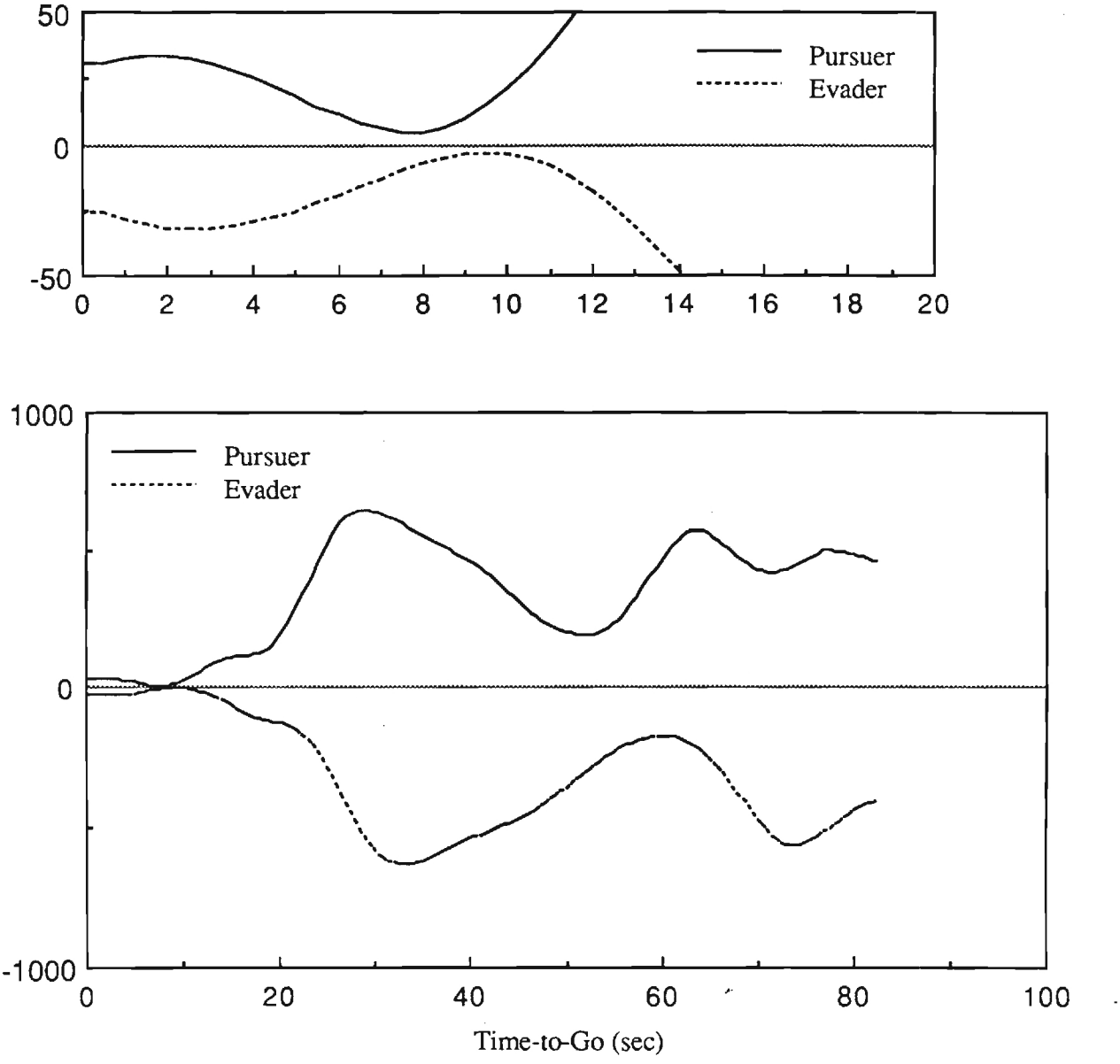

Figur 4.9 Legendre-Clebsch Test for the Pursuer and Evader

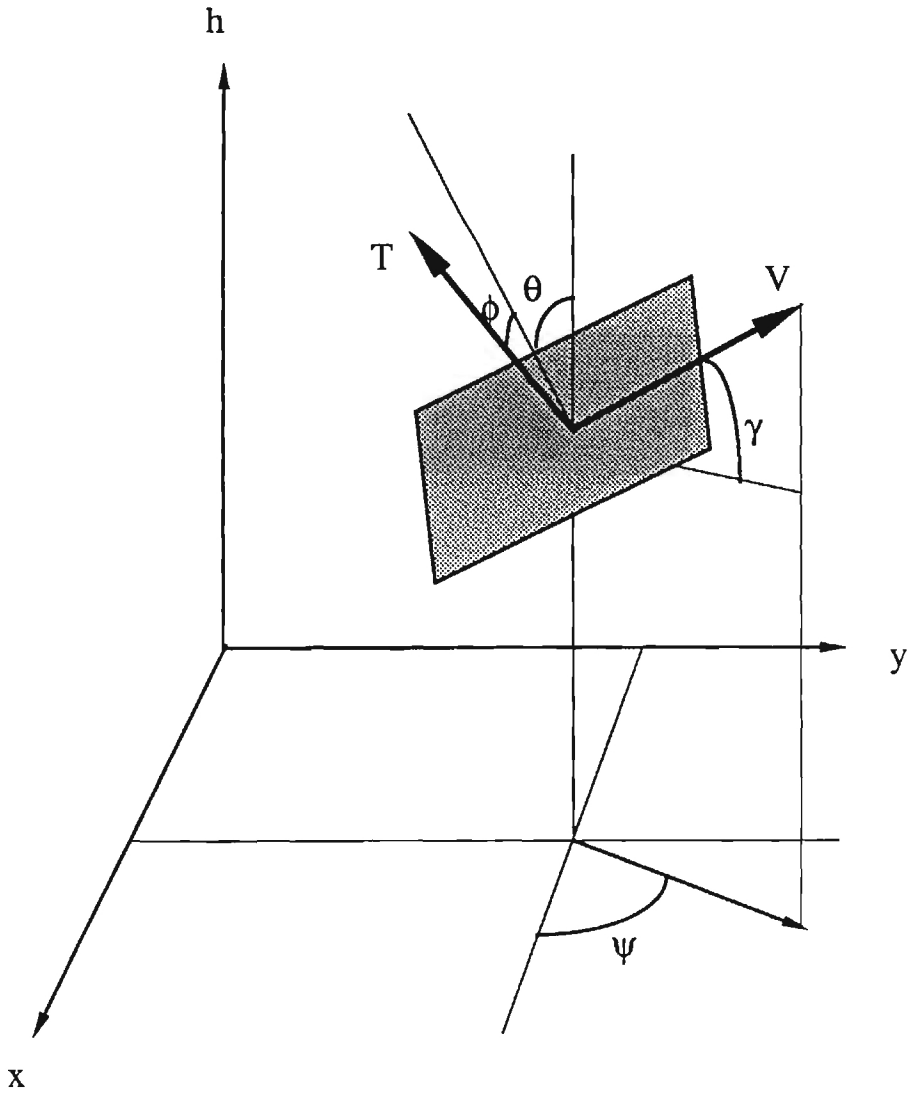

Figure 4.10 The Coordinate System

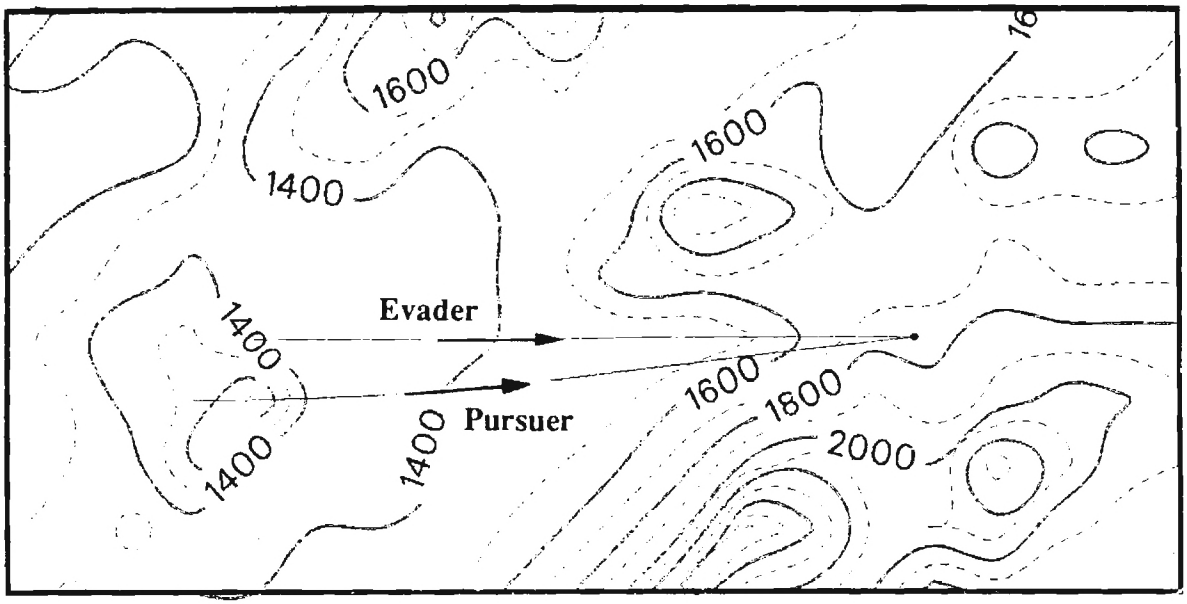

Figure 4.11 Trajectories for the Pursuer and Evader
($\sigma = 1.0$, $\alpha = 0.0007$, $\beta = 0.00001$)

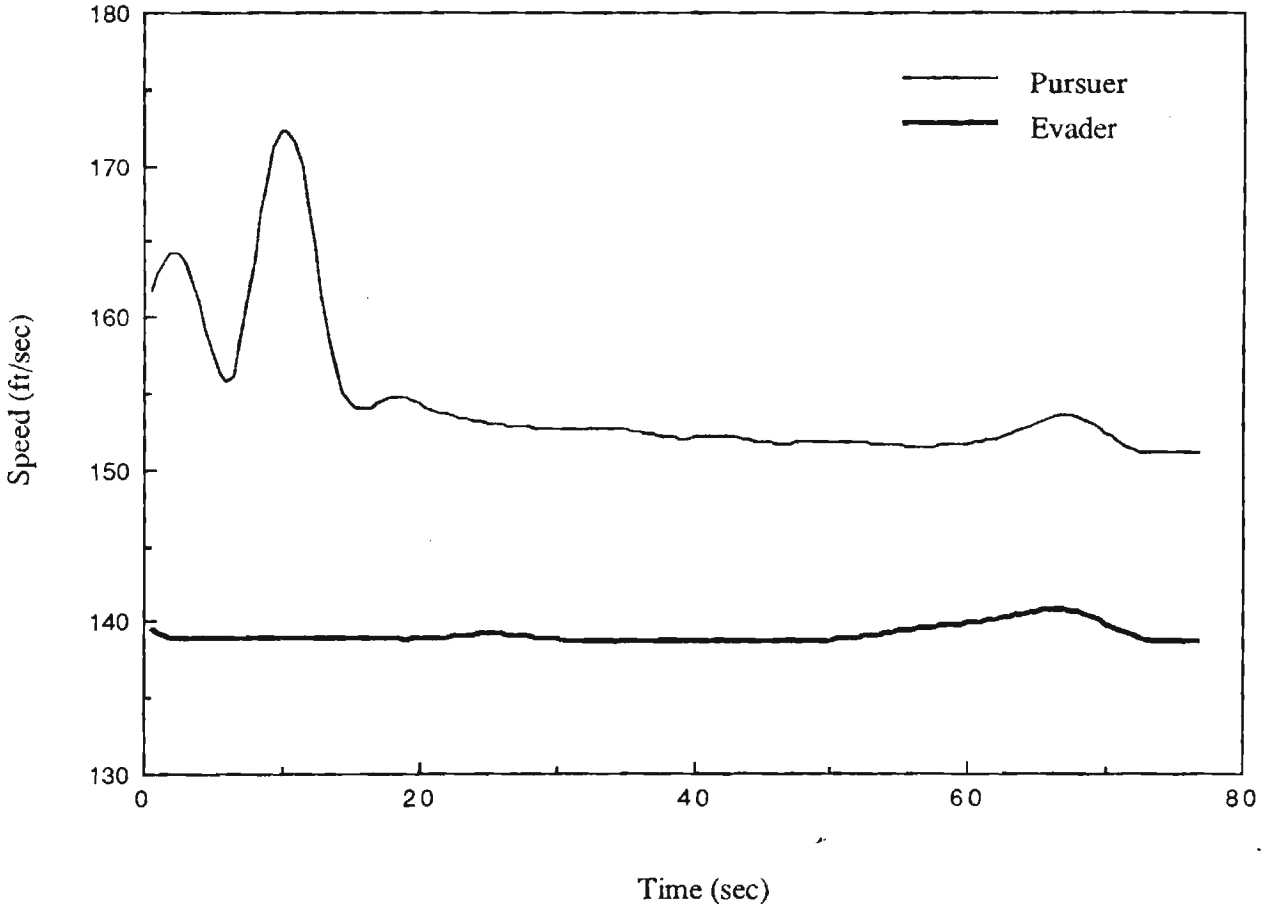

Figure 4.12 Speed Histories for the Pursuer and Evader

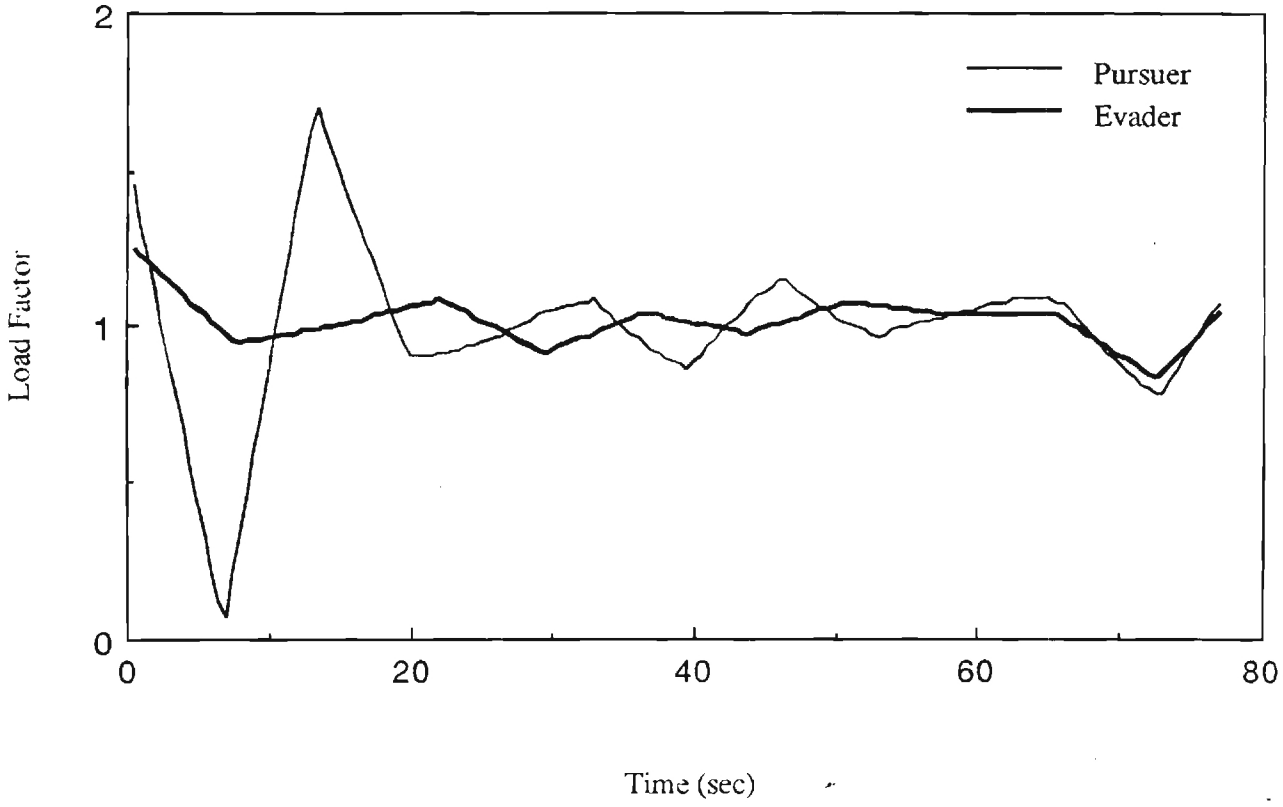

Figure 4.13 Load Factor Histories for the Pursuer and Evader

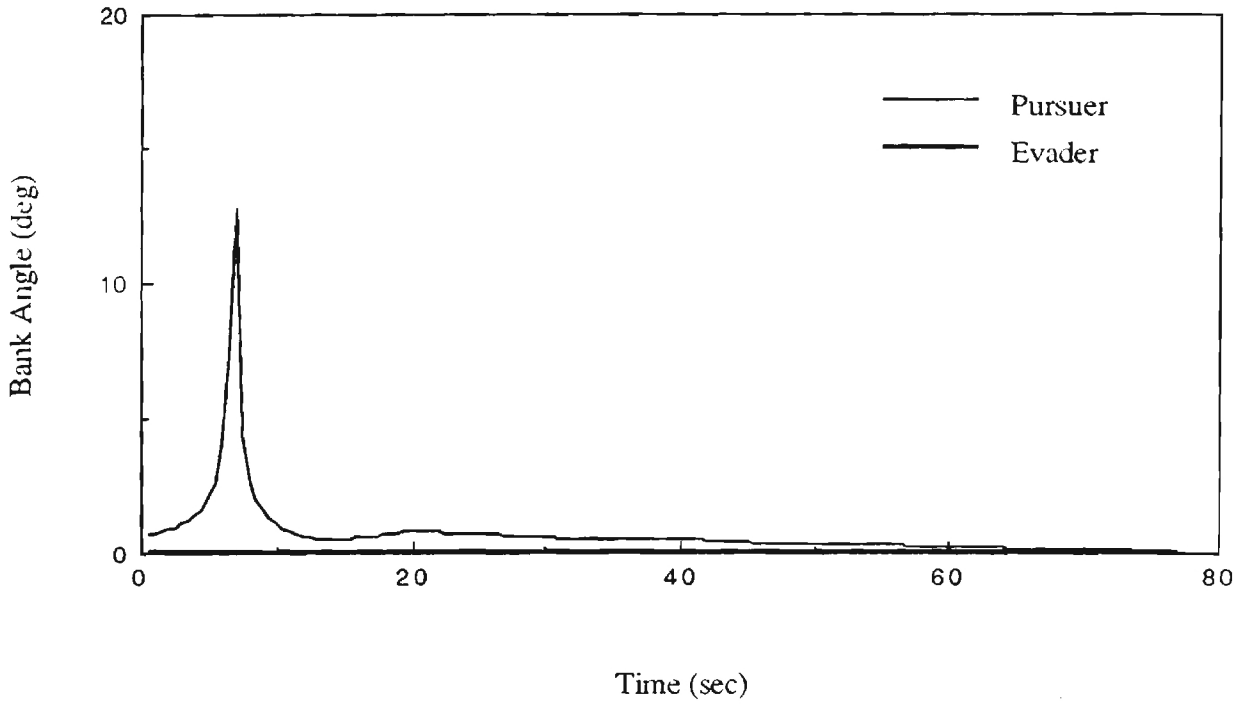

Figure 4.14 Bank Angle Histories for the Pursuer and Evader

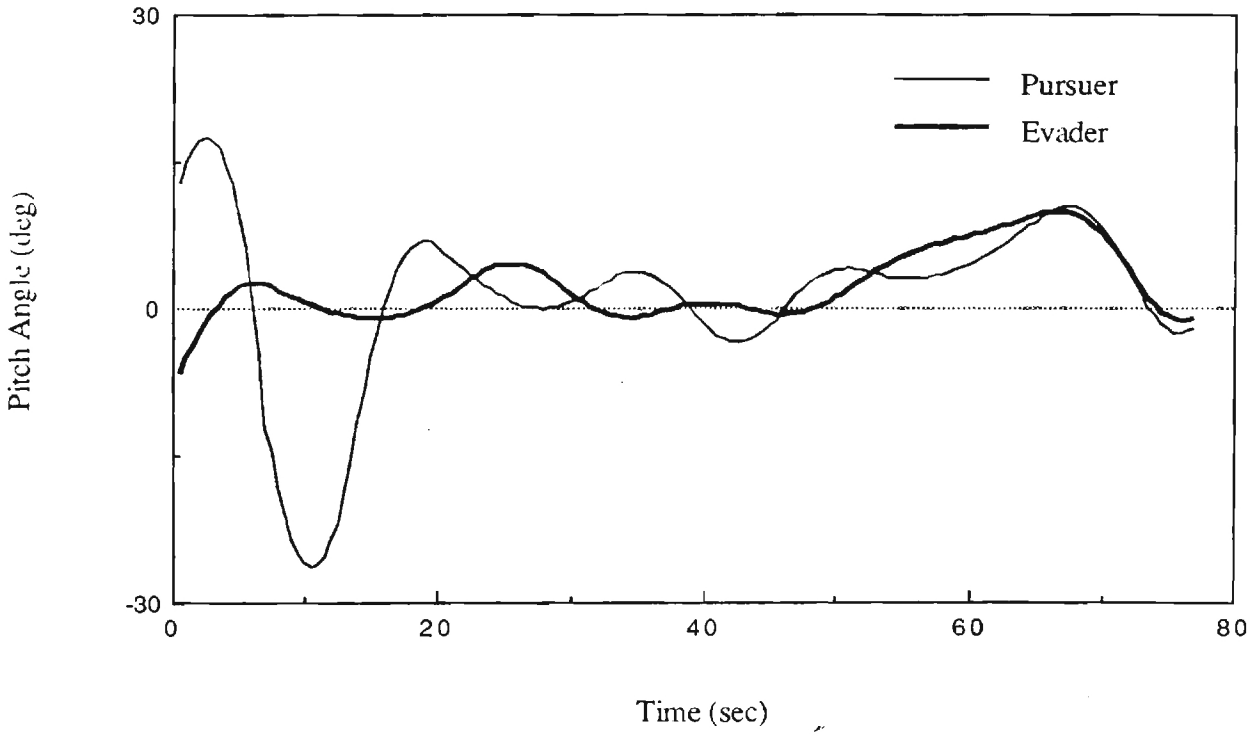

Figure 4.15 Pitch Angle Histories for the Pursuer and Evader

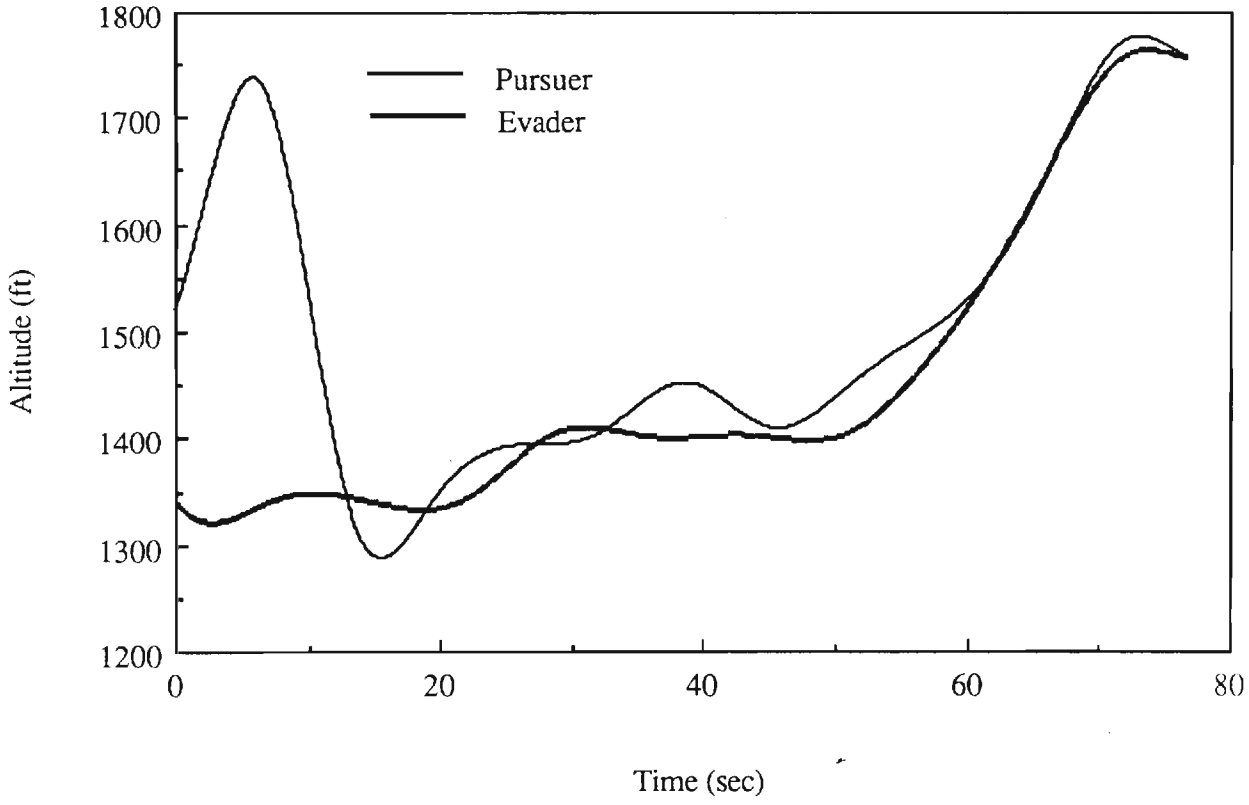

Figure 4.16 Altitude Histories for The Pursuer and Evader

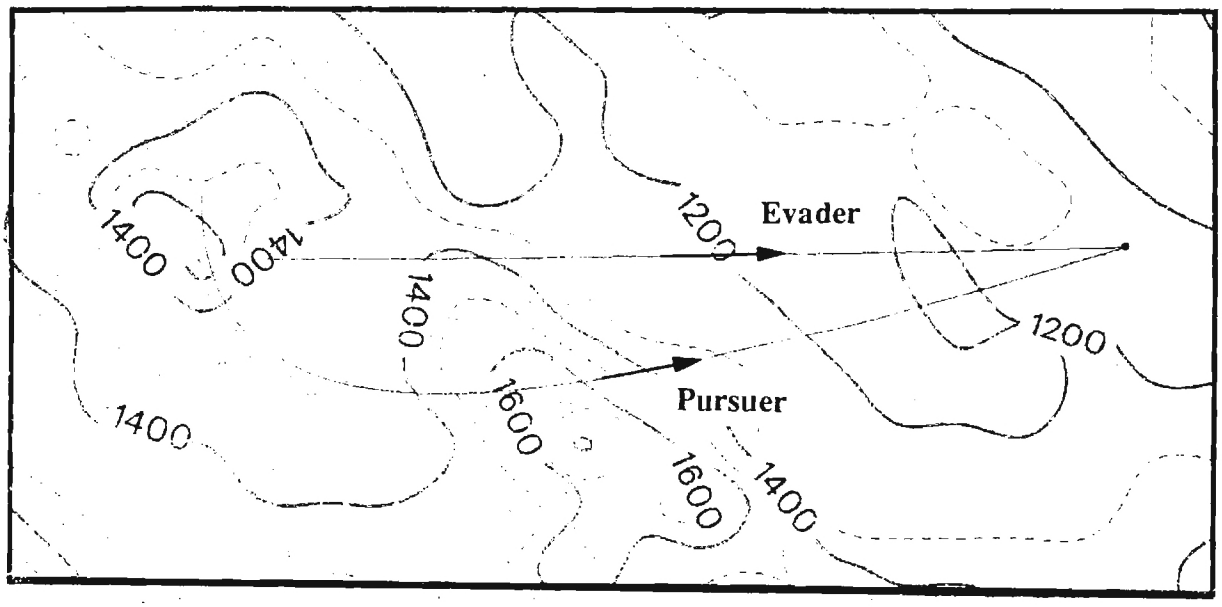

Figure 4.17 Trajectories for the Pursuer and Evader
($\sigma = 1.0$, $\alpha = 0.0007$, $\beta = 0.00001$)

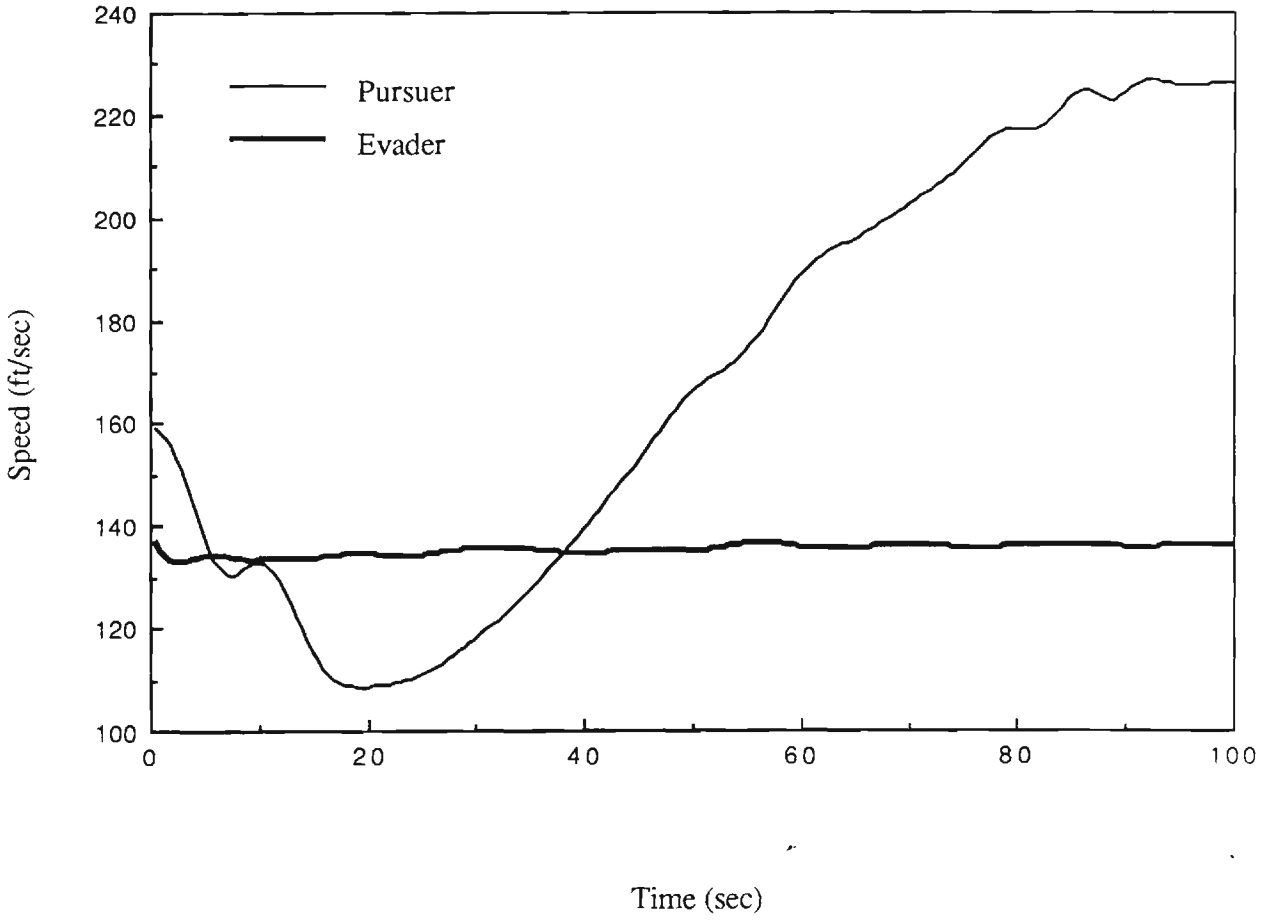

Figure 4.18 Speed Histories for the Pursuer and Evader

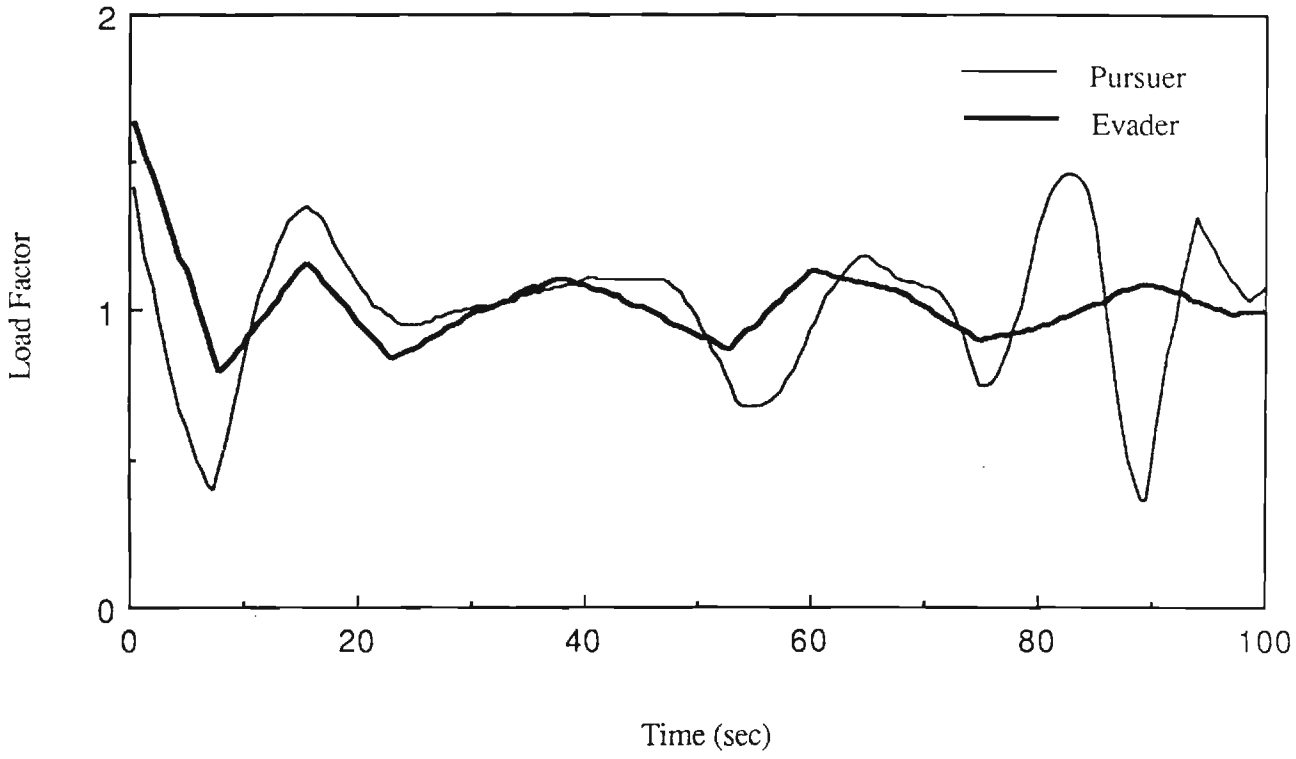

Figure 4.19 Load Factor Histories for the Pursuer and Evader

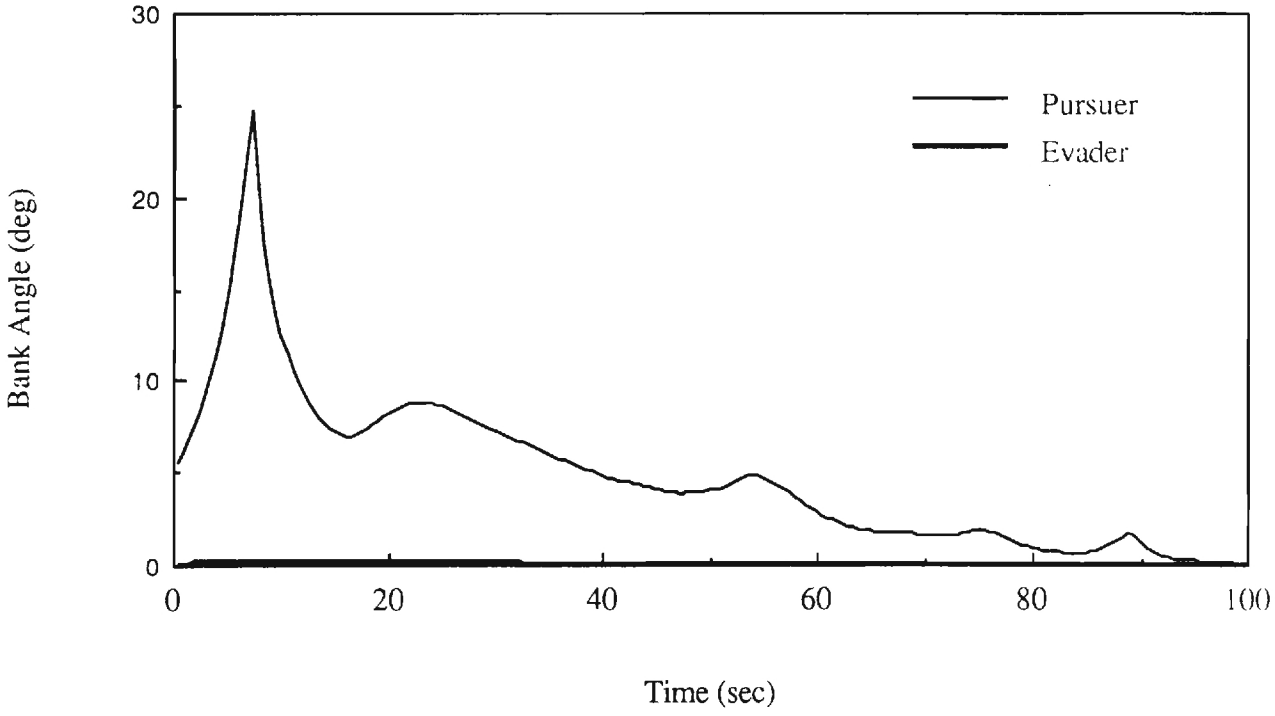

Figure 4.20 Roll Attitude Histories for the Pursuer and Evader

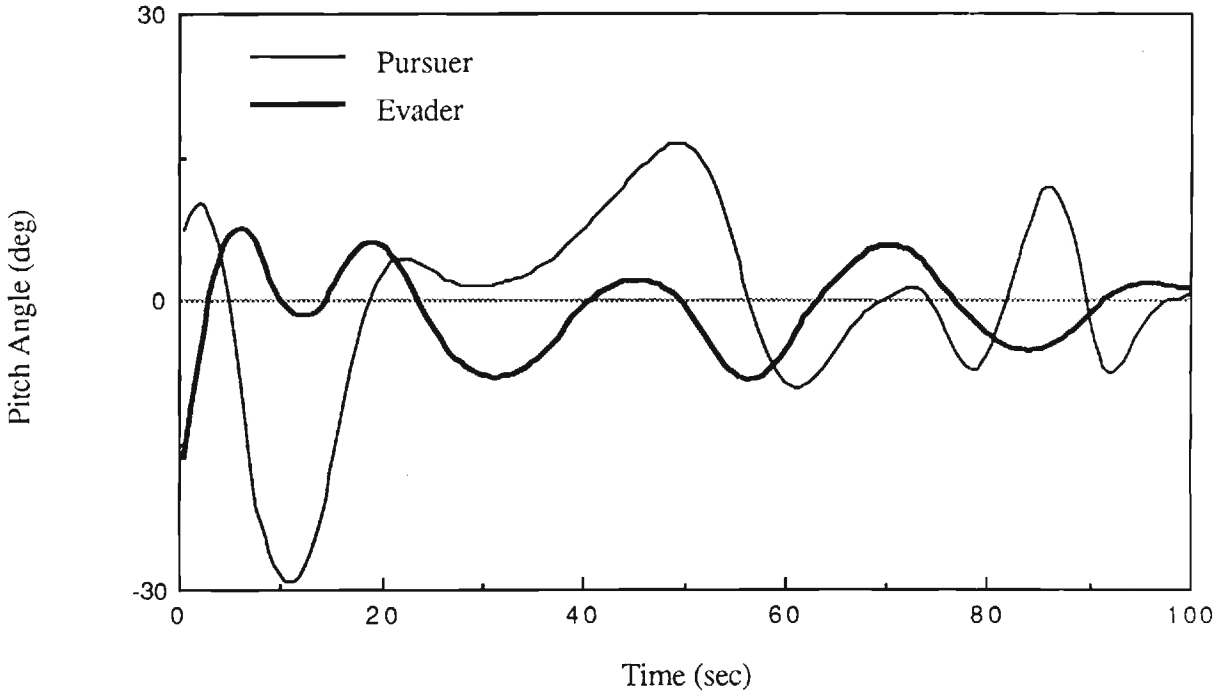

Figure 4.21 Pitch Attitude Histories fot the Pursuer and Evader

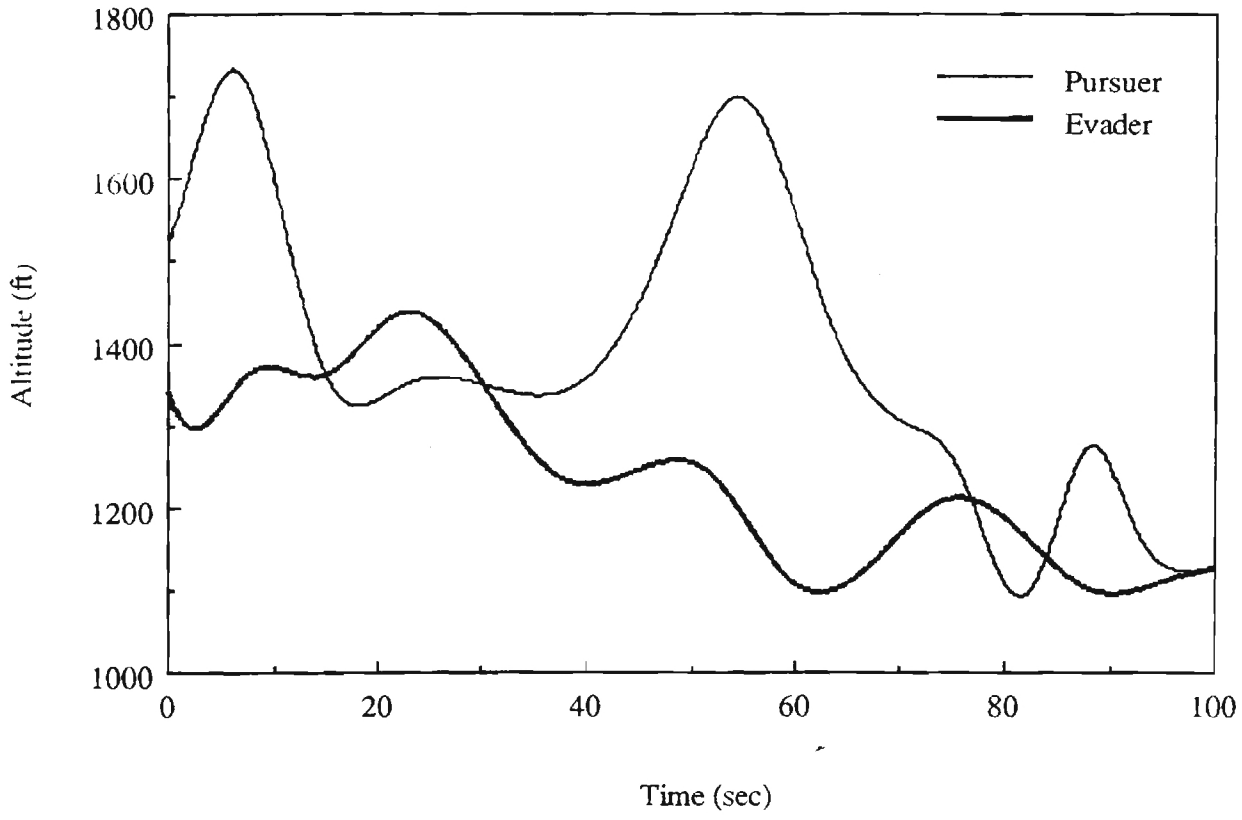

Figure 4.22 Altitude Histories for The Pursuer and Evader

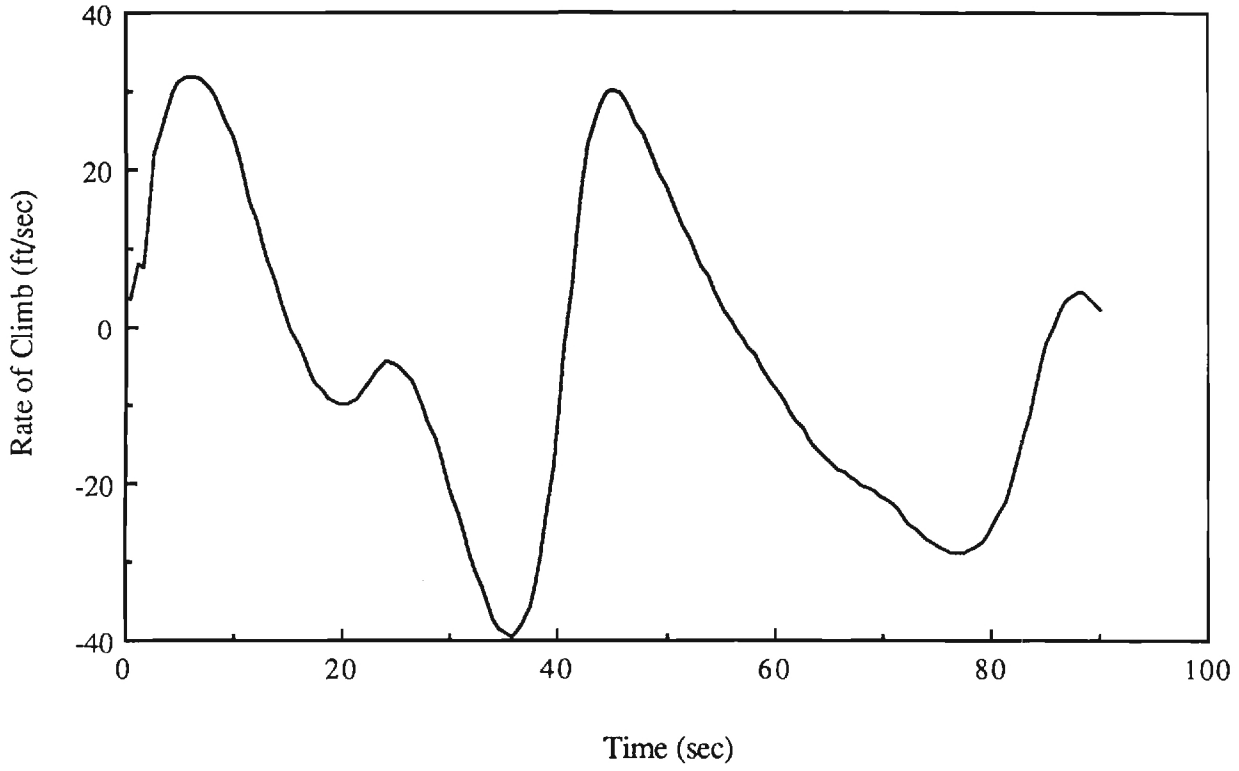

Figure 5.1 Rate of Climb for Maximum Terrain Masking Trajectory

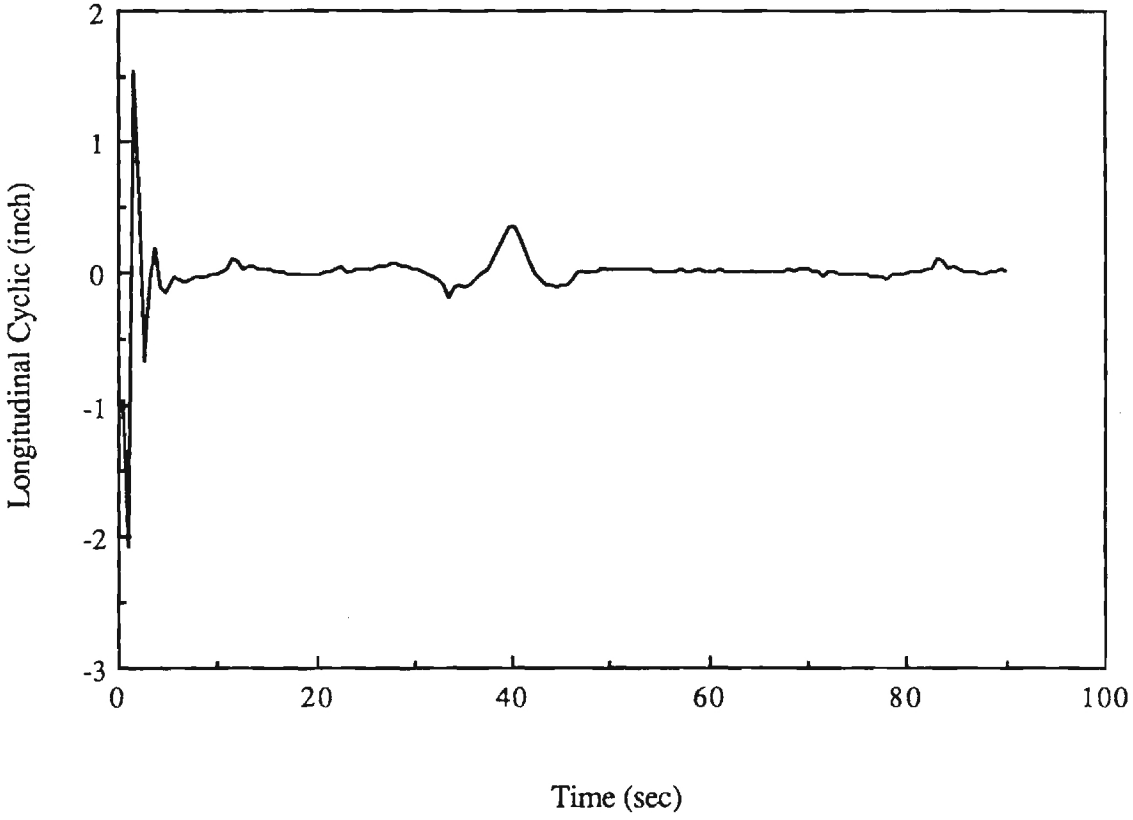

Figure 5.2 Longitudinal Cyclic Control for Maximum Masking Trajectory

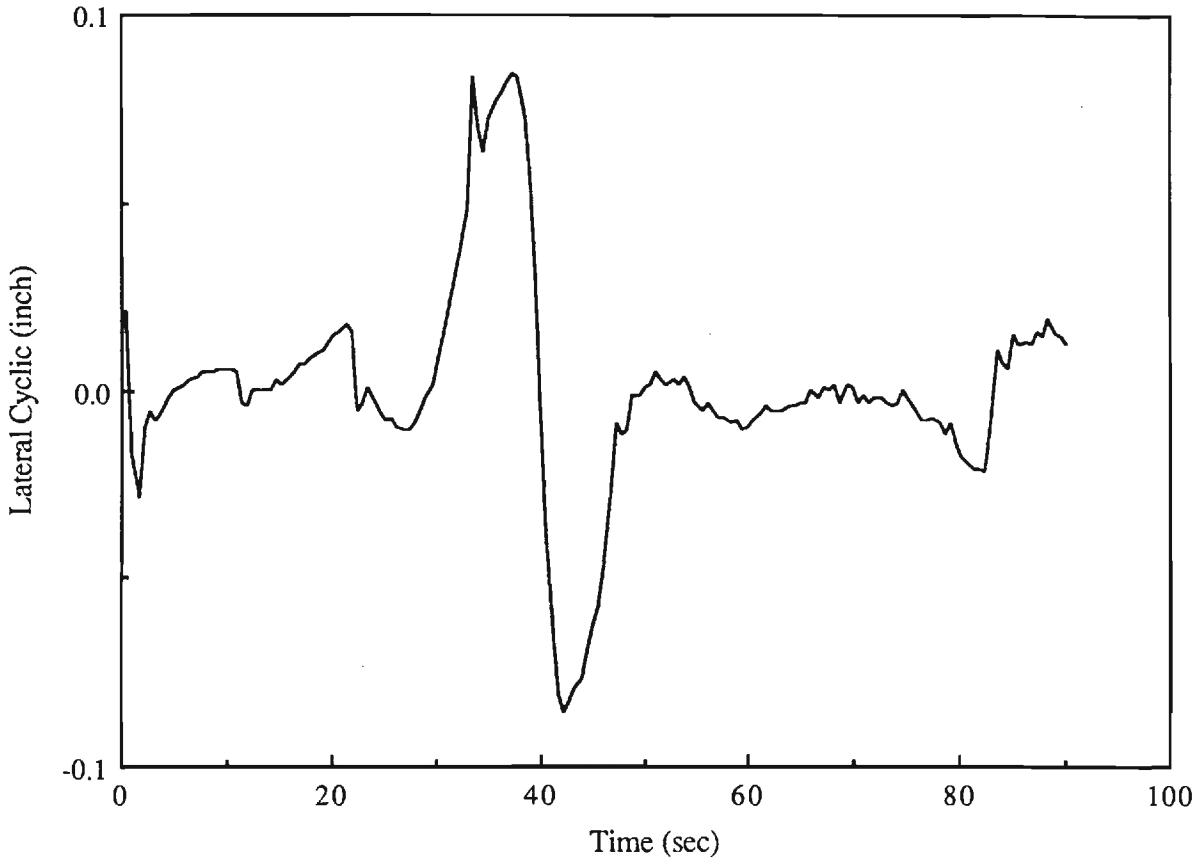

Figure 5.3 Lateral Cyclic Control for Maximum Masking Trajectory

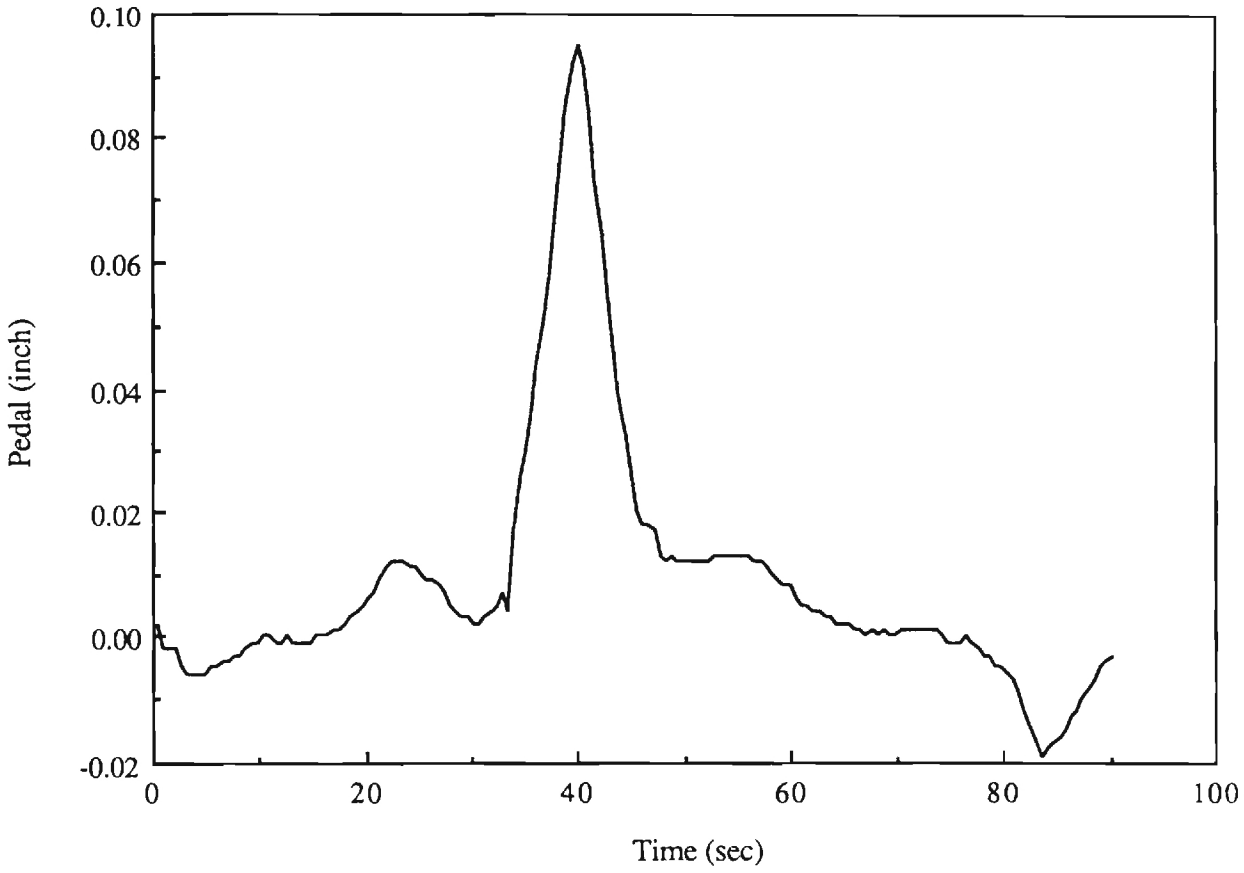

Figure 5.4 Pedal Control for Maximum Masking Trajectory

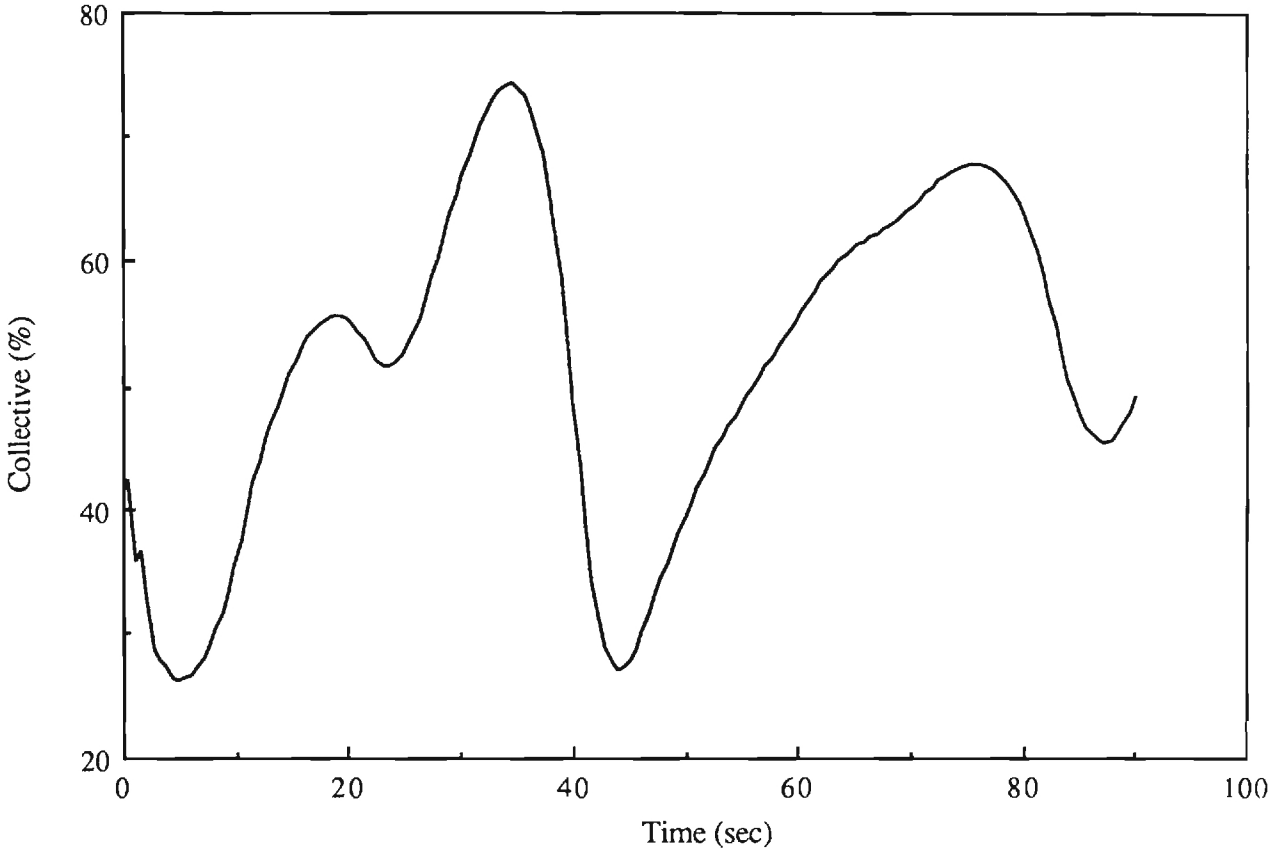

Figure 5.5 Collective Control for Maximum Masking Trajectory

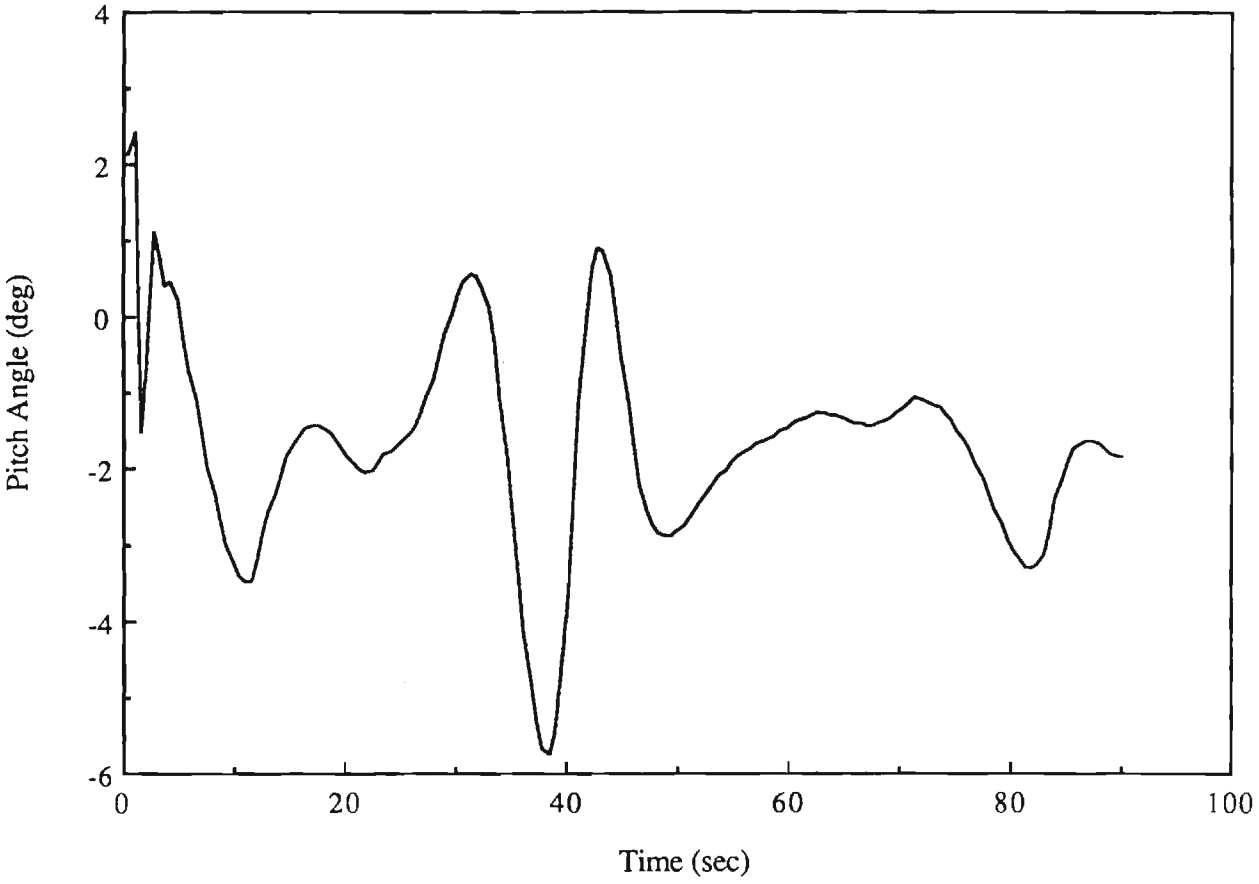

Figure 5.6 Pitch Attitude Response for Maximum Masking Trajectory

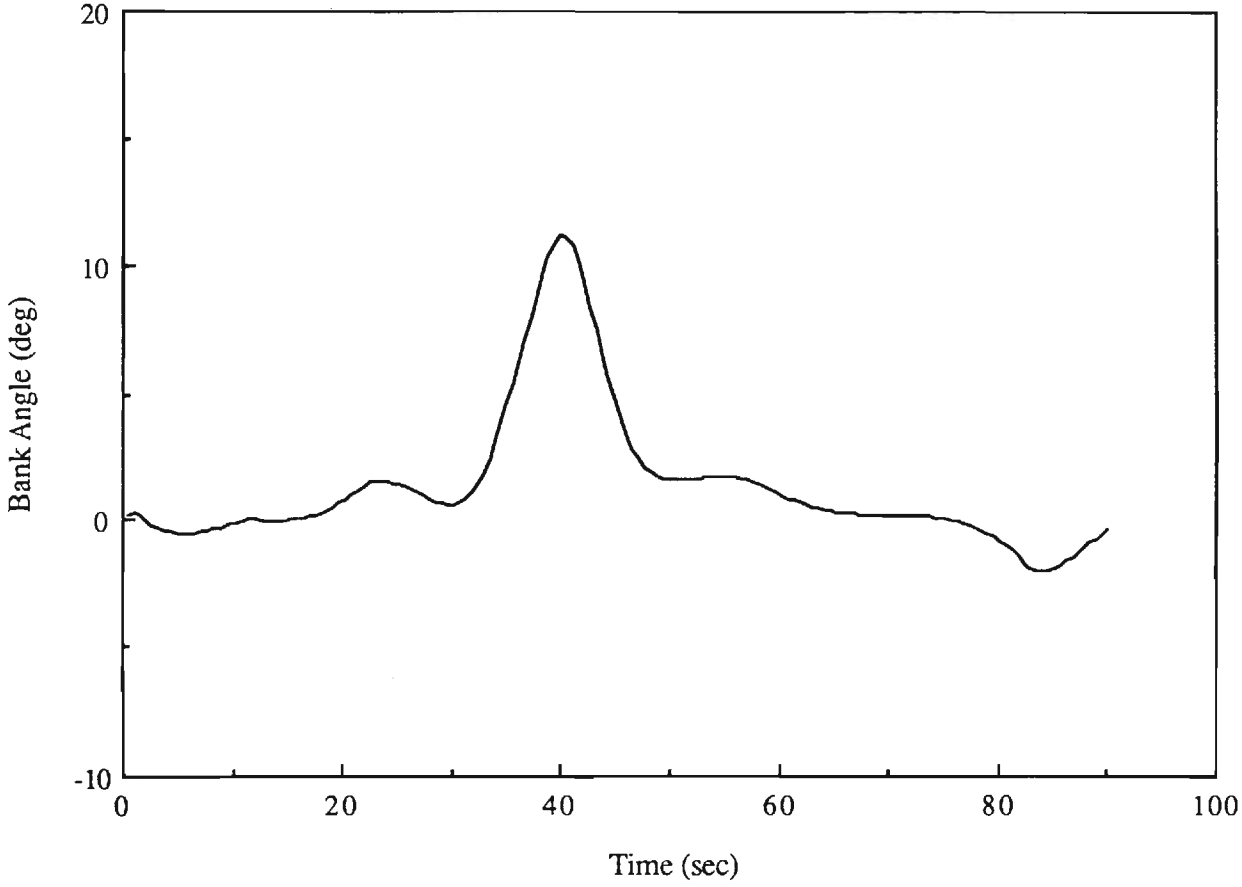

Figure 5.7 Roll Attitude Response for Maximum Masking Trajectory

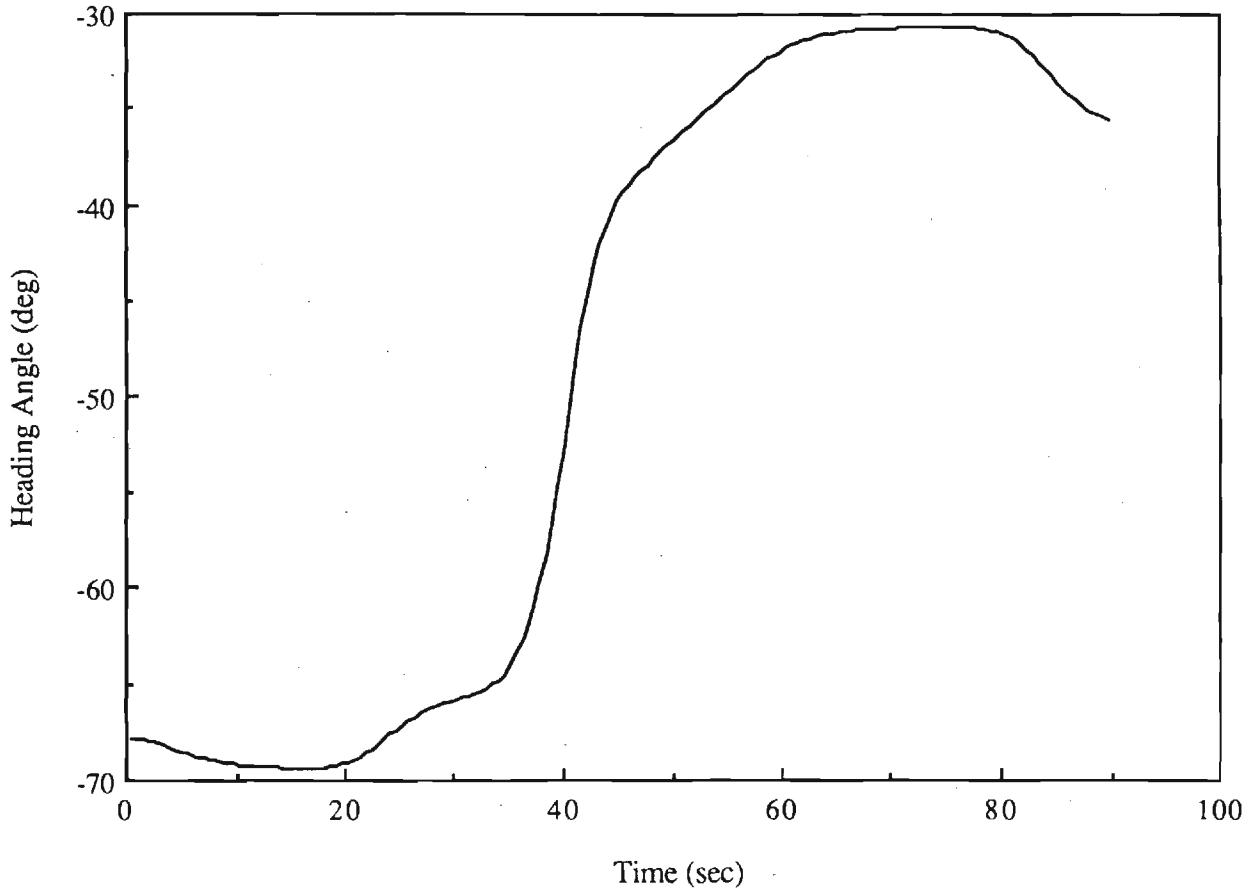

Figure 5.8 Yaw Attitude Response for Maximum Masking Trajectory

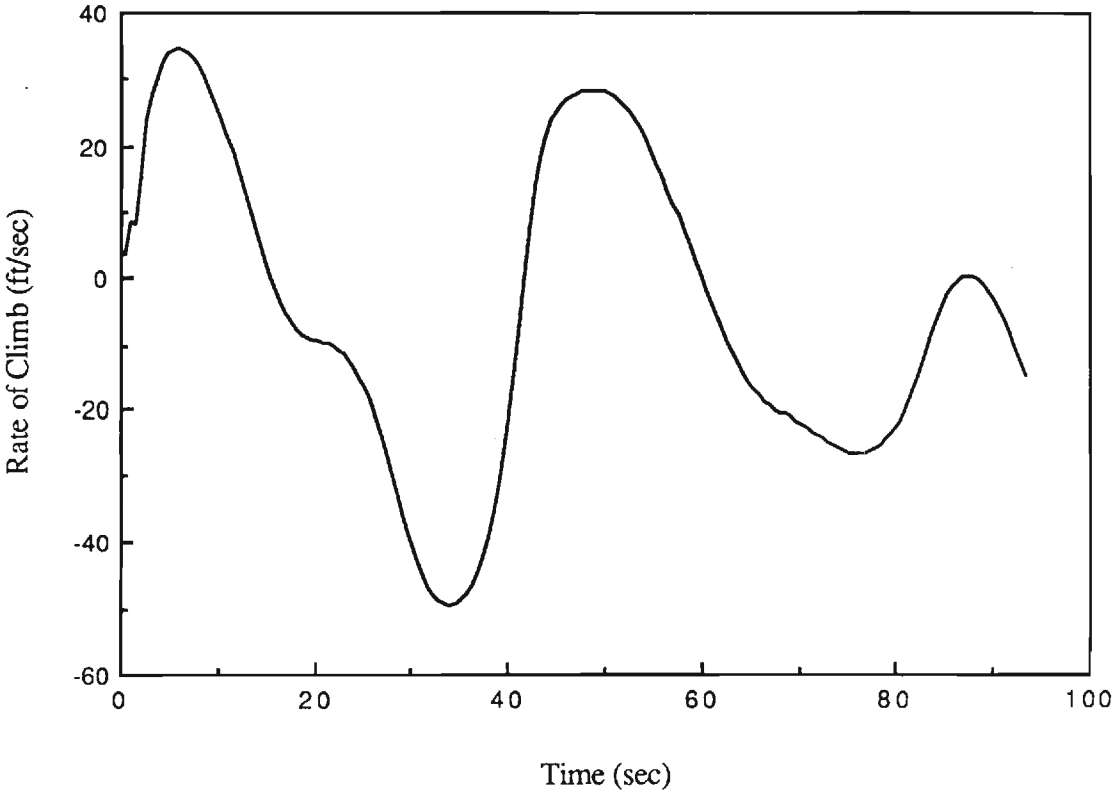

Figure 5.9 Rate of Climb for Minimum Time Trajectory

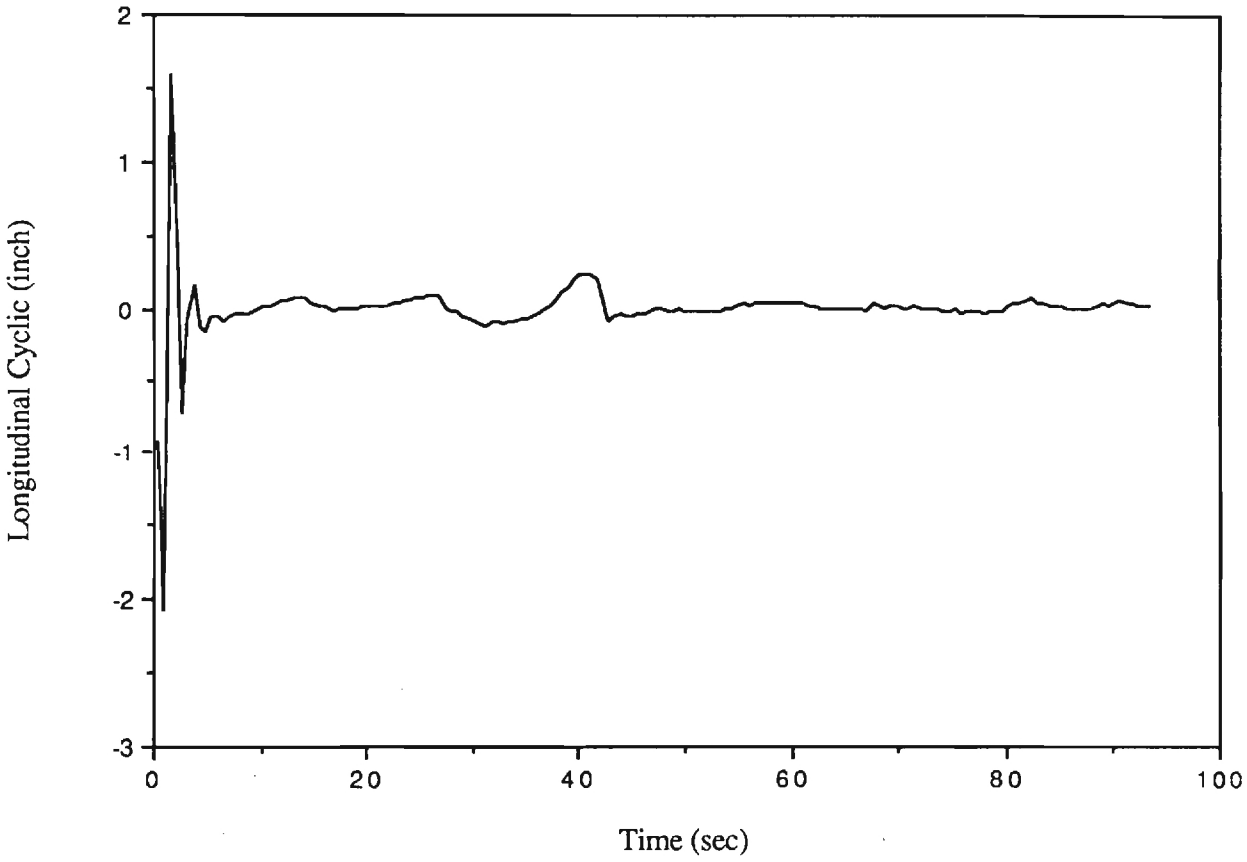

Figure 5.10 Longitudinal Cyclic Control for Minimum Time Trajectory

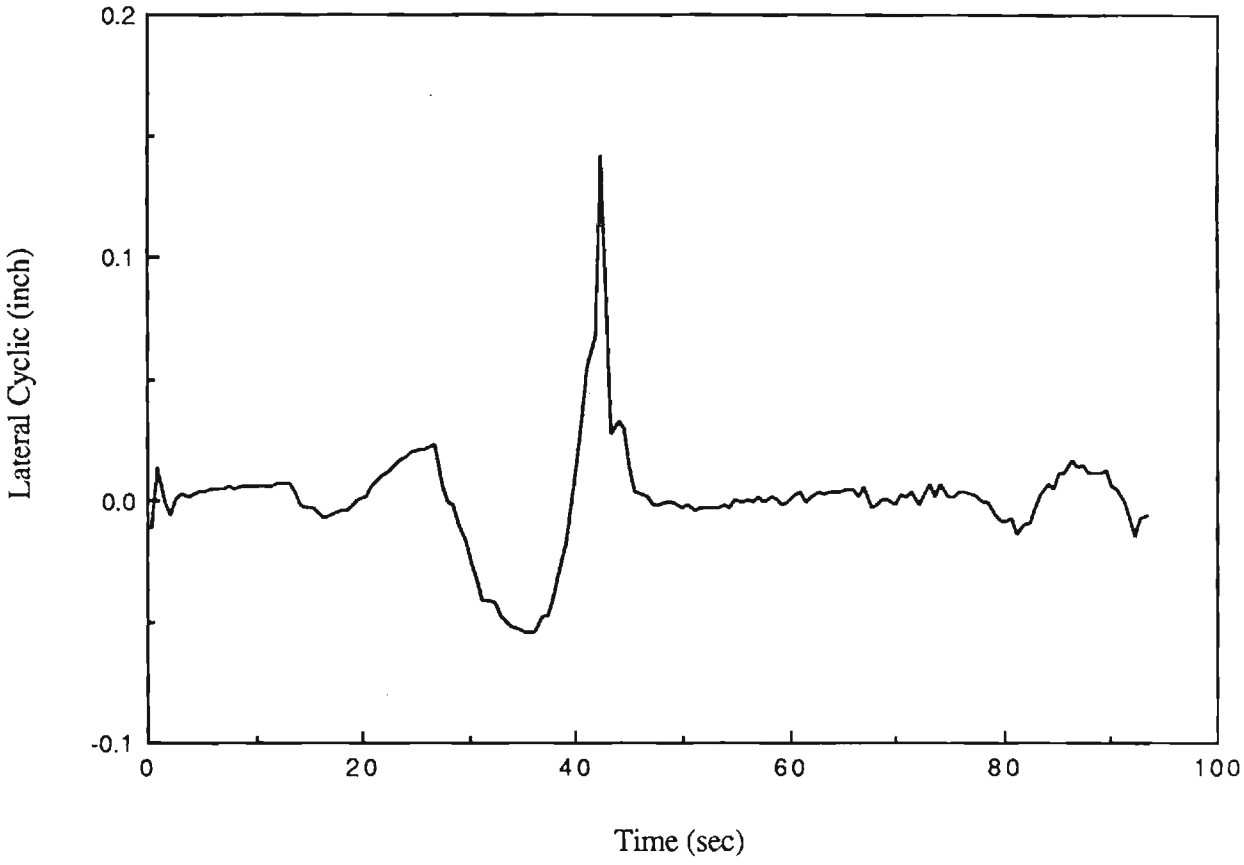

Figure 5.11 Lateral Cyclic Control for Minimum Time Trajectory

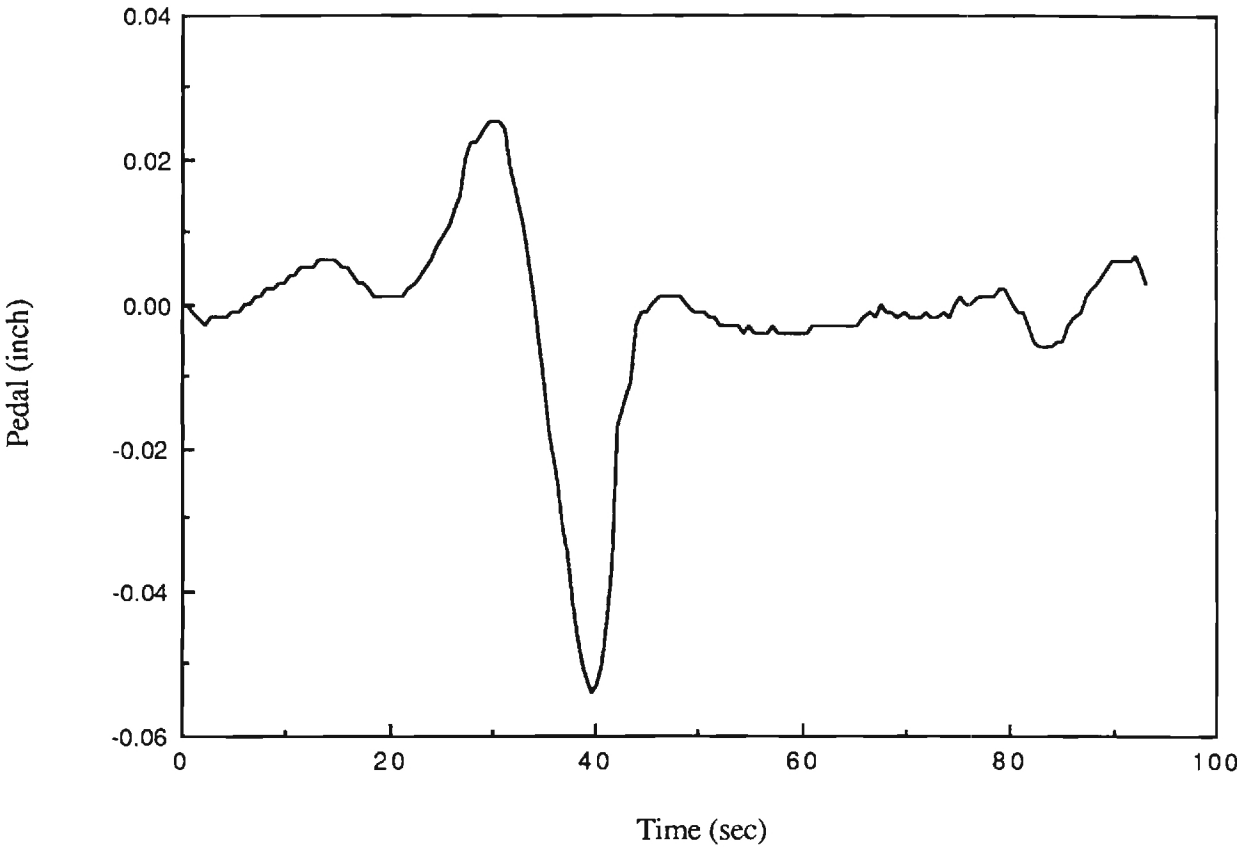

Figure 5.12 Pedal Control for Minimum Time Trajectory

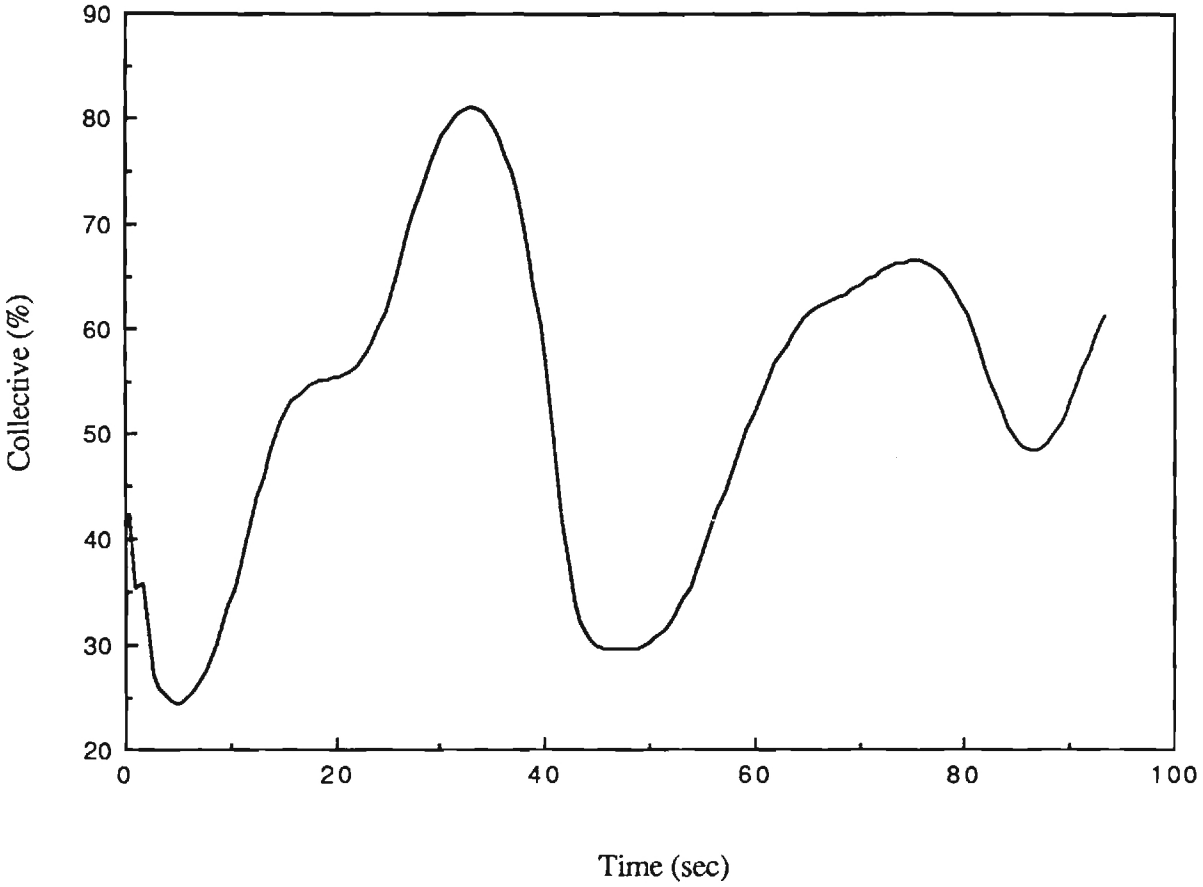

Figure 5. 13 Collective Control for Minimum Time Trajectory

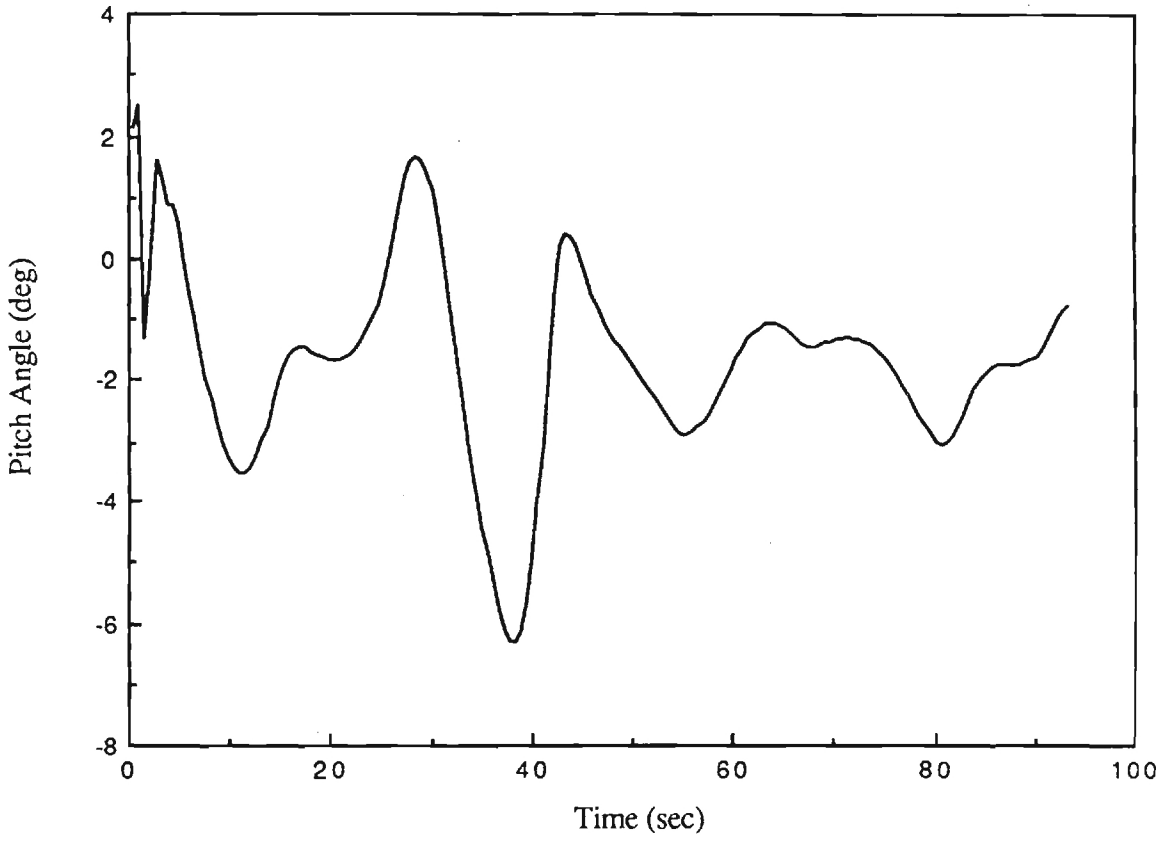

Figure 5.14 Pitch Attitude Response for Minimum Time Trajectory

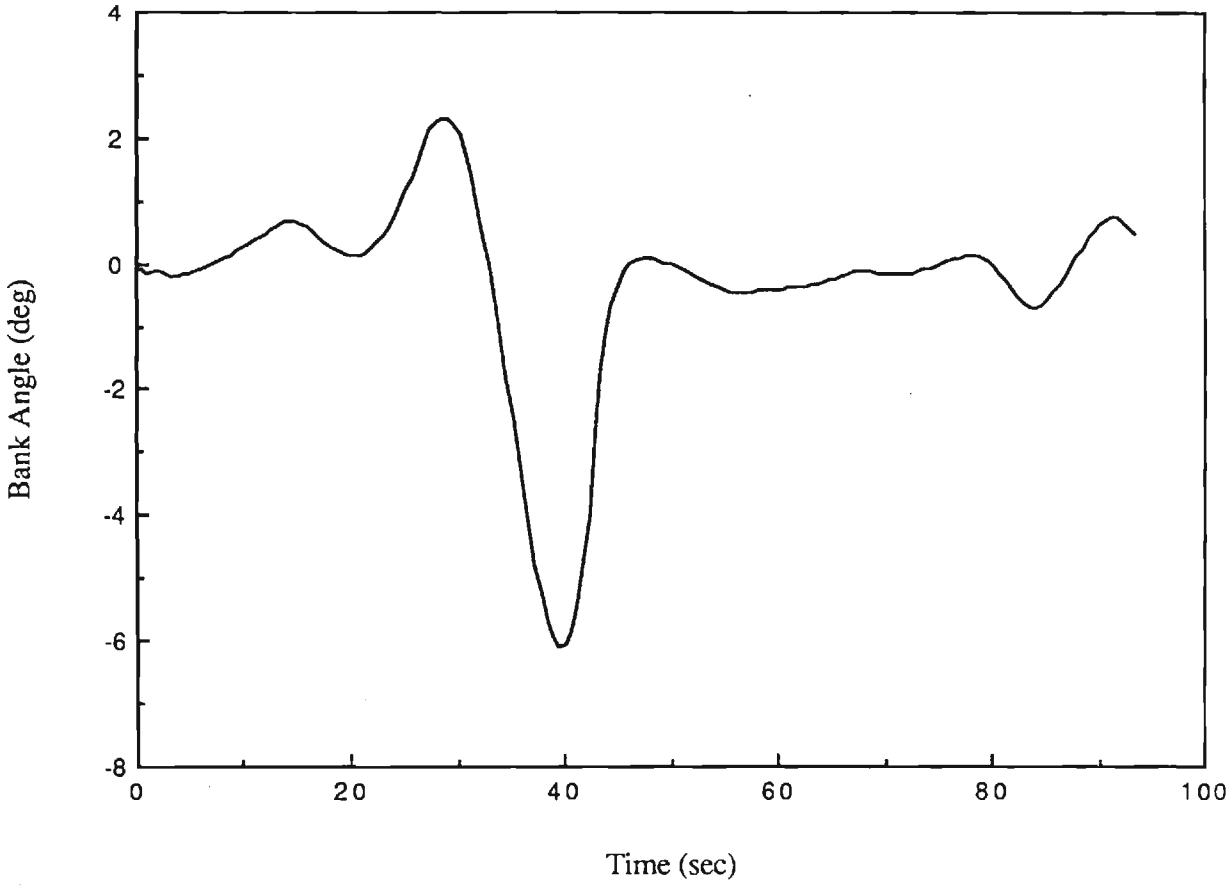

Figure 5.15 Roll Attitude Response for Minimum Time Trajectory

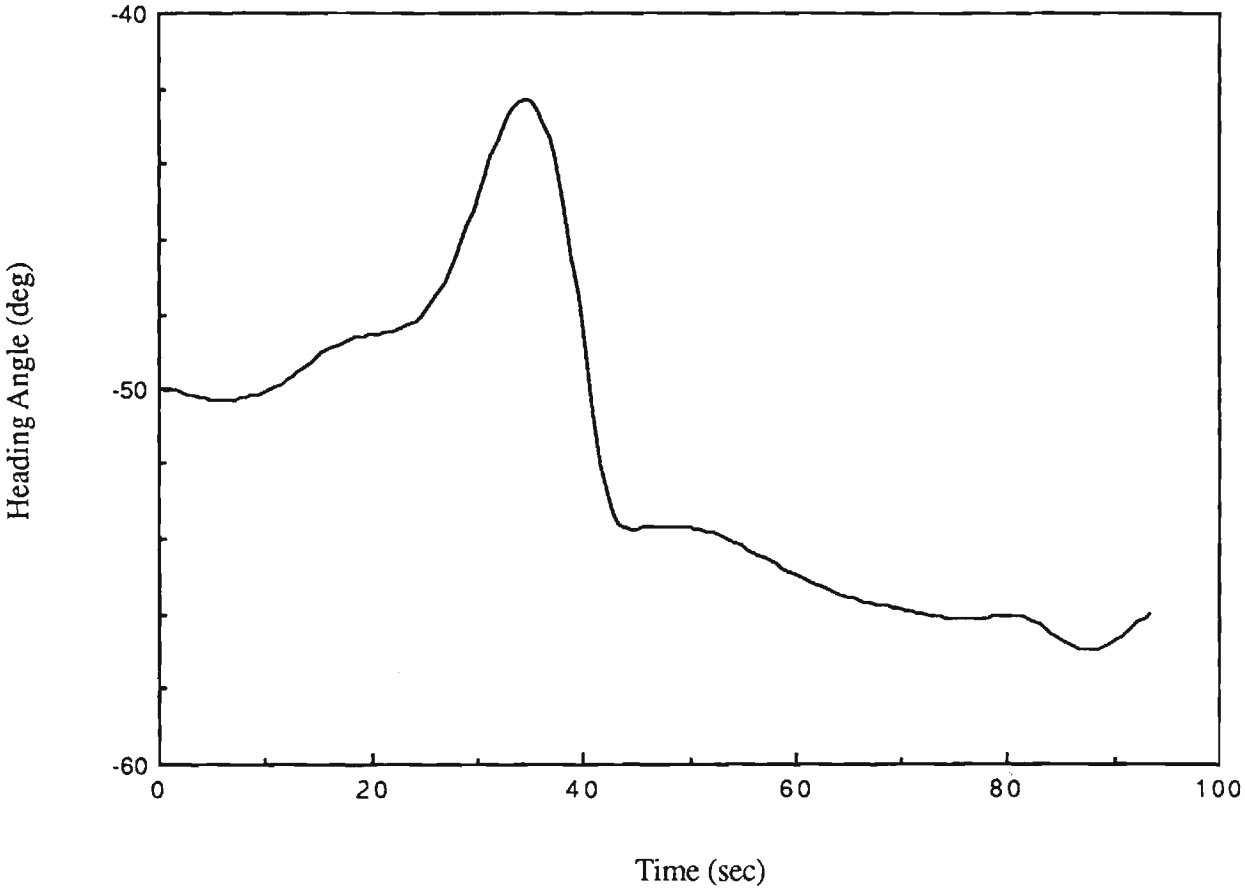

Figure 5.16 Yaw Attitude Response for Minimum Time Trajectory